Modeling high Reynolds number wall turbulence using the attached eddy hypothesis

Ivan Marusic

Department of Mechanical Engineering
University of Melbourne, Australia

THE UNIVERSITY OF MELBOURNE

Australian Government
Australian Research Council

Definitions

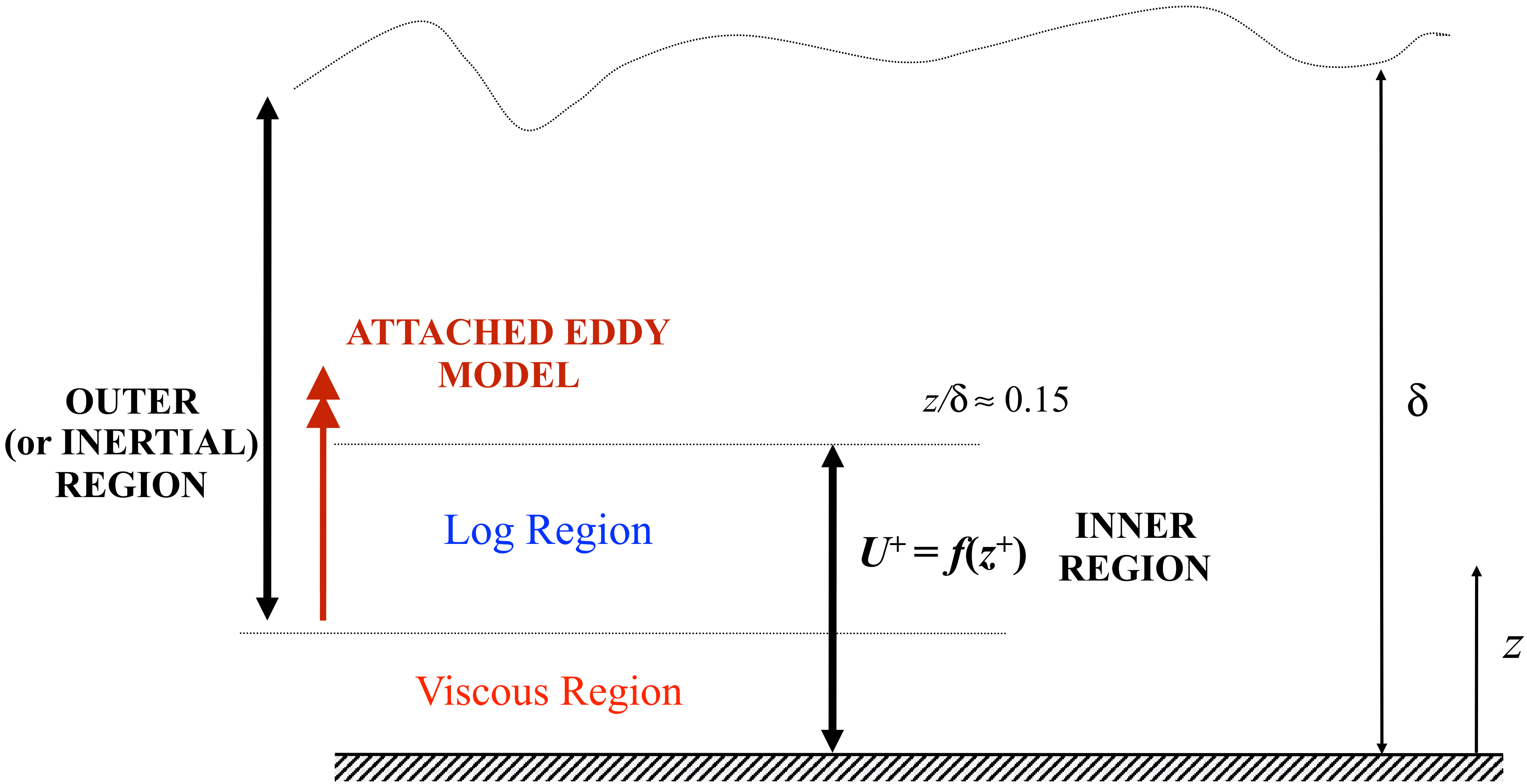

$$U^+ = \frac{U}{U_\tau}; \quad z^+ = \frac{zU_\tau}{\nu}; \quad \tau_0 = \rho U_\tau^2 \qquad Re_\tau = \frac{\delta U_\tau}{\nu}$$

Log region dominated at high Re

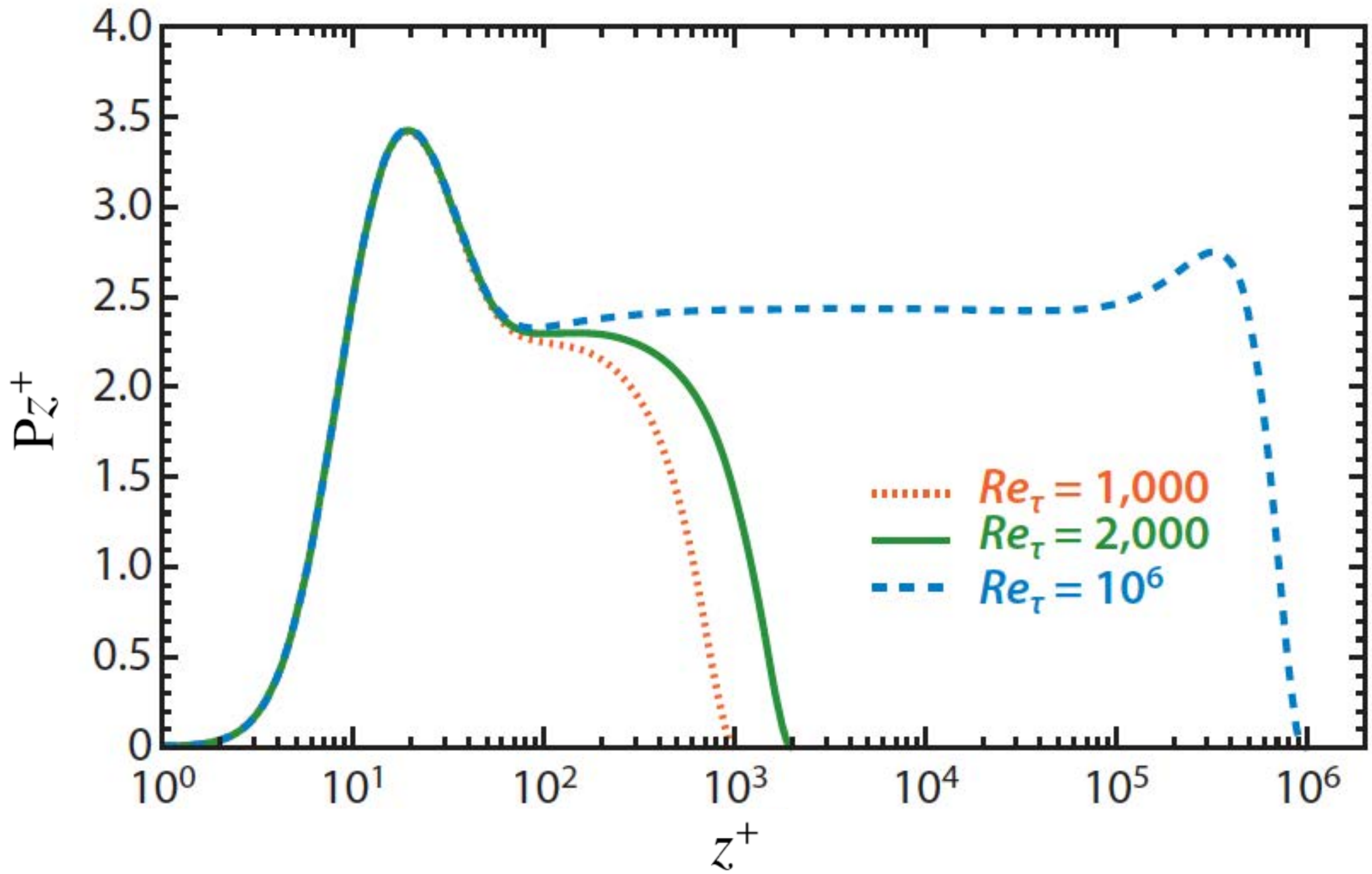

Bulk production = Area under curve

Bulk production ~ $\int P^+ dz^+ = \int z^+ P^+ d(\log z^+)$

Log region dominated at high Re

Contribution to Bulk Production vs *Re*

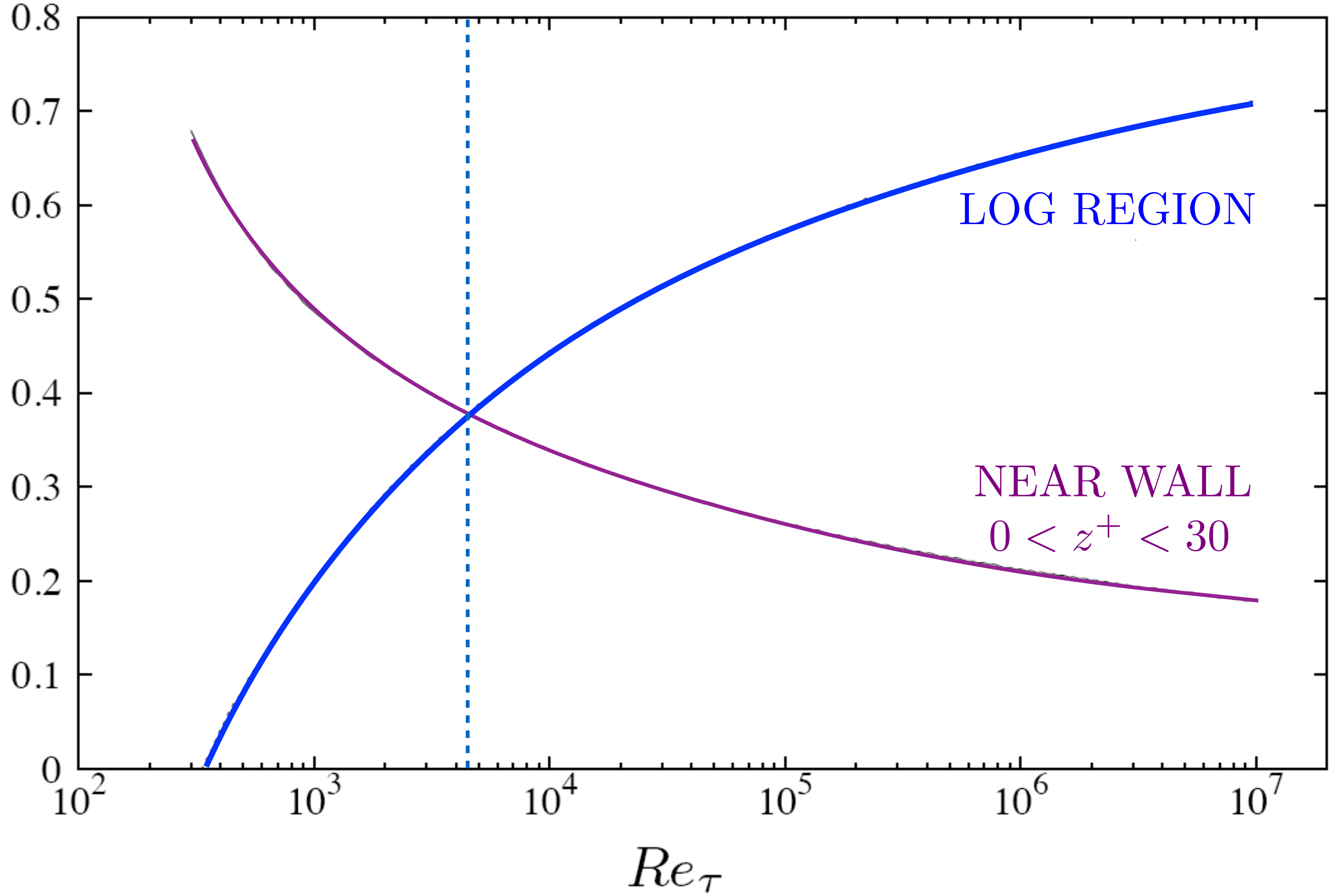

Bulk production = Main contributor to skin friction drag
(Renard & Deck 2016)

Attached eddy hypothesis of A. A. Townsend

Townsend (1976), Page 153:

It is difficult to imagine how the presence of the wall could impose a dissipation length-scale proportional to distance from it unless the main eddies of the flow have diameters proportional to distance of their ‘centres’ from the wall because their motion is directly influenced by its presence. In other words, the velocity fields of the main eddies, regarded as persistent, organised flow patterns, extend to the wall and, in a sense, they are *attached* to the wall. We proceed to consider the observed characteristics of a motion made up from the superposition of attached eddies of a wide range of sizes.

Let us suppose that the main, energy-containing motion is made up of contributions from ‘attached’ eddies with similar velocity distributions,

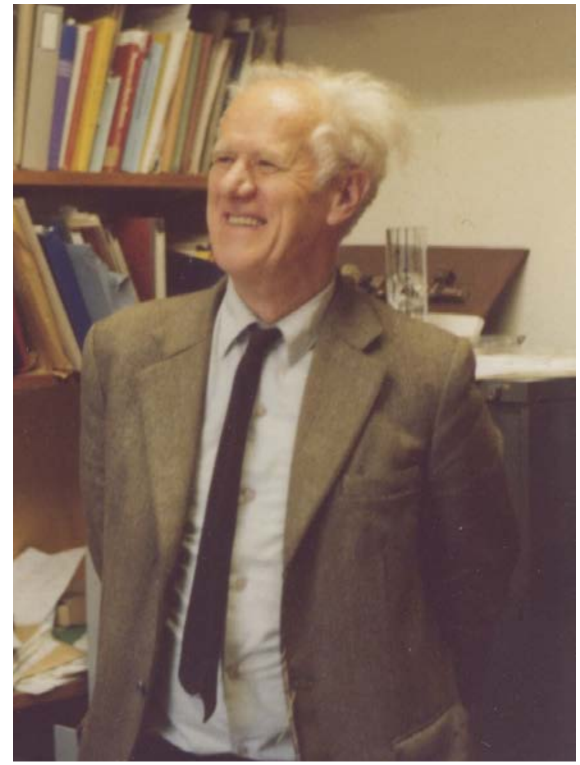

Attached eddy hypothesis of A. A. Townsend
(and Perry & Chong 1982)

for $z_0 \ll z \ll \delta$

$$\overline{u^2}^+ = B_1 - A_1 \log(z/\delta),$$
$$\overline{v^2}^+ = B_2 - A_2 \log(z/\delta),$$
$$\overline{w^2}^+ = A_3, \quad -\overline{uw}^+ = 1.$$

$A_1 \equiv$ Townsend-Perry constant

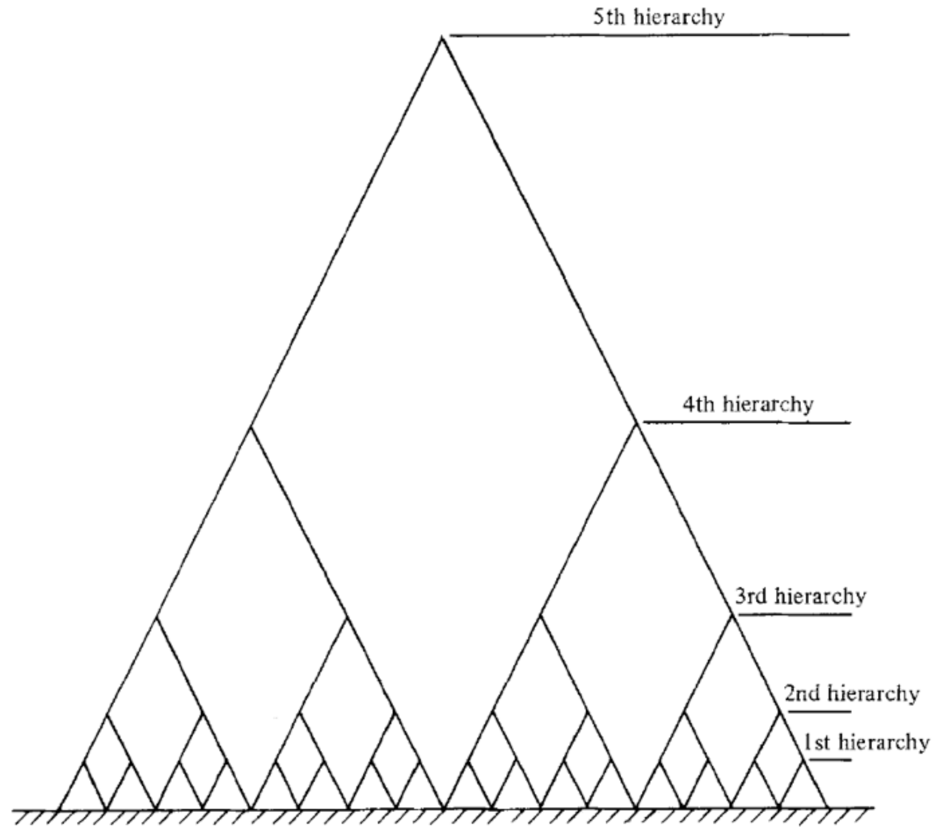

FIGURE 14. Symbolic representation of a discrete system of hierarchies.

Log law in mean flow follows from -1 power law PDF of representative eddy length scales

Implications for turbulence models

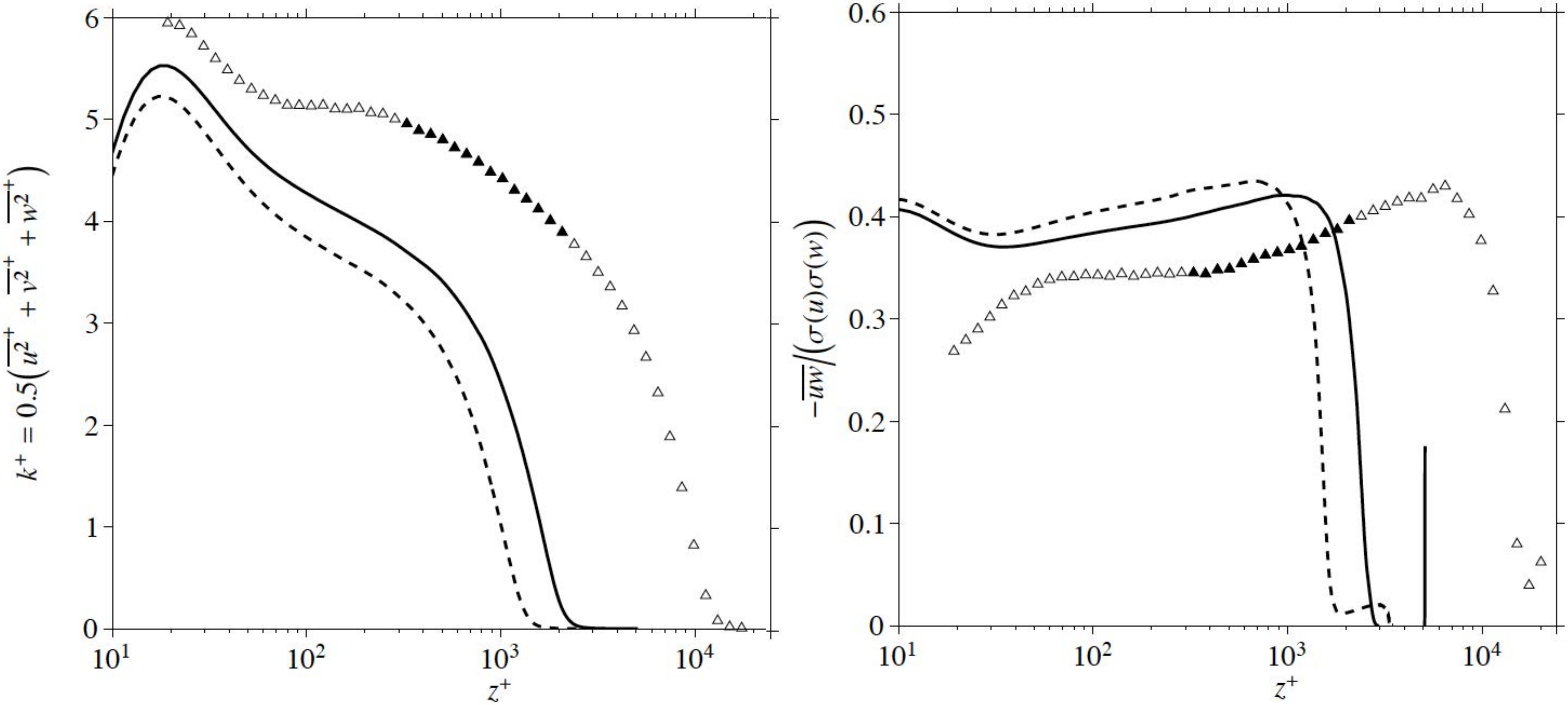

DNS data shown as lines: - - $Re_\tau \approx 1,200$ [Schlatter and Örlü, 2010] $\triangle$ $Re_\tau \approx 15,000$

— $Re_\tau \approx 2,000$ [Sillero et al., 2013]

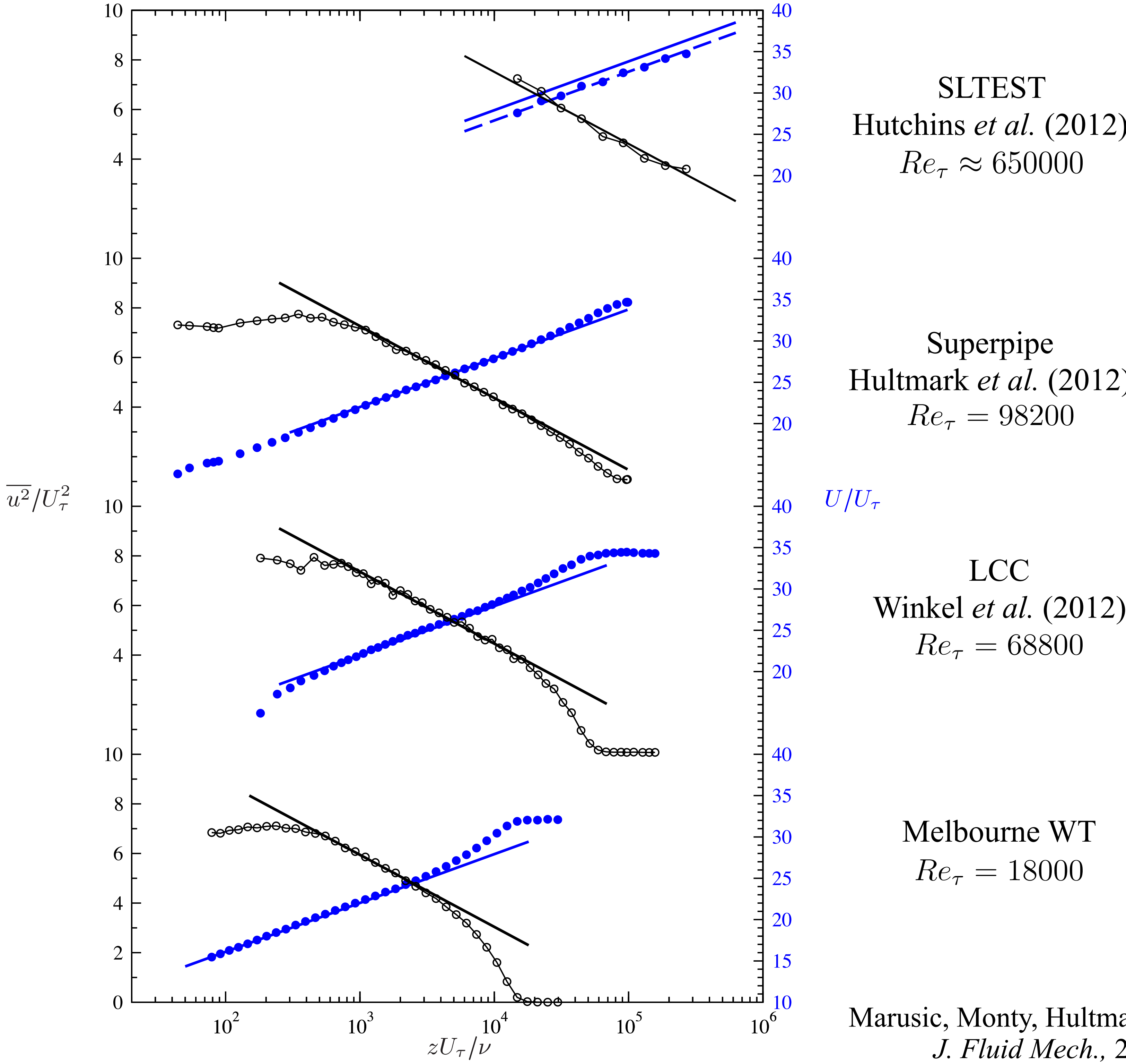

Marusic, Monty, Hultmark & Smits
J. Fluid Mech., 2013

Talluru et al. JFM, 2014

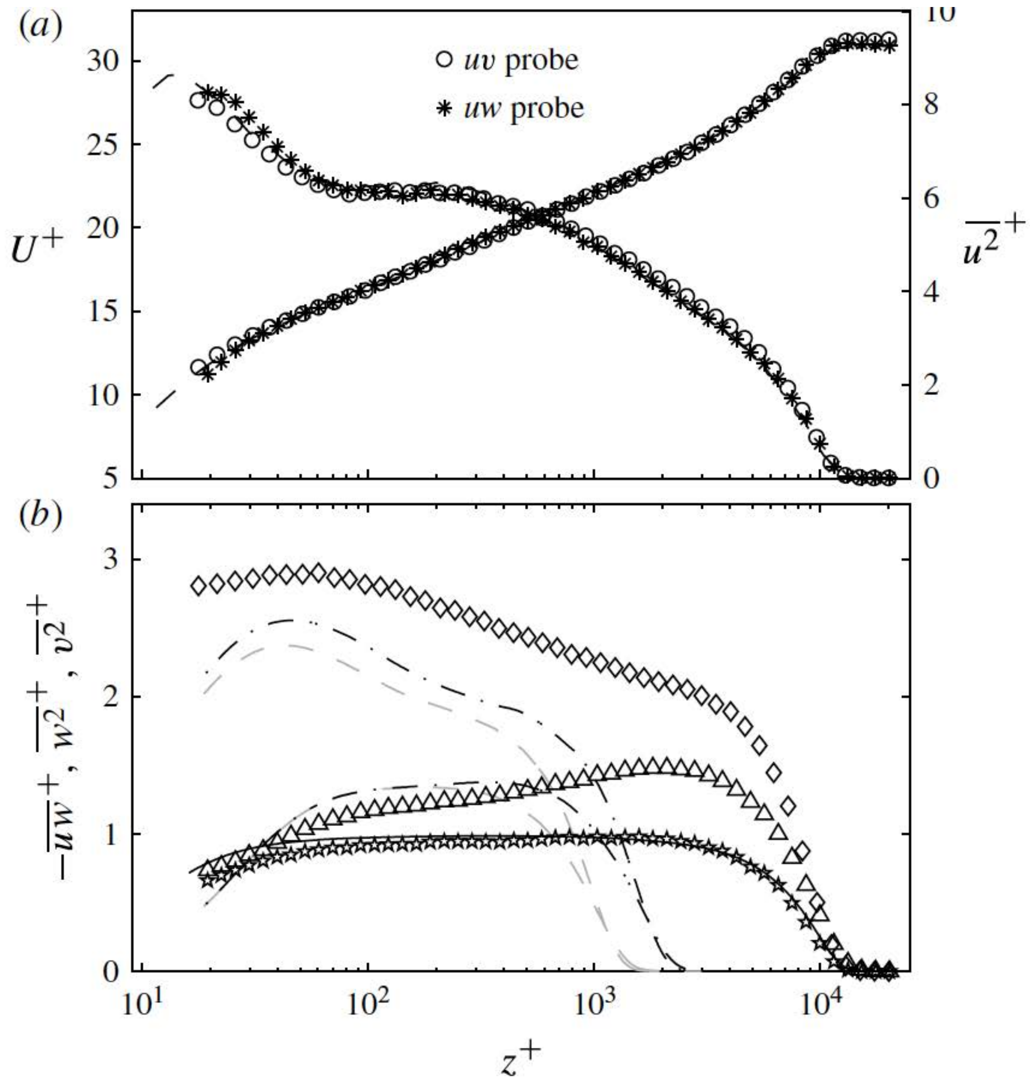

FIGURE 1. (*a*) The mean and variance of the u component as measured by (○) the *uv* probe and (∗) the *uw* probe; dashed lines show the data of Hutchins *et al.* (2011) at comparable Reynolds number. (*b*) Comparison of variance of v and w (◇ and △ symbols respectively) against the DNS data of (grey dashed line) Schlatter & Örlü (2010*a*) at $Re_\tau = 1271$ and (dot-dashed line) Sillero *et al.* (2013) at $Re_\tau = 1989$. The measured $-\overline{uw}$ profile (☆) is also compared with the (solid line) Reynolds shear stress obtained from the mean velocity profile.

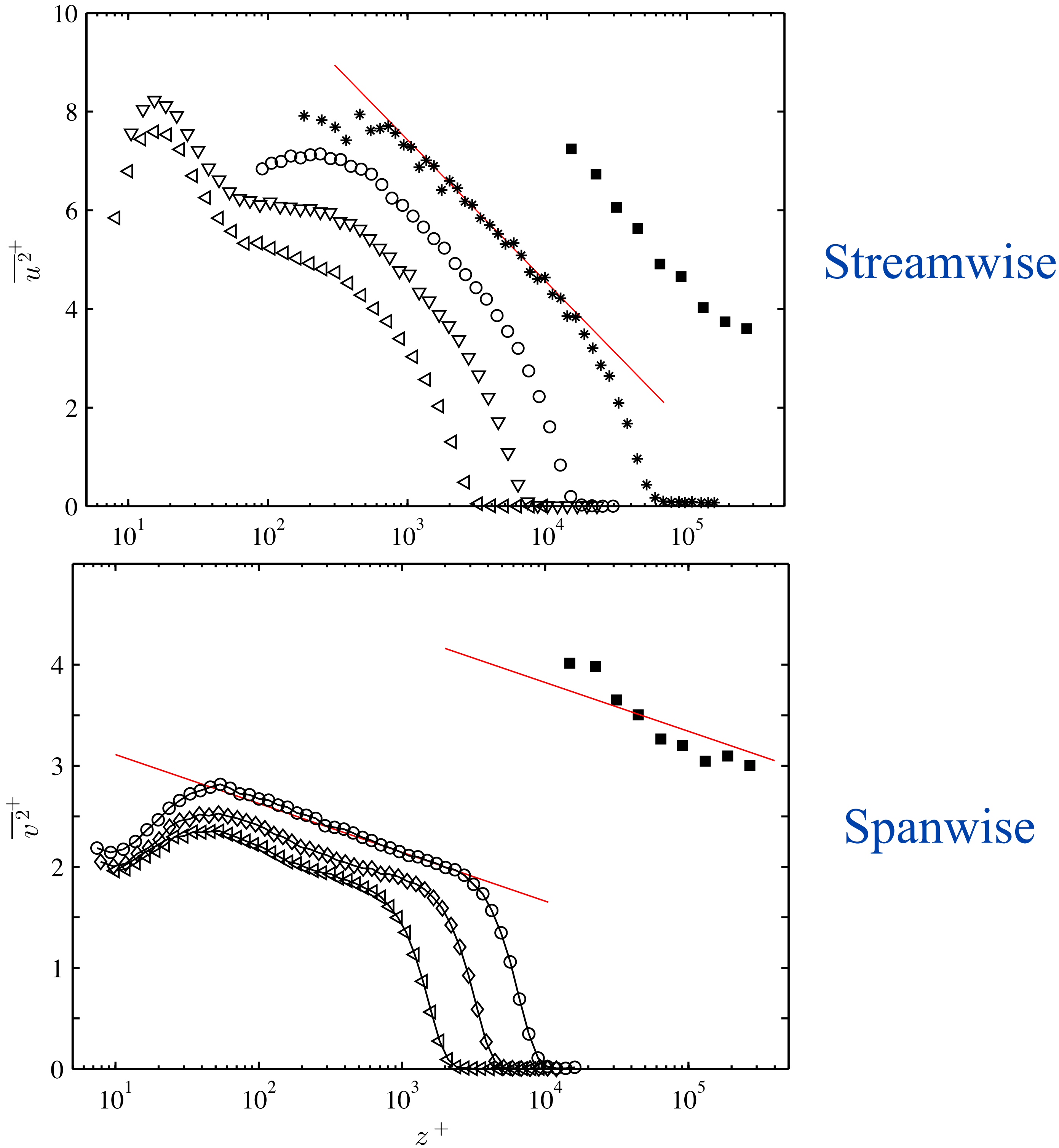

Streamwise
Spanwise
$\overline{u^2}^+$
$\overline{v^2}^+$
z^+

Attached eddy model

Two concepts:

1. Range of scales with changing Reynolds number

2. Geometric progression of scales

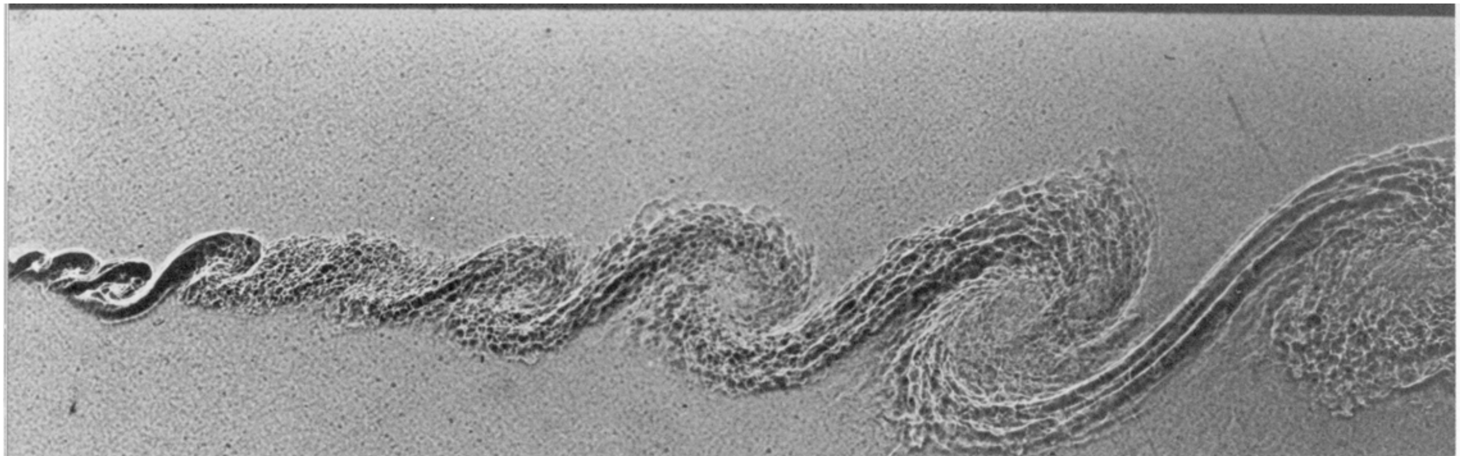

176. Large-scale structure in a turbulent mixing layer. Nitrogen above flowing at 1000 cm/s mixes with a helium-argon mixture below at the same density flowing at 380 cm/s under a pressure of 4 atmospheres. Spark shadow photography shows simultaneous edge and plan views, demonstrating the spanwise organization of the large eddies. The streamwise streaks in the plan view (of which half the span is shown) correspond to a system of secondary vortex pairs oriented in the streamwise direction. Their spacing at the downstream side of the layer is larger than near the beginning. *Photograph by J. H. Konrad, Ph.D. thesis, Calif. Inst. of Tech., 1976.*

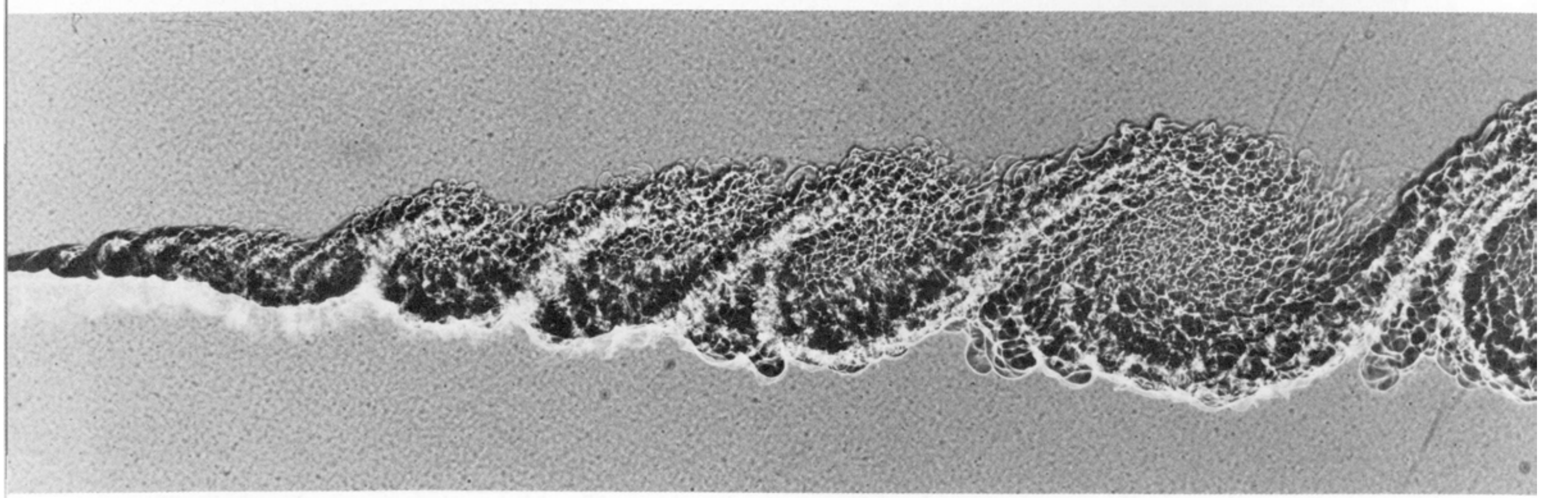

177. Coherent structure at higher Reynolds number. This flow is as above but at twice the pressure. Doubling the Reynolds number has produced more small-scale structure without significantly altering the large-scale structure. *M. R. Rebollo, Ph.D. thesis, Calif. Inst. of Tech., 1976; Brown & Roshko 1974*

Van Dyke (1982)

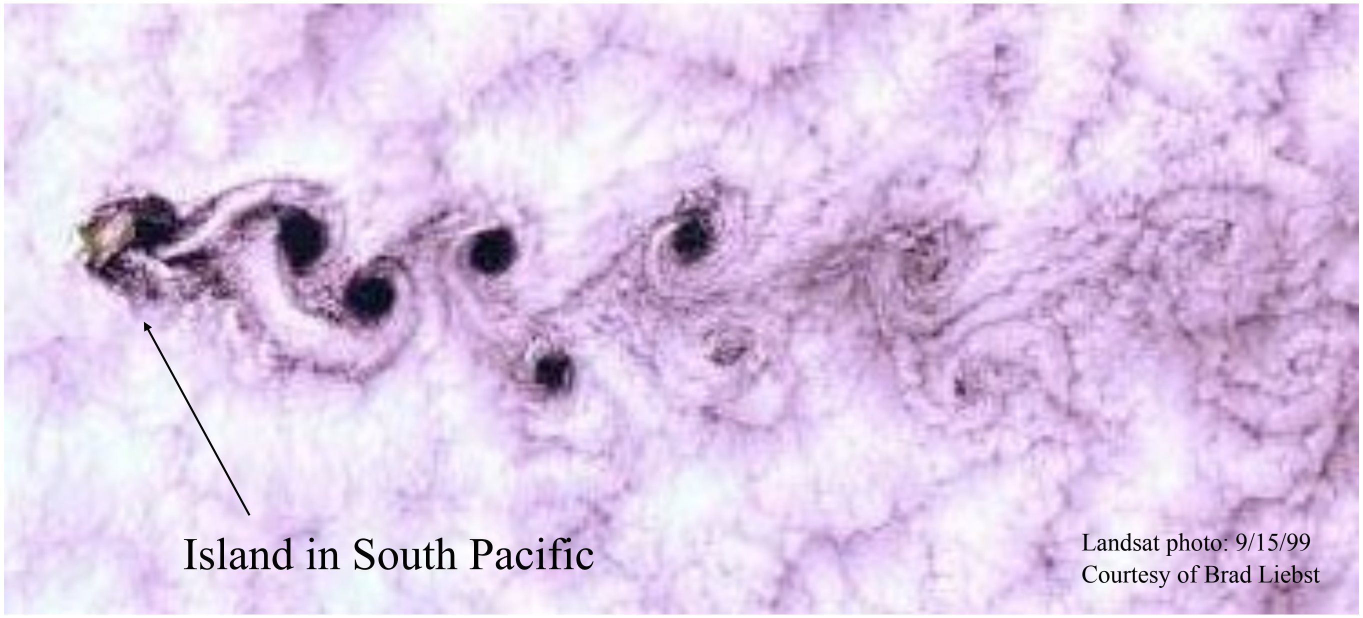

Landsat photo: 9/15/99
Courtesy of Brad Liebst

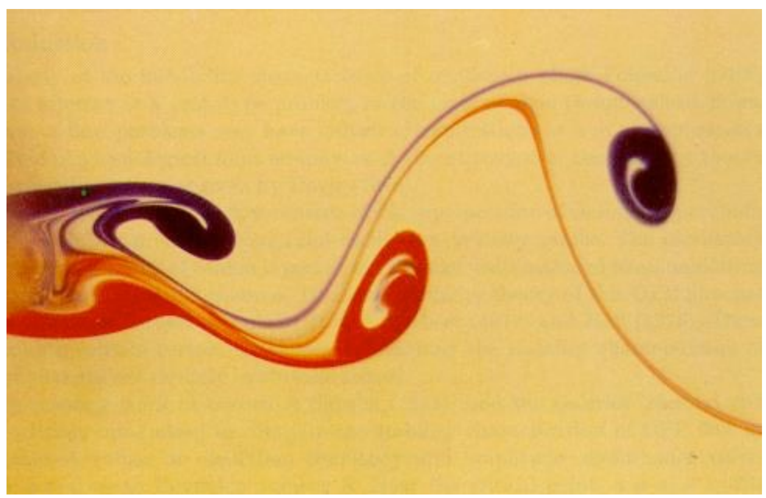

Perry, Lim & Chong

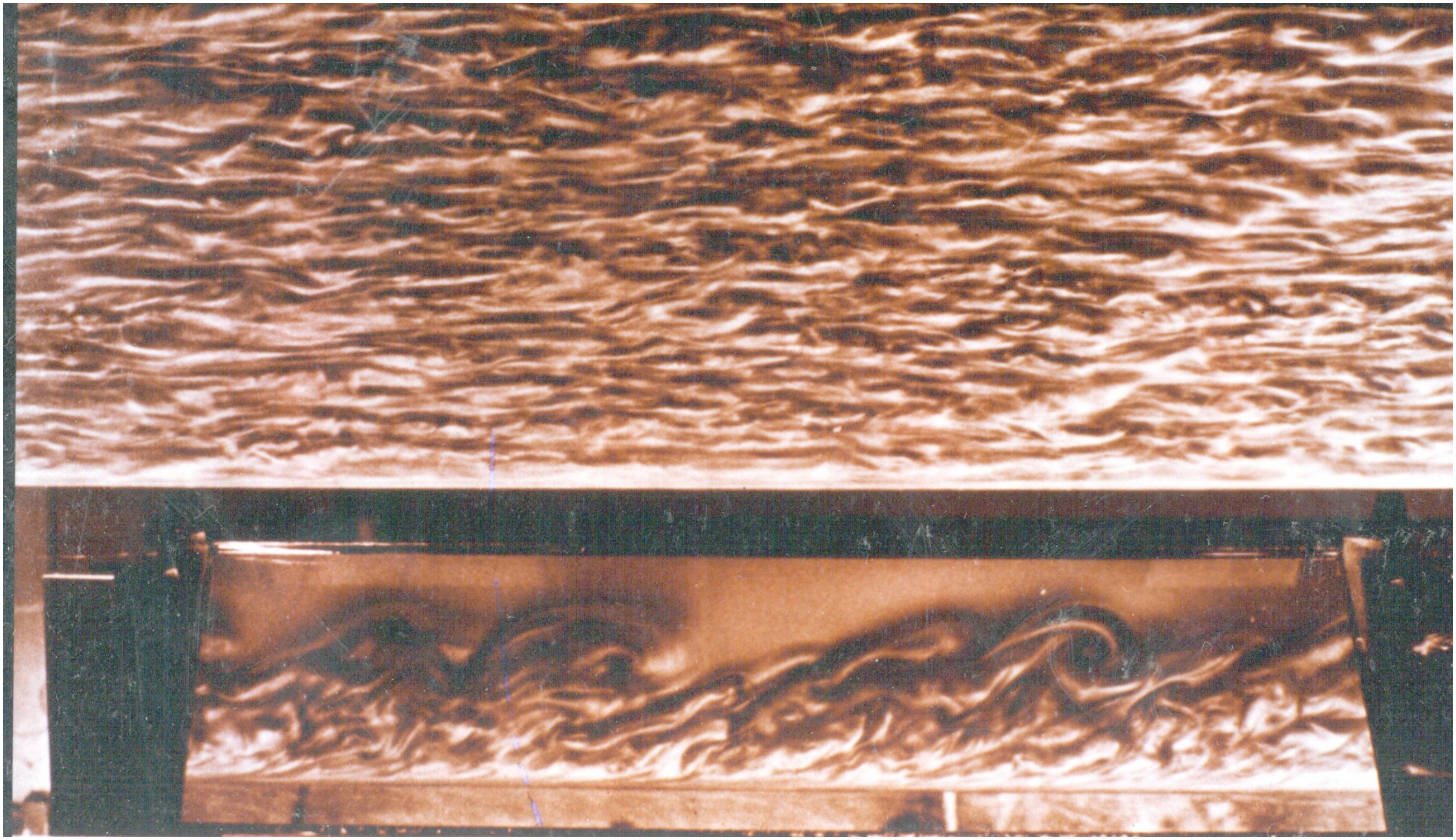

Cantwell, Dimotakis & Coles

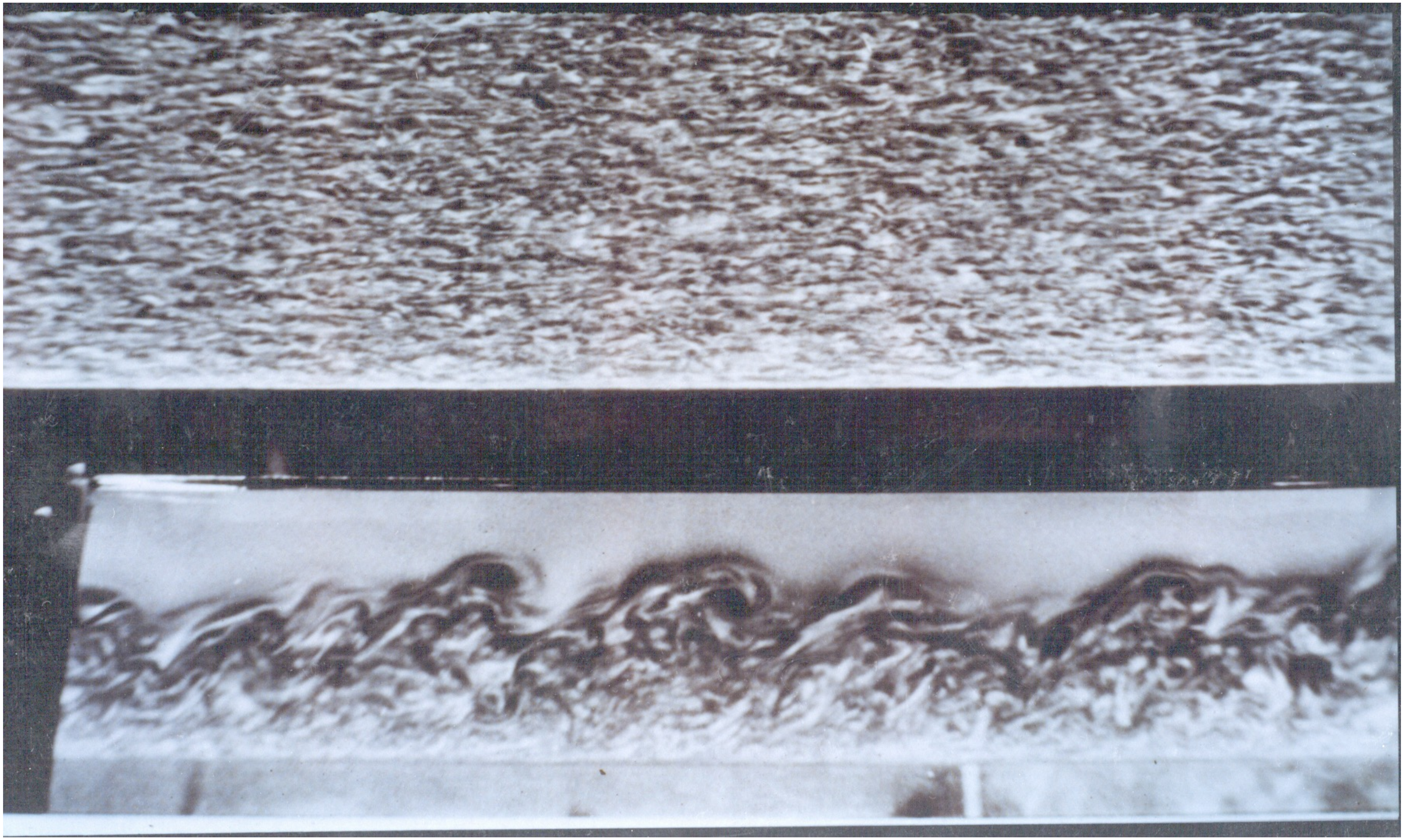

Cantwell, Dimotakis & Coles

Geometric progression of scales

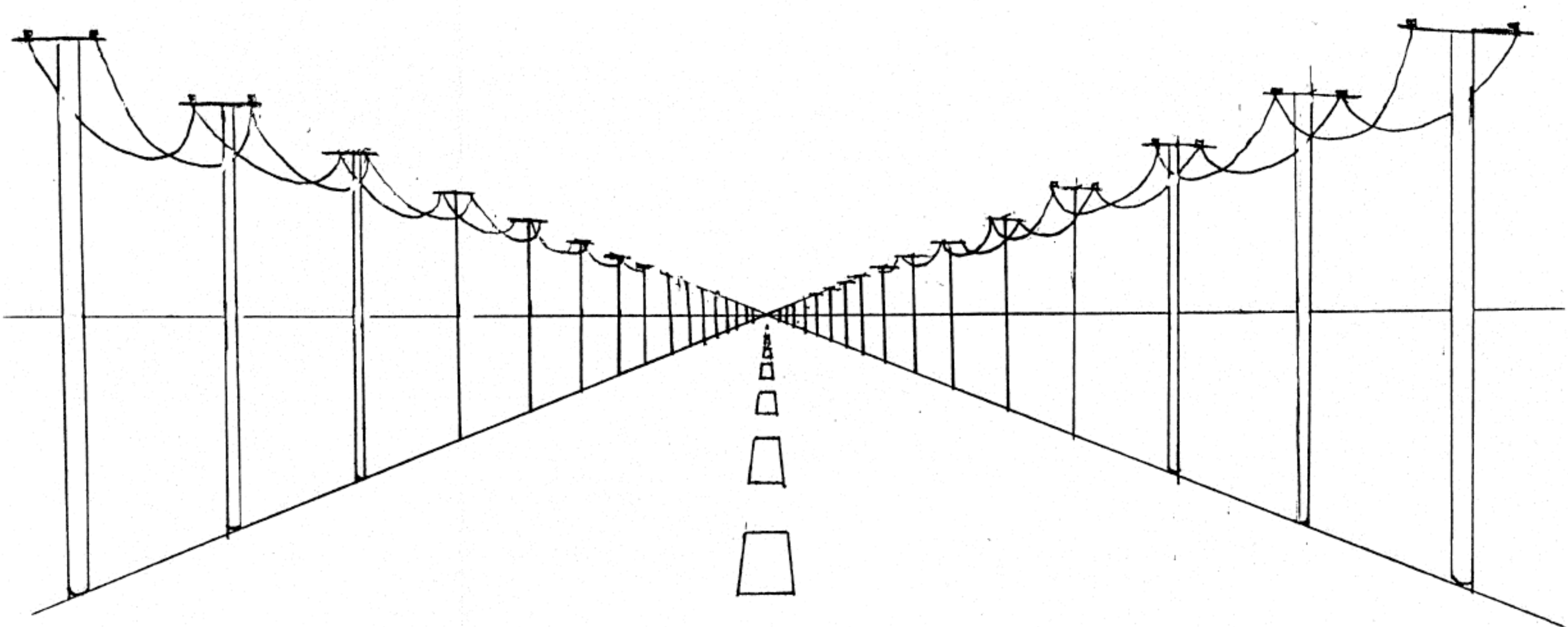

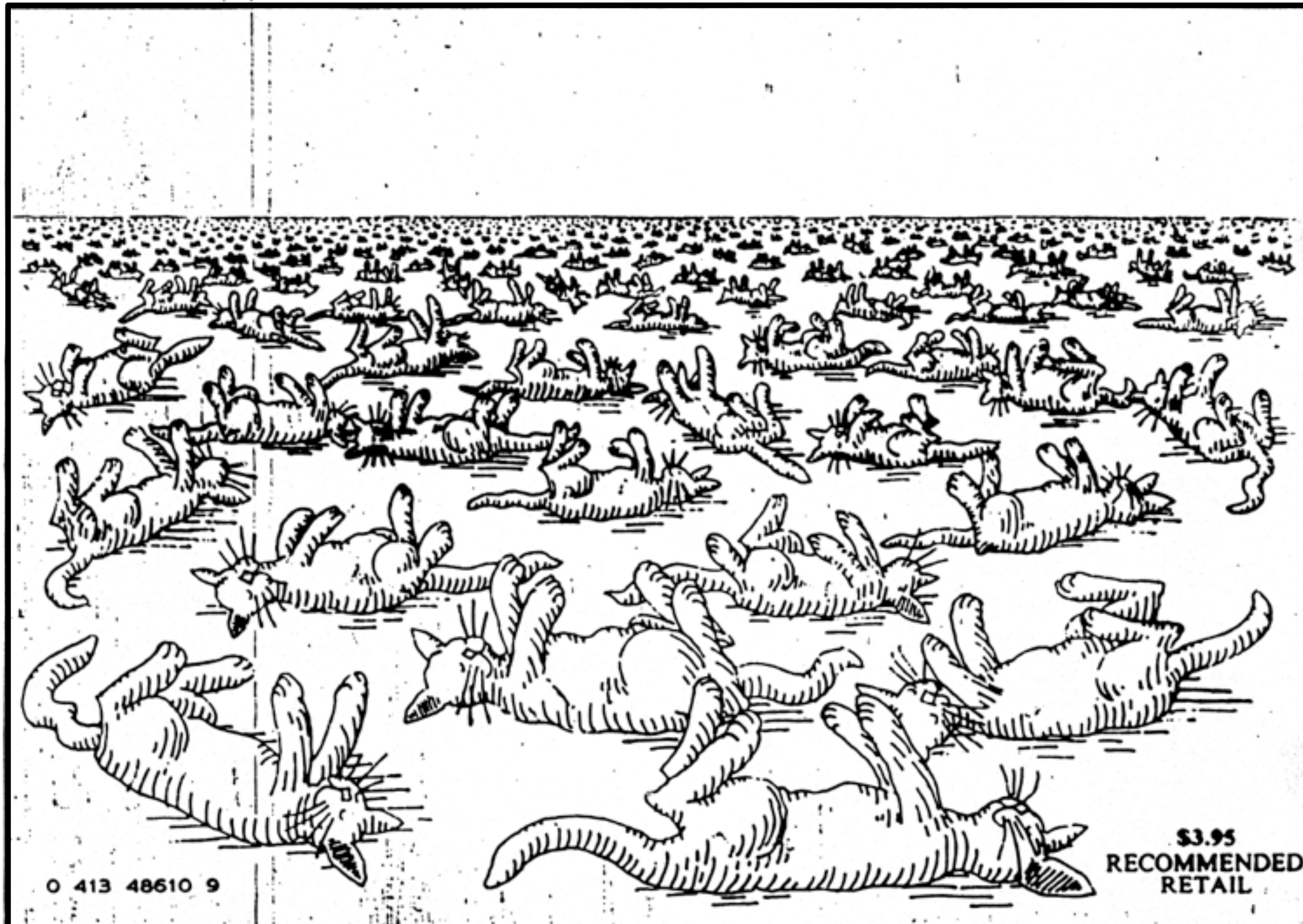

0 413 48610 9

$3.95
RECOMMENDED
RETAIL

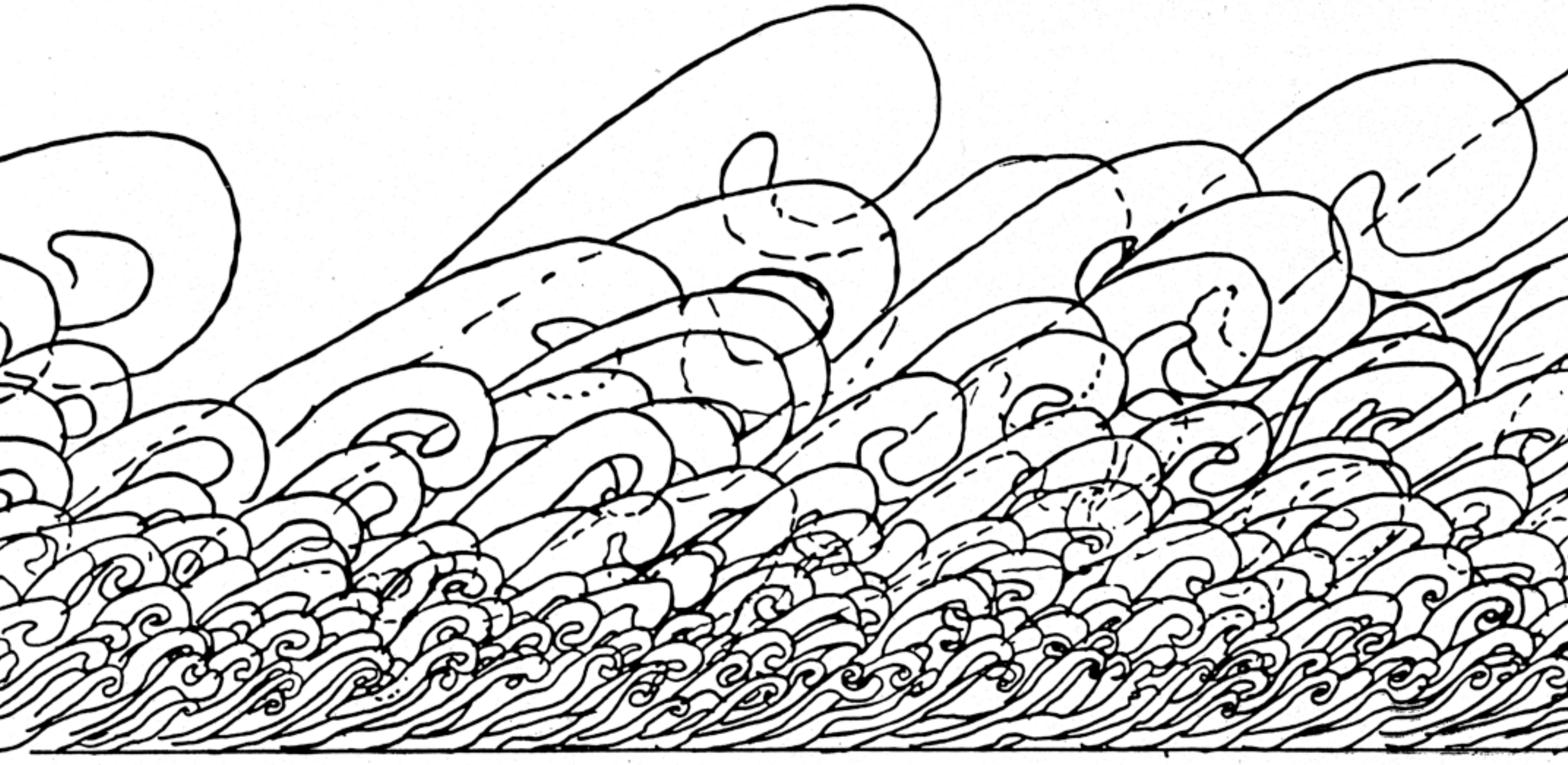

Attached eddy model
- Main assumptions/issues

- Attached eddies - do they exist or are they just a statistical construct?

- Statistical self-similarity of eddies that scale with distance from the wall.

- Random spatial distribution of attached eddies in plane of the wall, which are independent of each other.

1. Are attached eddies real or just a statistical construct?

Hairpin-vortices as candidate attached eddies

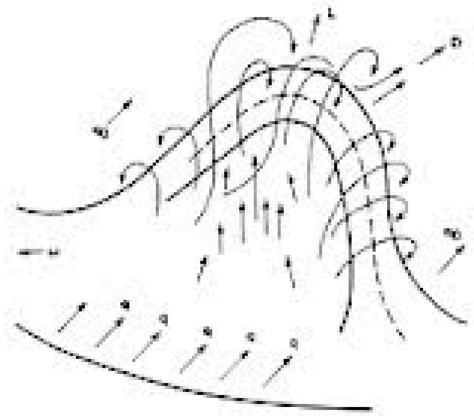

Theodorsen (1952) “hairpin vortex”

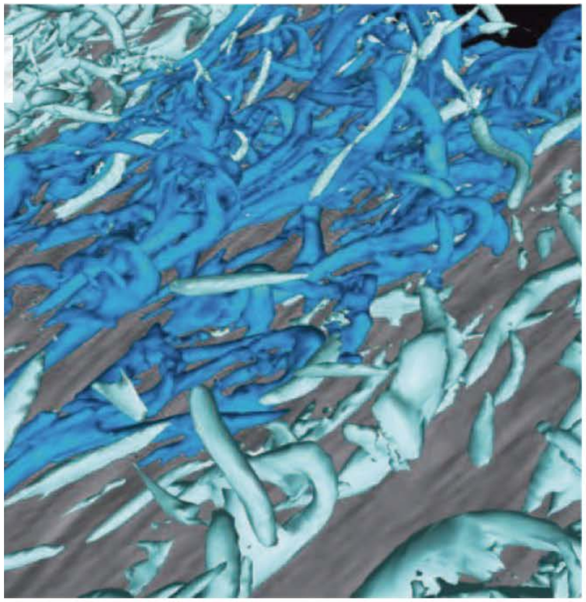

Ganapathisubramani, Longmire & Marusic

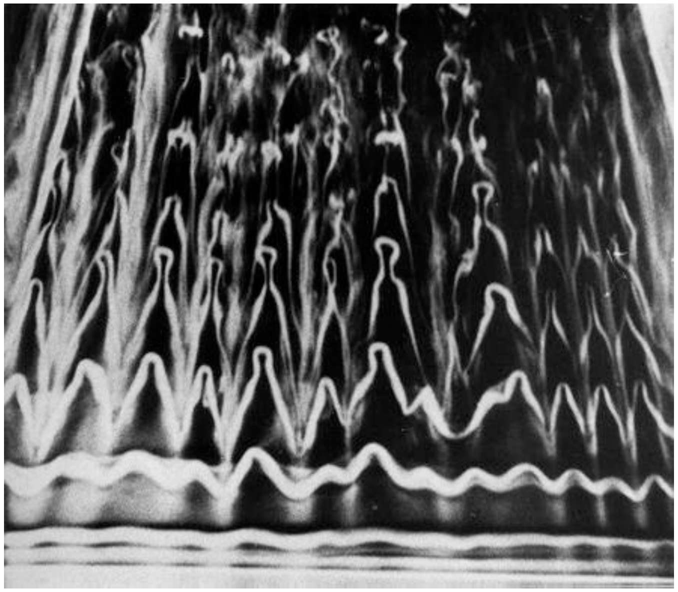

Perry, Lim & Teh

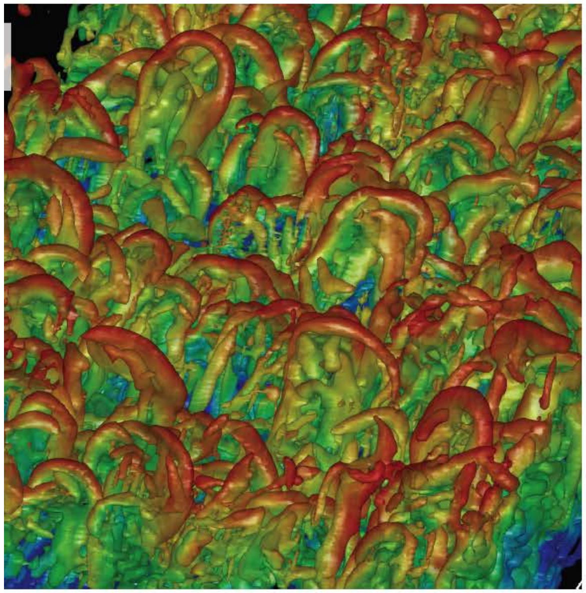

Wu & Moin

Existence of hairpin vortices at high Re?

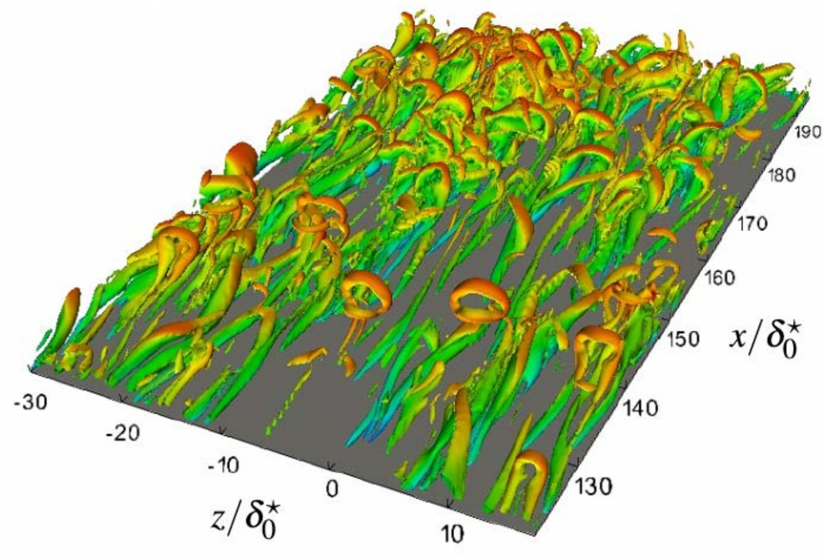

$Re_\theta = 273 - 370$

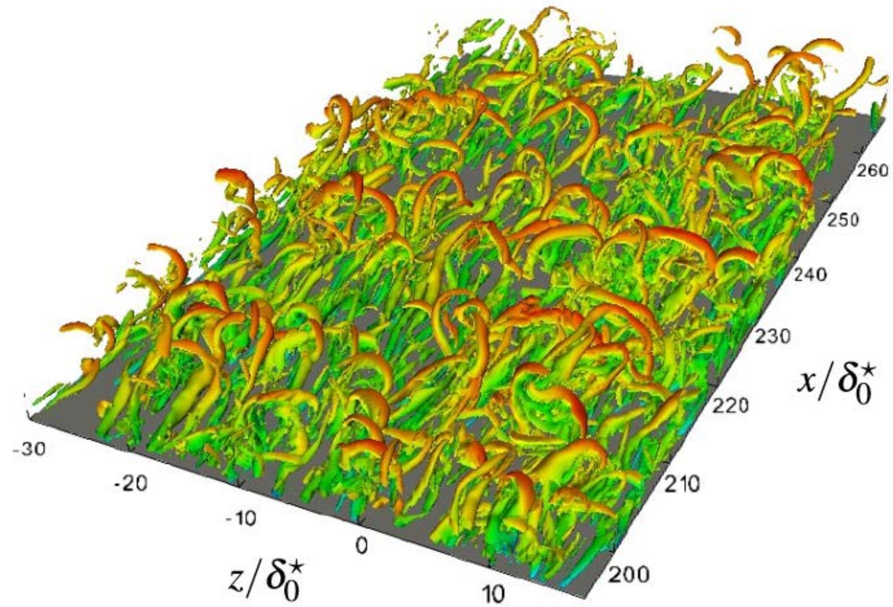

$Re_\theta = 370 - 445$

"A qualitative analysis of the present data suggests that the flow is not dominated by wall-attached hairpins beyond $Re_\theta = 350$"

Eitel-Amor, Orlu, Schlatter & Flores (2015) *Phys. Fluids*

Flow topology classification

Velocity gradient tensor

$$A_{ij} = \frac{\partial u_j}{\partial x_i}$$

Characteristic equation: $\lambda^3 + P\lambda^2 + Q\lambda + R = 0$

Discriminant: $\Delta = \frac{1}{4}R^2 + \frac{1}{27}Q^3$

Invariants

$$\begin{aligned} P &= -A_{ii} = 0 \quad \text{(incompressible)} \\ Q &= -\frac{1}{2}A_{im}A_{mi} \\ R &= -\frac{1}{3}A_{im}A_{mk}A_{ki} \end{aligned}$$

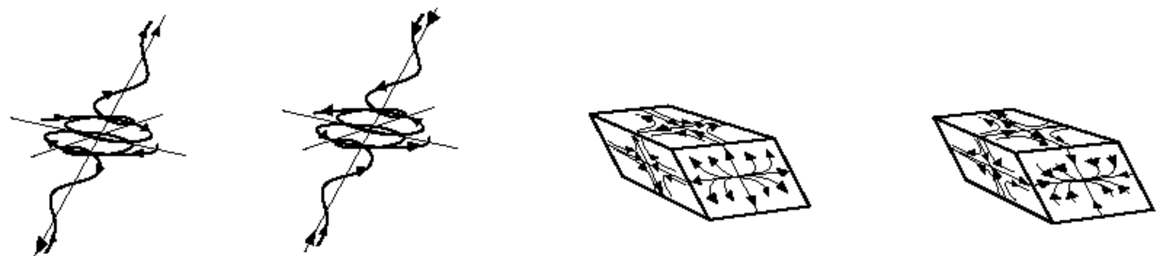

I Stable-focus stretching ($\Delta > 0$)

II Unstable-focus compressing ($\Delta > 0$)

III Unstable-node saddle-saddle ($\Delta < 0$)

IV Stable-node saddle-saddle ($\Delta < 0$)

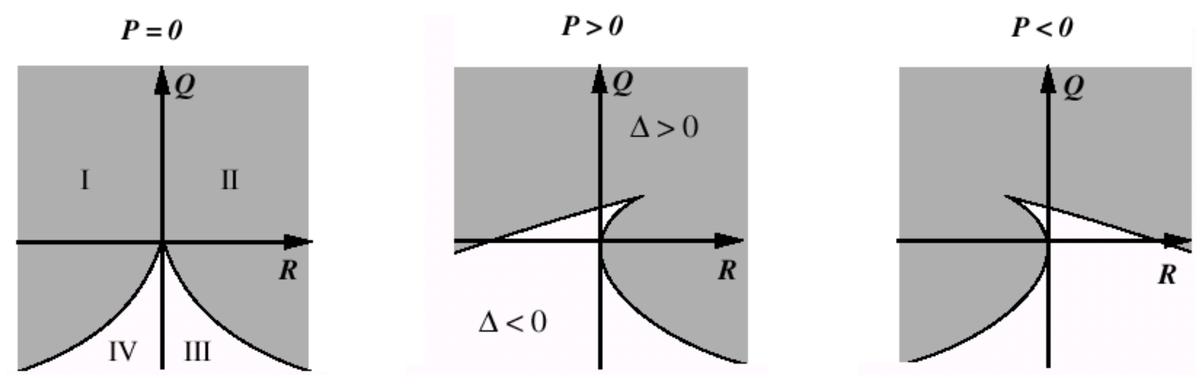

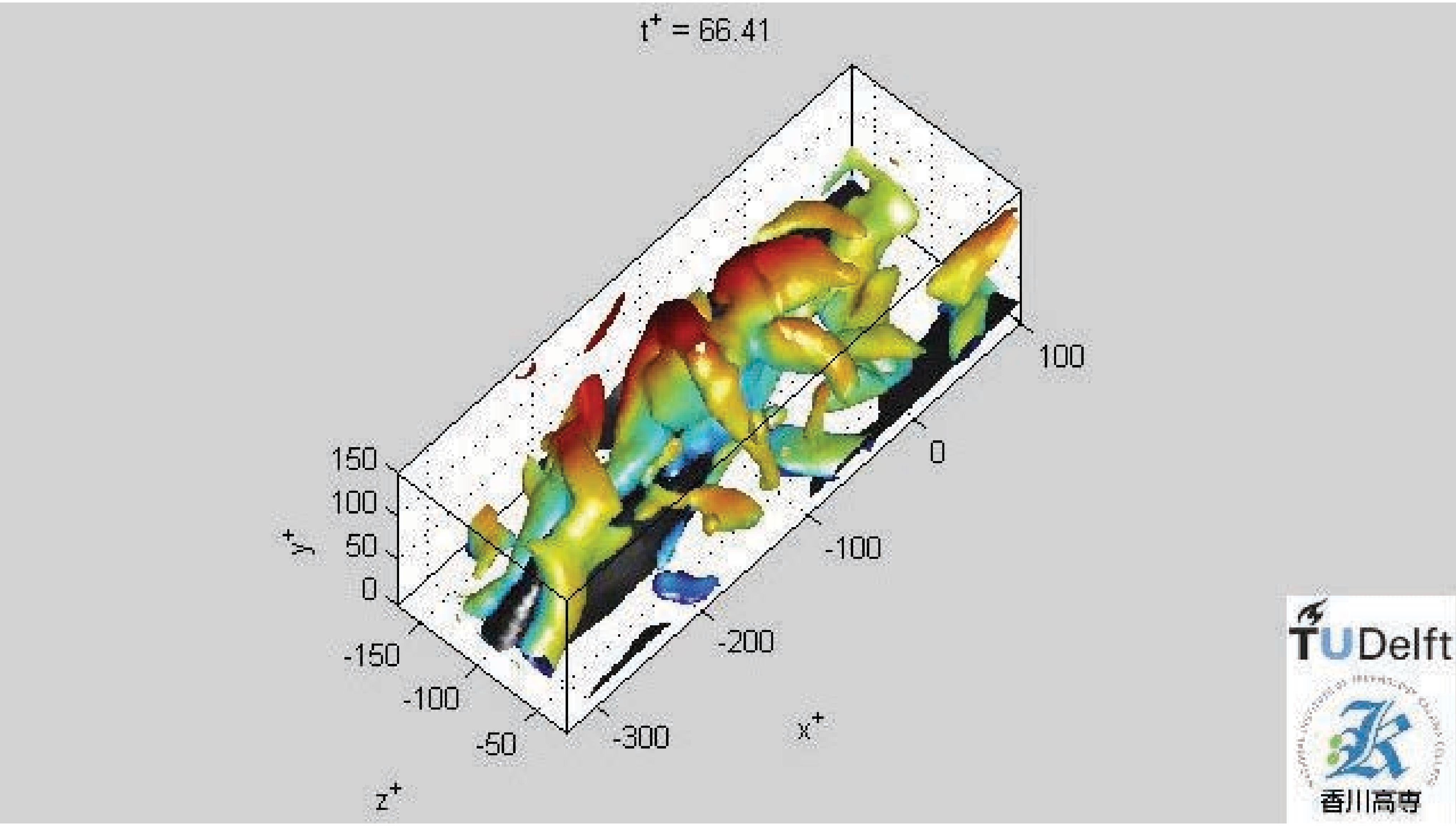

Courtesy of Gerrit Elsinga (Jodie & Elsinga. *JFM*. In press)

Energy vs. enstrophy contributing scales

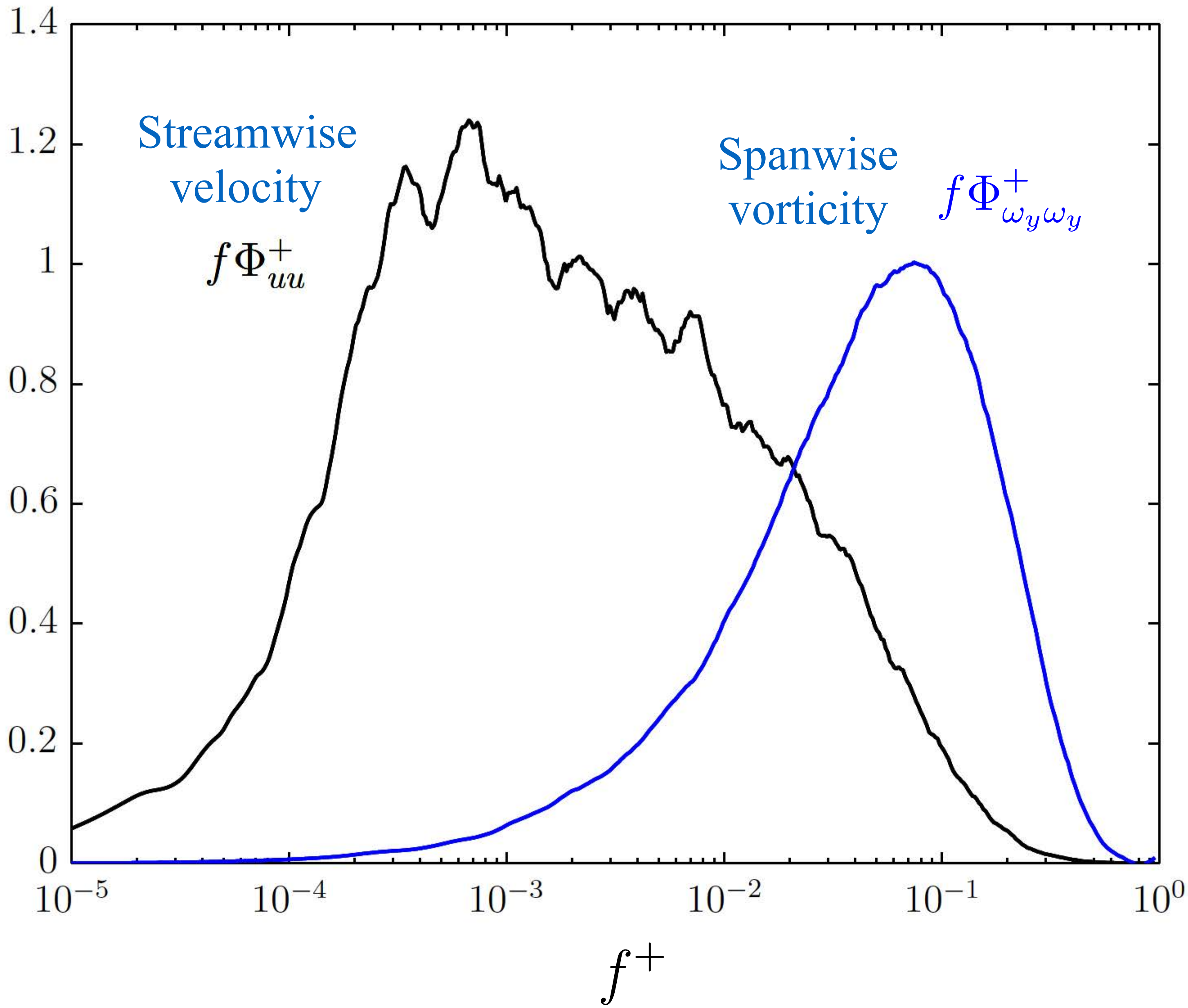

Focus on instantaneous (changes) in velocity fields

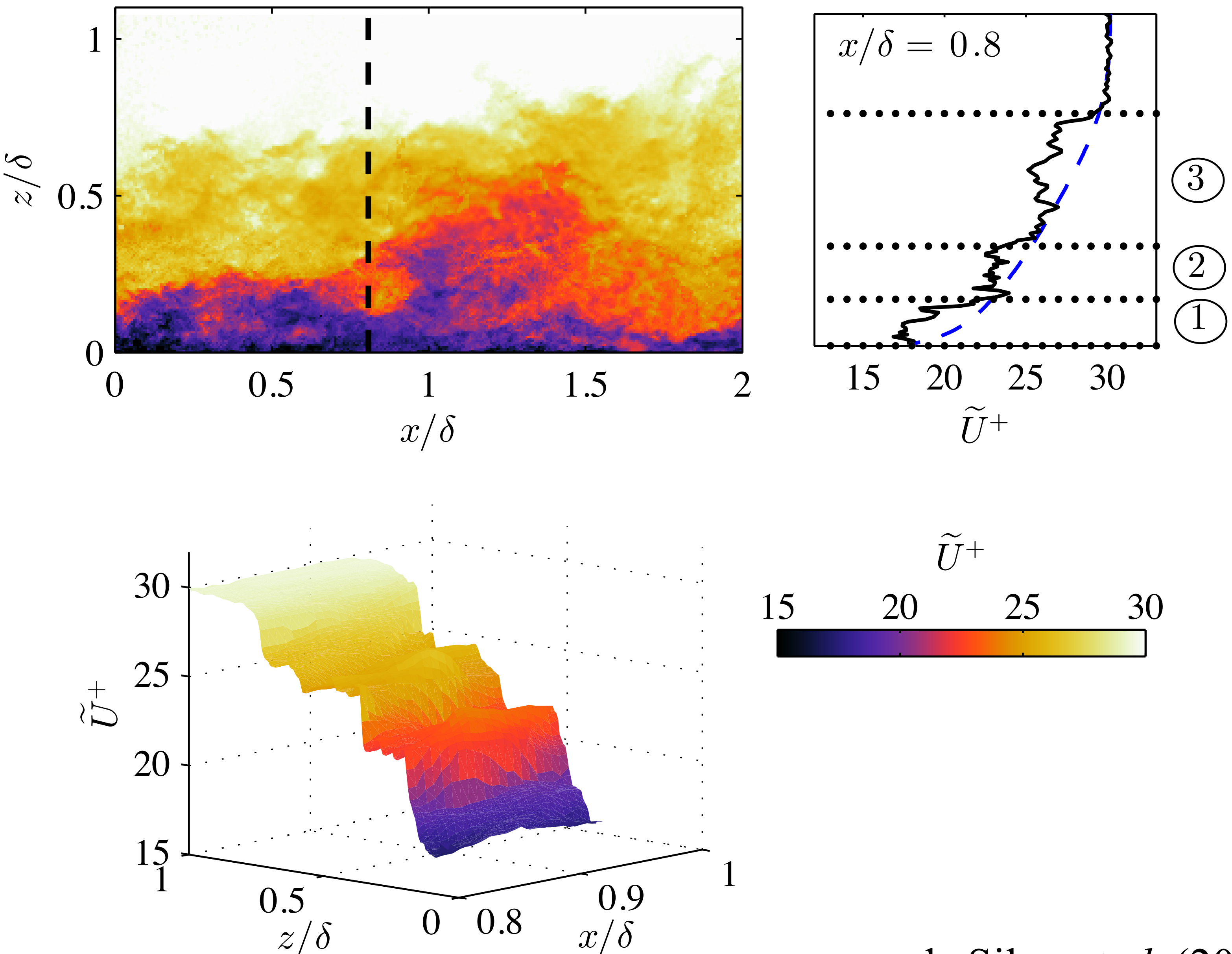

de Silva *et al.* (2016)

Adrian, Meinhart and Tomkins (2000)

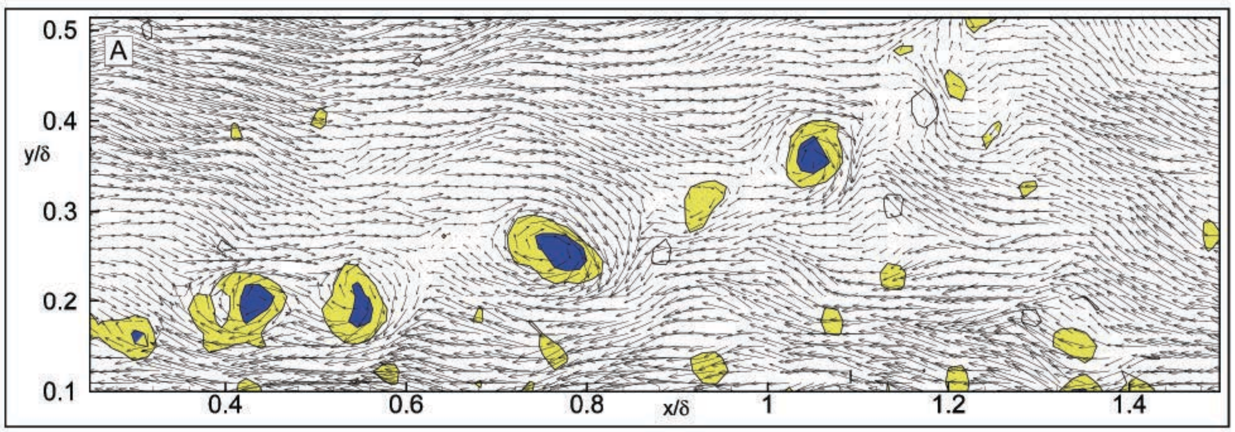

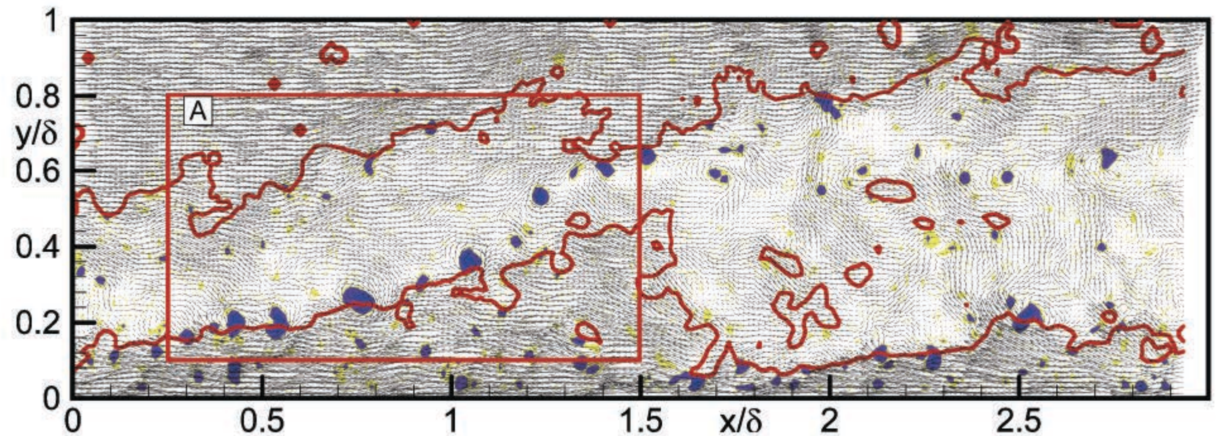

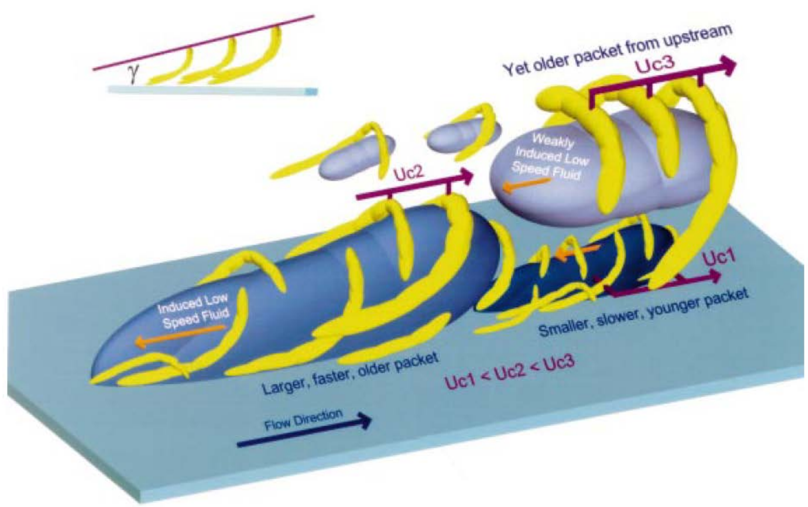

Zhou et al (1999)
Christensen & Adrian (2001)
Tomkins & Adrian (2003)

Blue: $-v$, low speed | Red: $+v$, high speed

Black: $-u$, low speed | Grey: $+u$, high speed

Focus on v in wall-normal $(x-z)$ plane and examine u in spanwise $(x-y)$ plane simultaneously

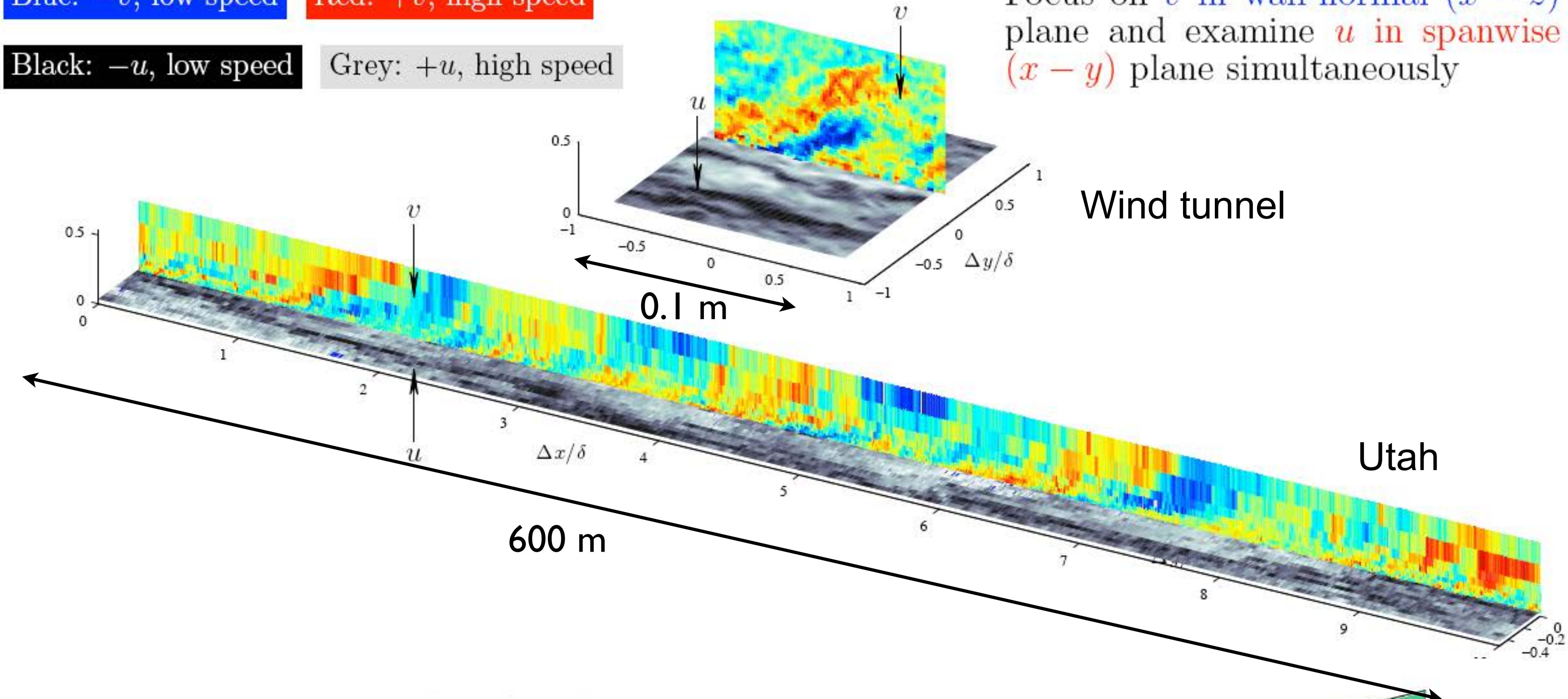

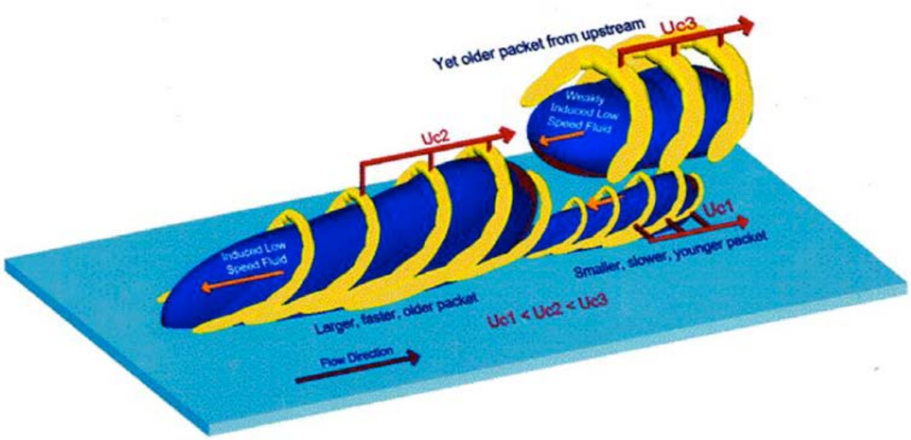

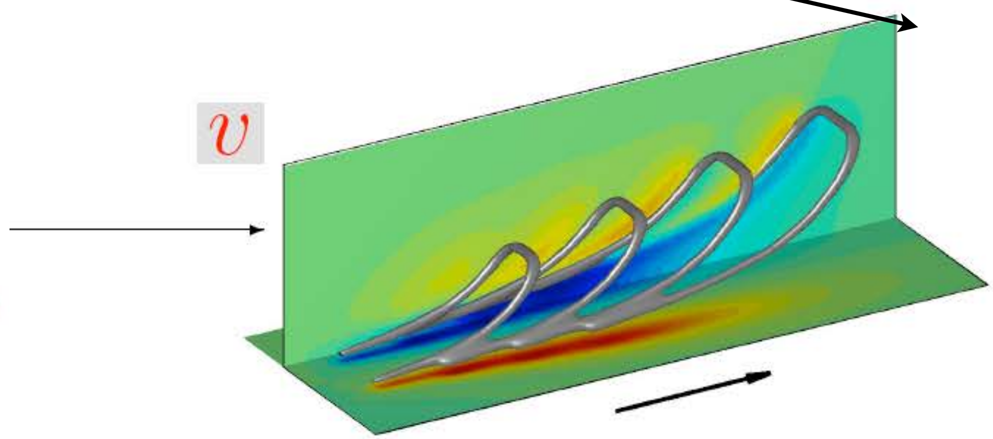

Spanwise velocity

2. Statistically self-similar attached eddies?

Evidence for self-similarity

Uniform Momentum Zones

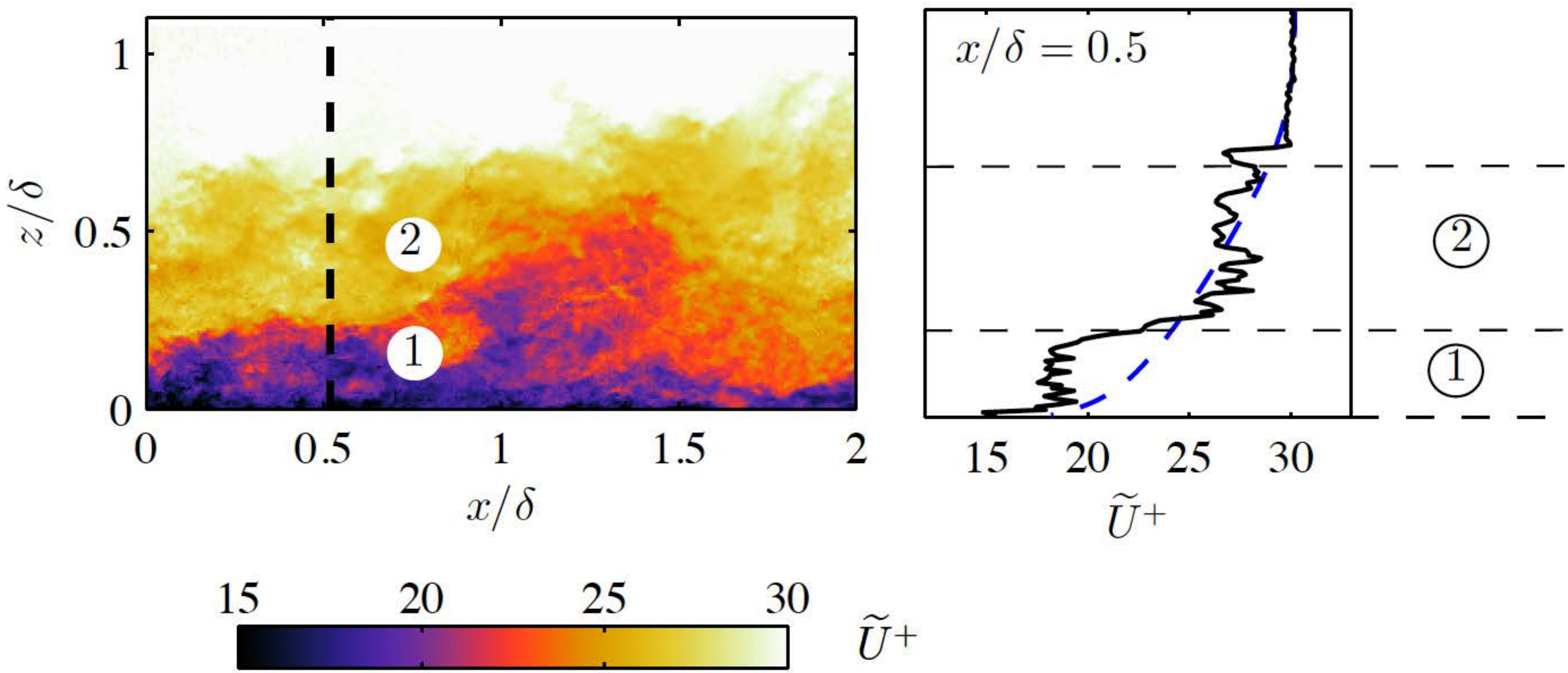

de Silva, Hutchins & Marusic (2016) *J. Fluid Mech.*
Eisma, Westerweel, Ooms, Elsinga (2015) *Phys. Fluids*

Extracting Uniform Momentum Zones (UMZs)

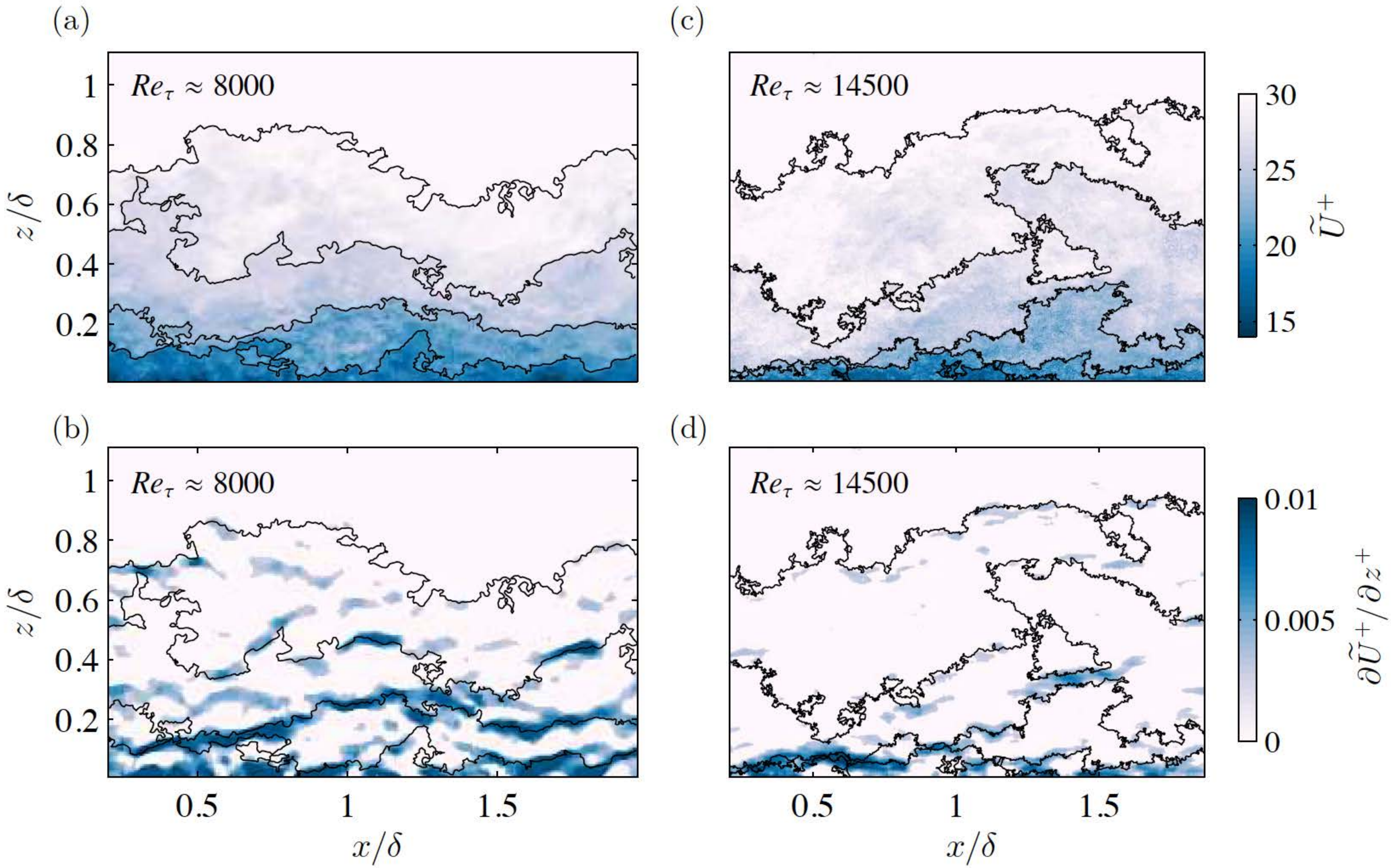

UMZ - Characterisation

- How many UMZ are present on average?

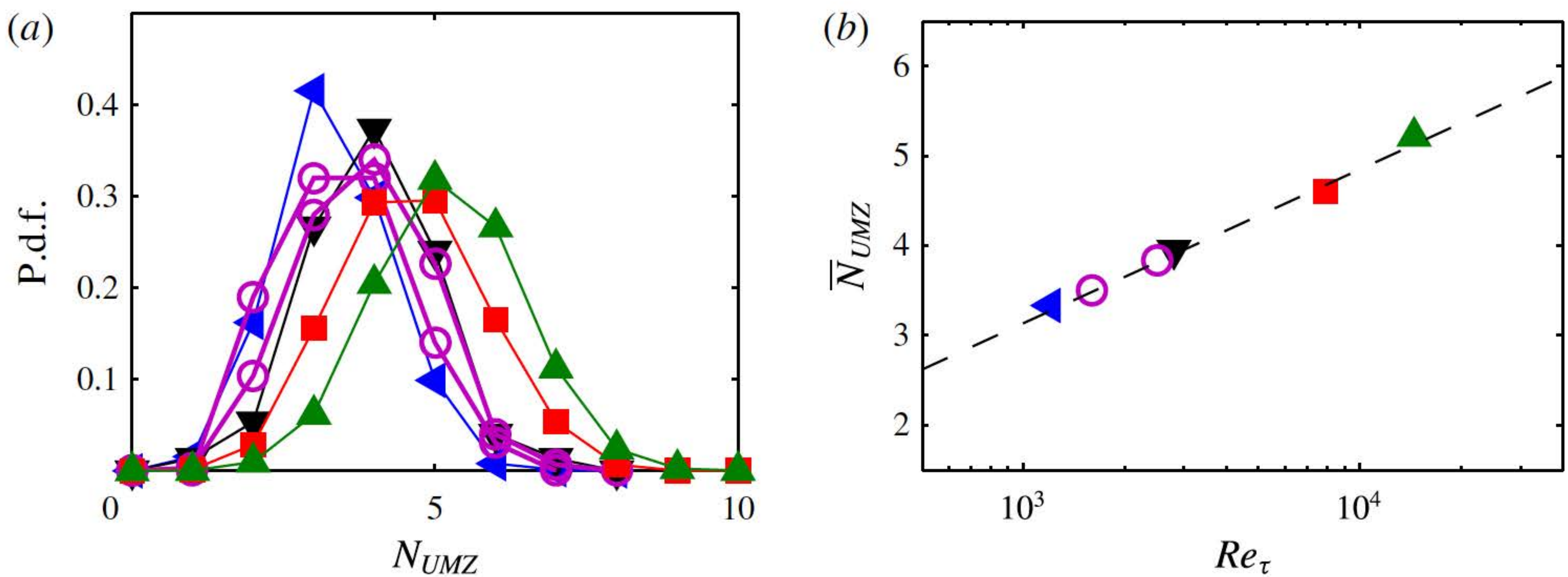

$Re_\tau \approx 1000$ (Hambleton *et al.* 2006)

$Re_\tau \approx 2800$ (Adrian *et al.* 2000)

$Re_\tau \approx 8000$

$Re_\tau \approx 14500$

DNS (Sillero et al. 2013)

UMZ - Characterisation

- How many UMZ are present on average?

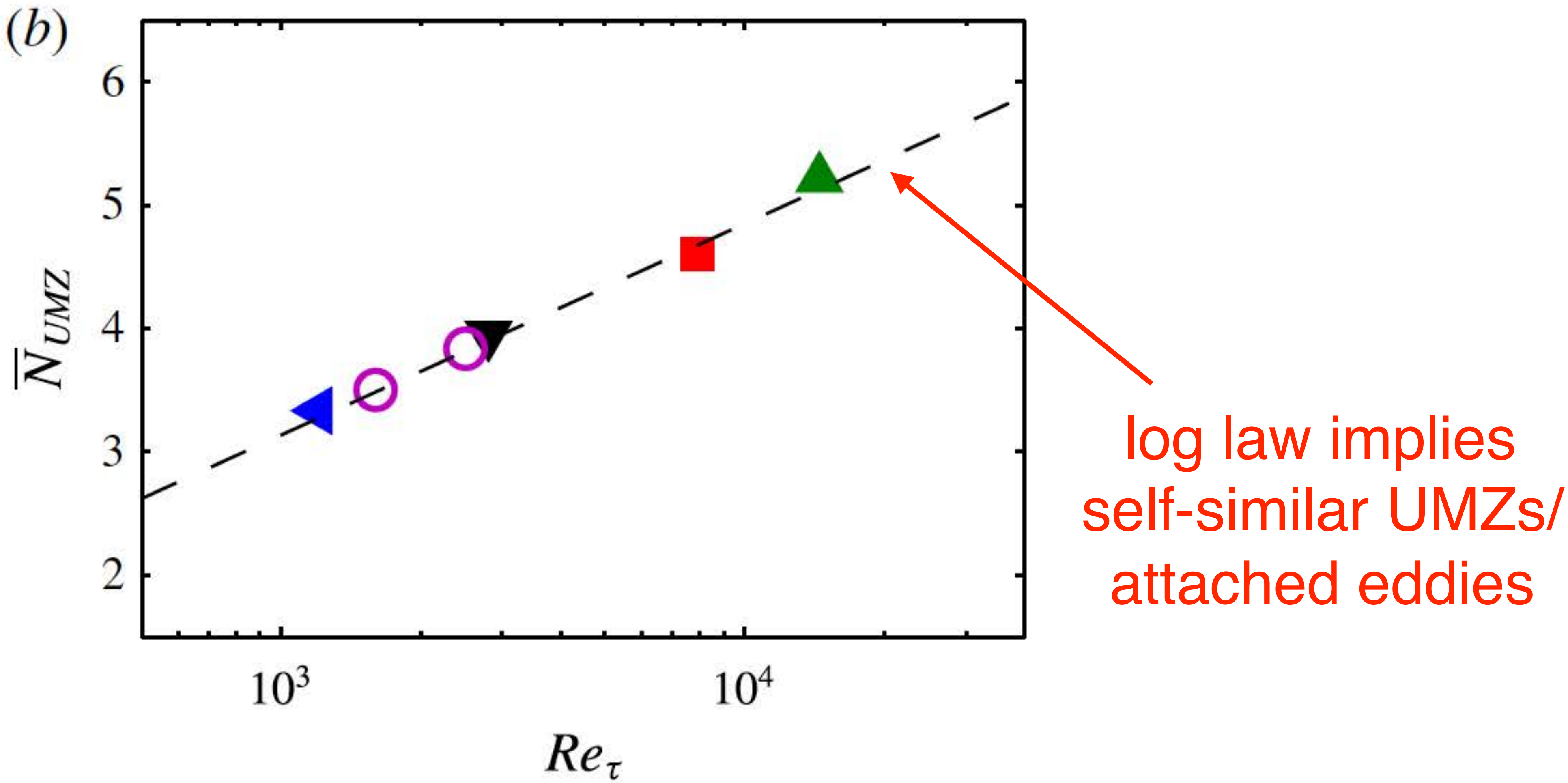

Packet as representative attached eddy

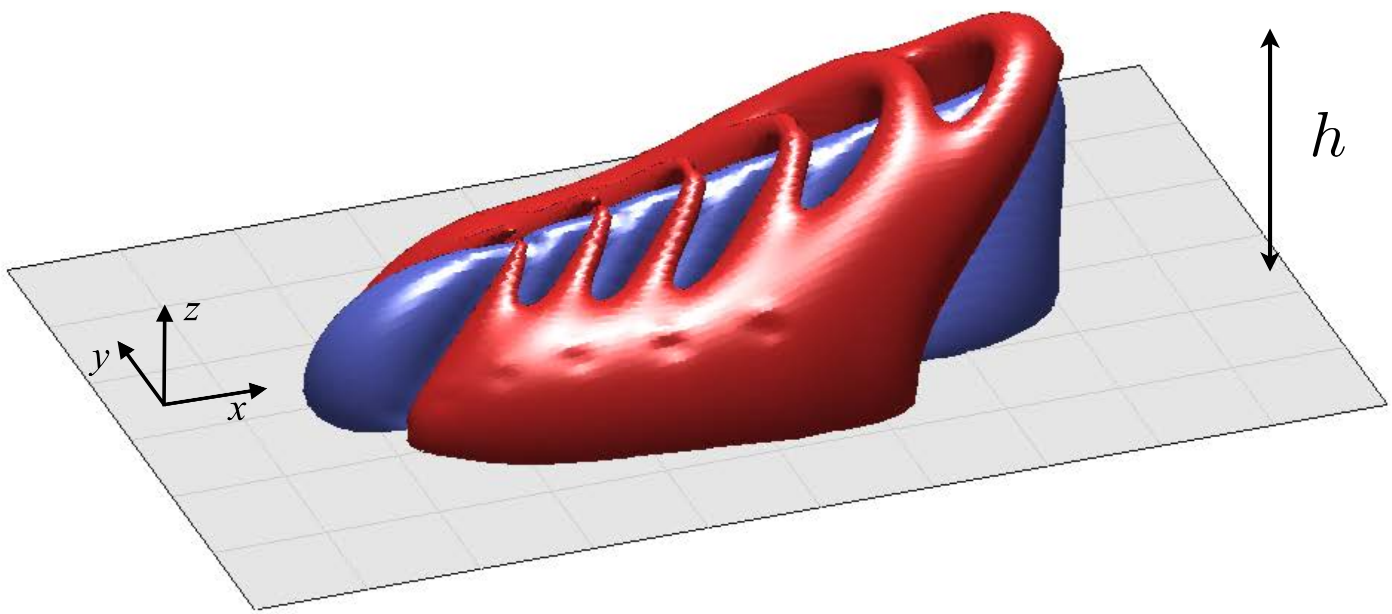

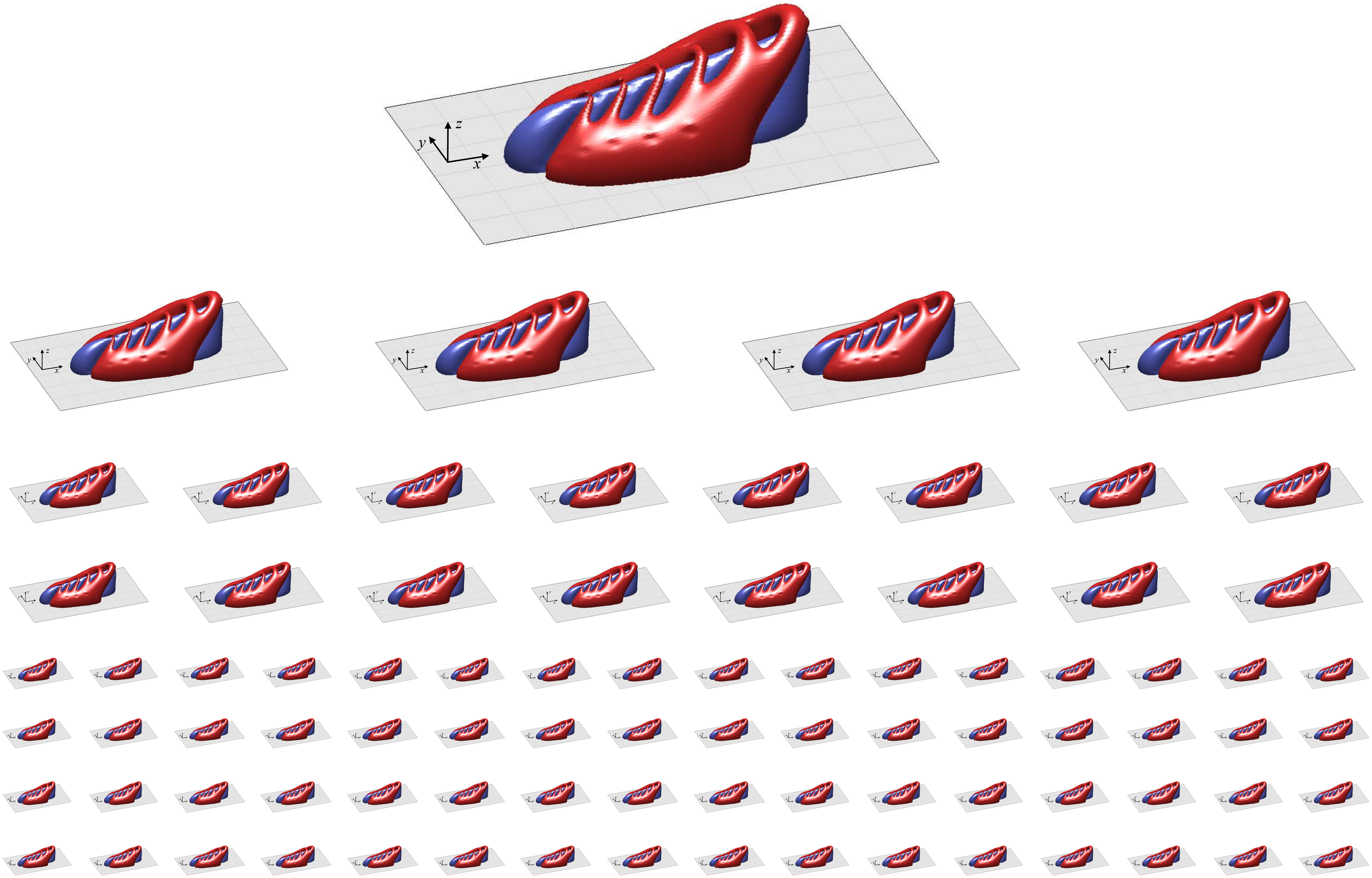

z
y
x

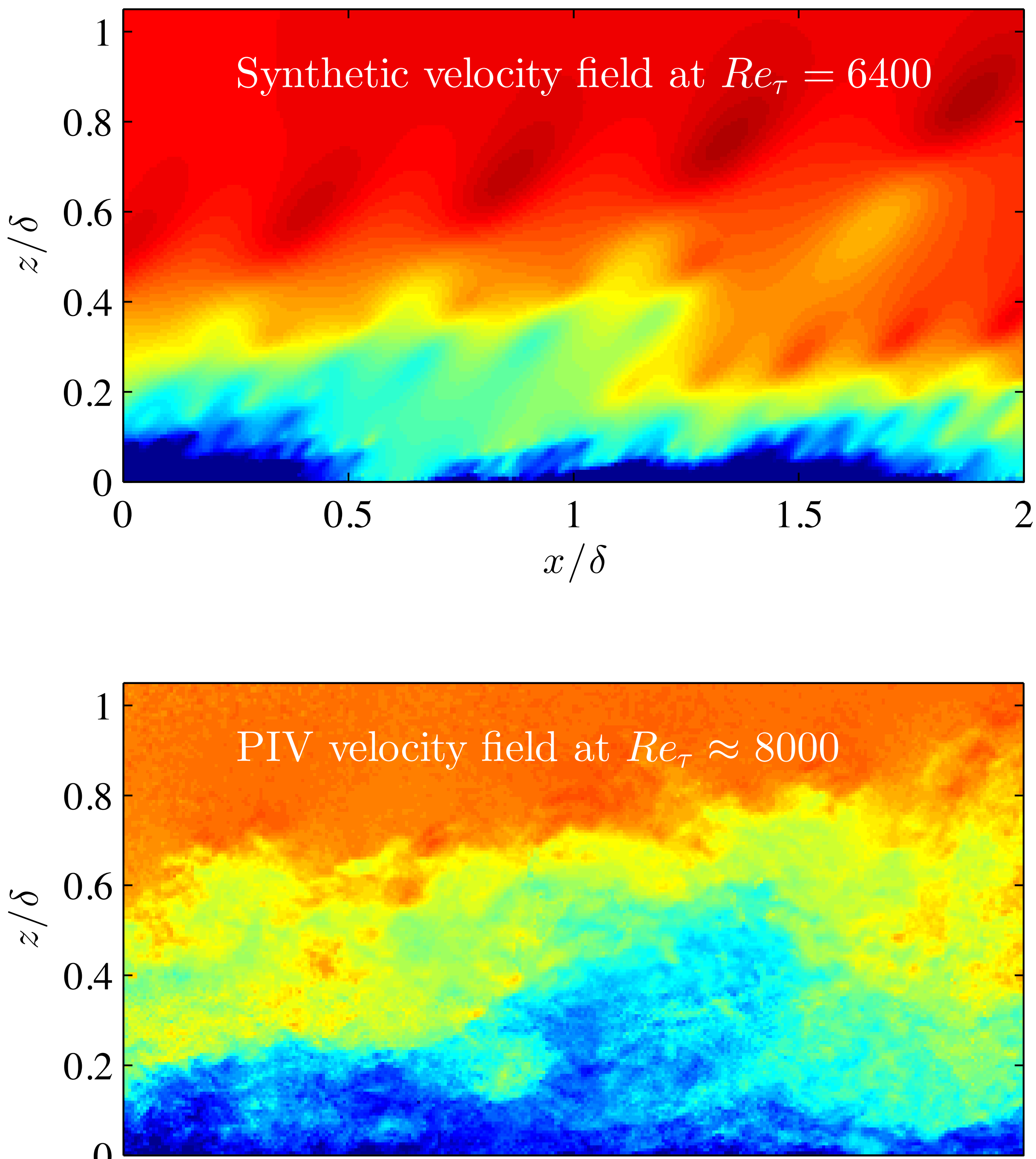

Synthetic velocity field at $Re_\tau = 6400$
PIV velocity field at $Re_\tau \approx 8000$
z/δ
x/δ
0
0.2
0.4
0.6
0.8
1
0.5
1.5
2

UMZ - Attached eddy model

$\mathcal{L}_x \approx \delta$

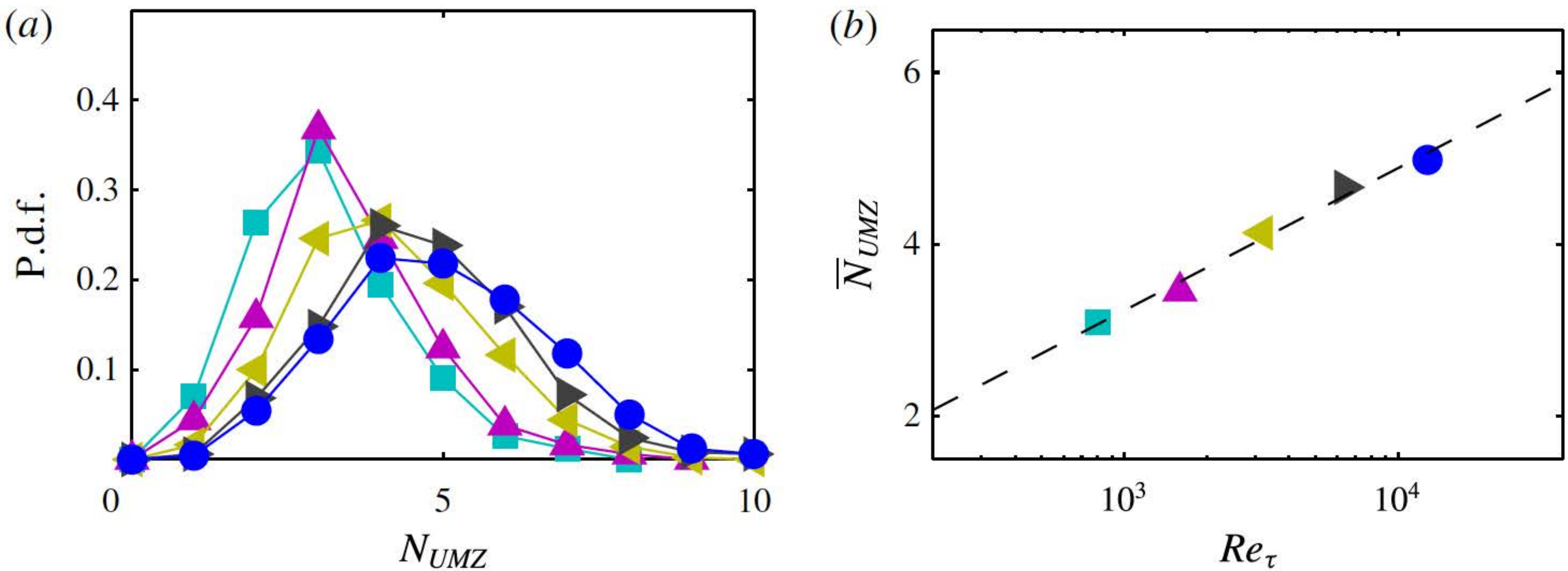

Symbol	Re_τ	Eddy hierarchies	$L_x \times L_z$	$\Delta x^+,\ \Delta z^+$	Frames
■	800	4	$2\delta \times 1.2\delta$	30×30	500
▲	1 600	5	$2\delta \times 1.2\delta$	30×30	500
◀	3 200	6	$2\delta \times 1.2\delta$	30×30	500
▶	6 400	7	$2\delta \times 1.2\delta$	30×30	500
●	12 800	8	$2\delta \times 1.2\delta$	30×30	500

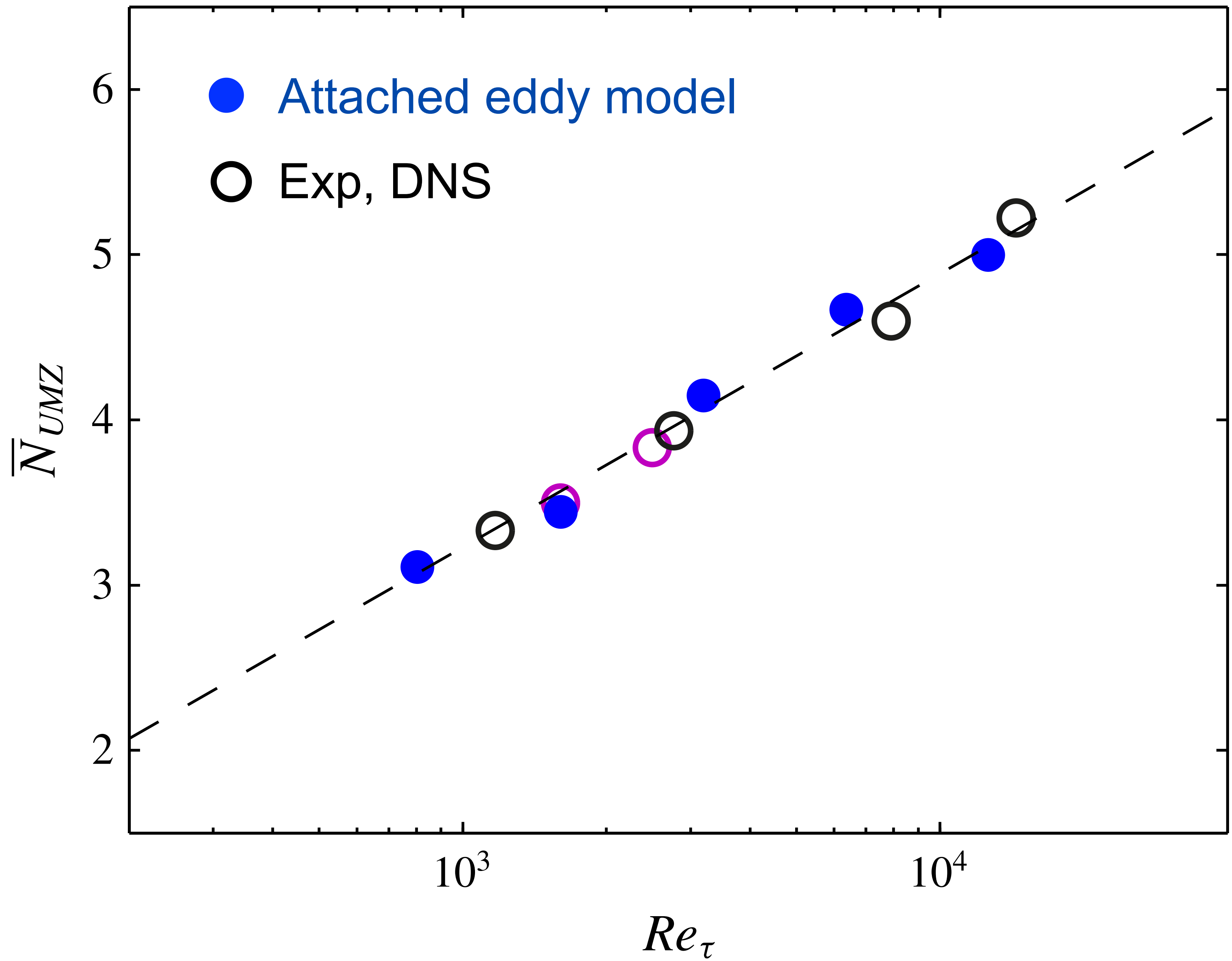

Attached eddy model
Exp, DNS
6
5
4
3
2
10^3
10^4
$\overline{N}_{UMZ}$
Re_τ

Evidence for self-similarity

POD modes in turbulent pipe flow: $\Phi^{(n)}(m;\, r)$

n=1 n=2 n=3

m=5

m=15

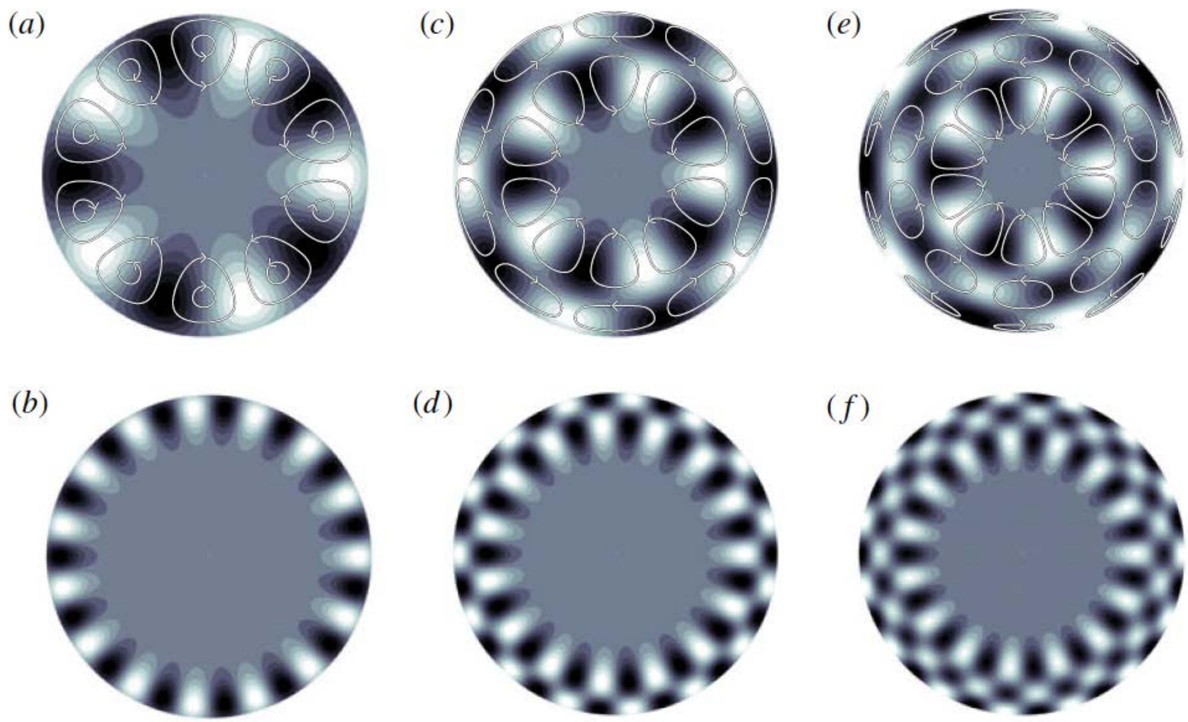

Hellstrom, Marusic, Smits (2016) *J. Fluid Mech., 709 Rapids*

Larger-scale (m=5)

Smaller-scale (m=40)

n=1

n=2

n=3

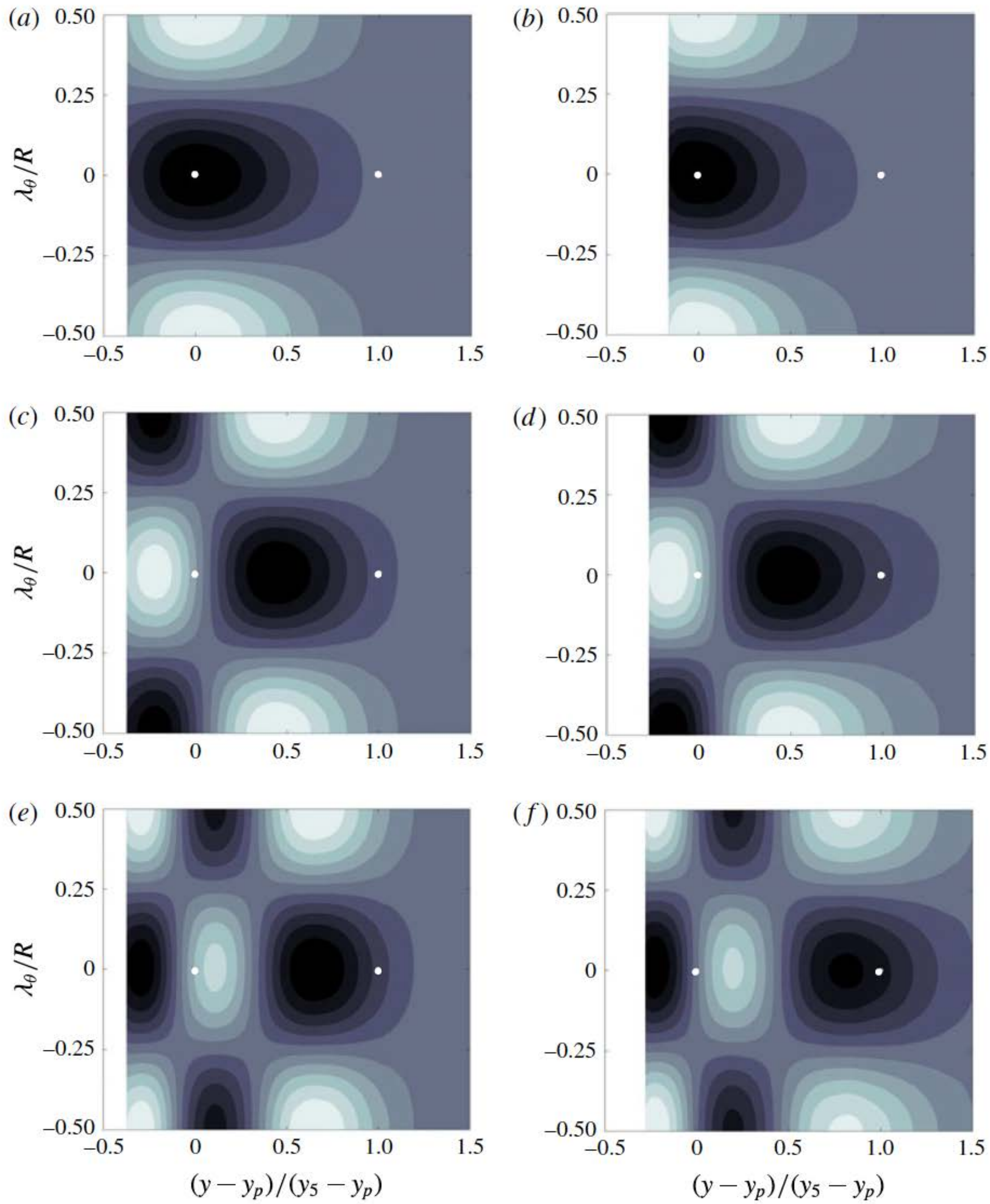

FIGURE 7. Scaled modes: (a) $(n, m) = (1, 5)$, (b) $(n, m) = (1, 40)$, (c) $(n, m) = (2, 5)$, (d) $(n, m) = (2, 20)$, (e) $(n, m) = (3, 5)$, (f) $(n, m) = (3, 15)$. White represents positive and black negative values; the white marks indicate the points used for scaling.

Self-similarity of modes

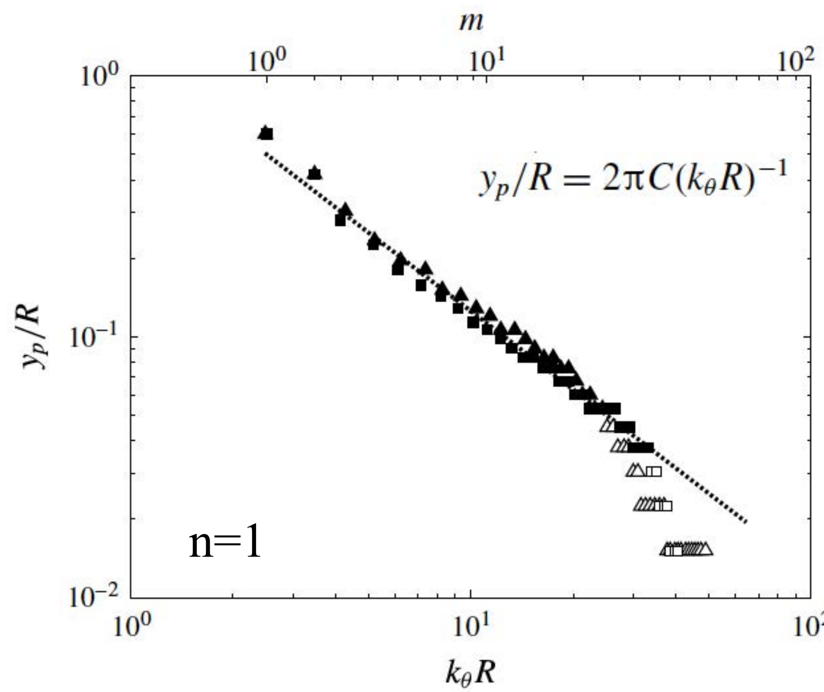

Evidence for self-similarity

- McKeon & Sharma (2010, 2013), Moarref *et al.* (2013)

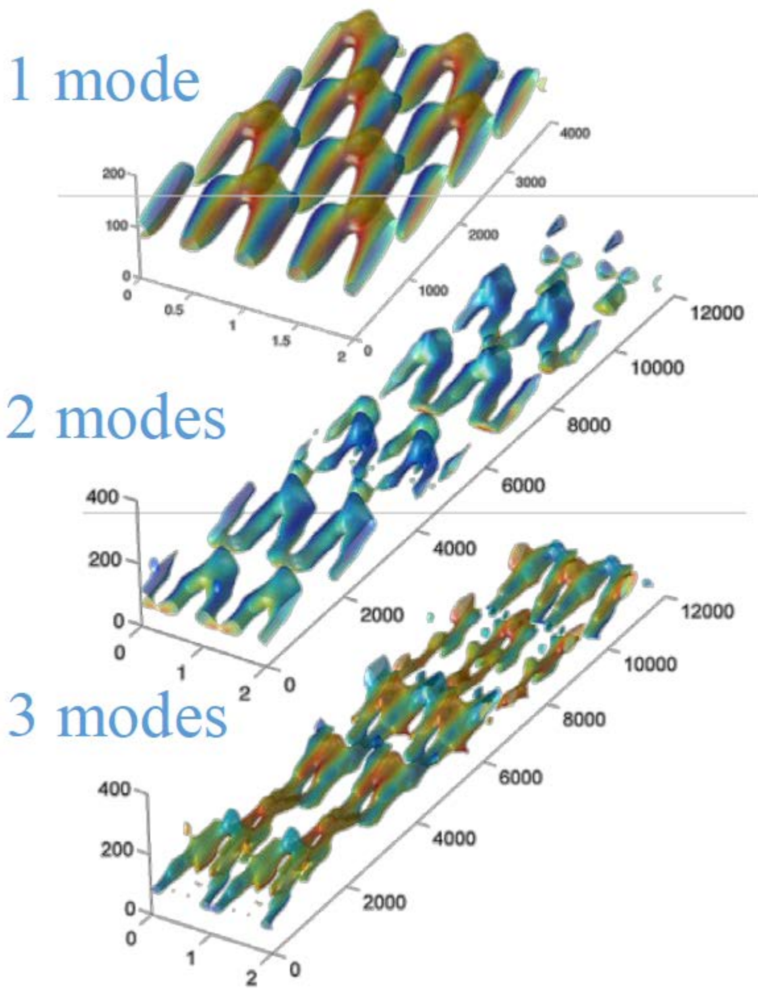

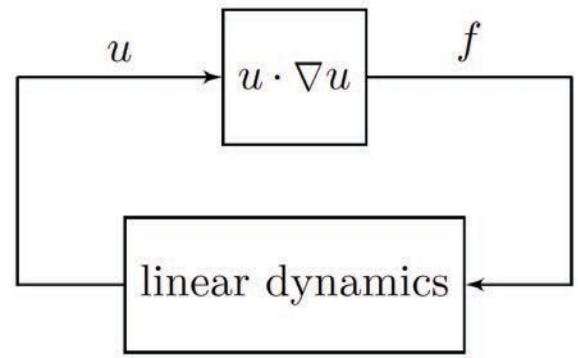

Self-similar resolvent modes

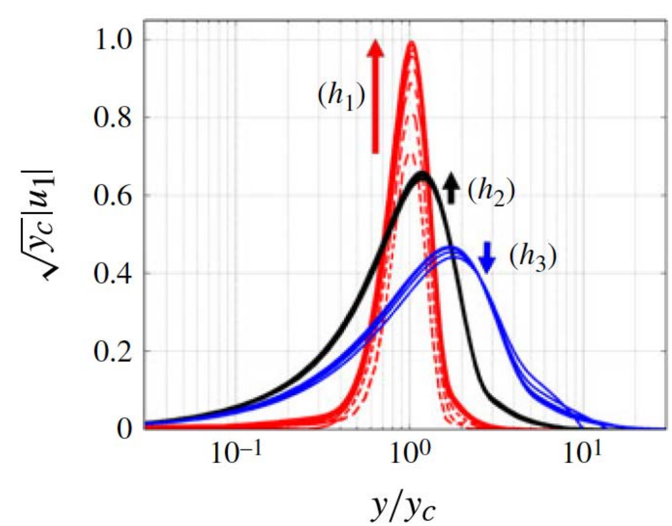

Evidence for self-similarity

- Flores & Jimenez (2010), Lozano-Duran, Flores & Jimenez (2012), Jimenez (2015)

Self-similar, attached
Q, sweep, & ejection structures

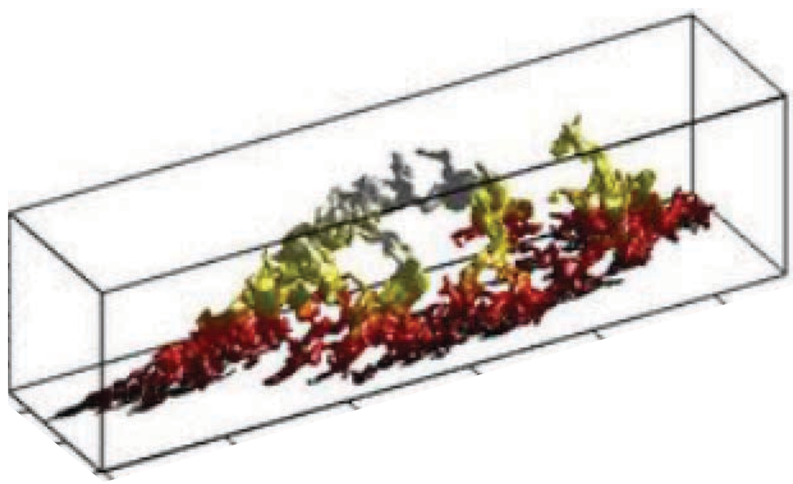

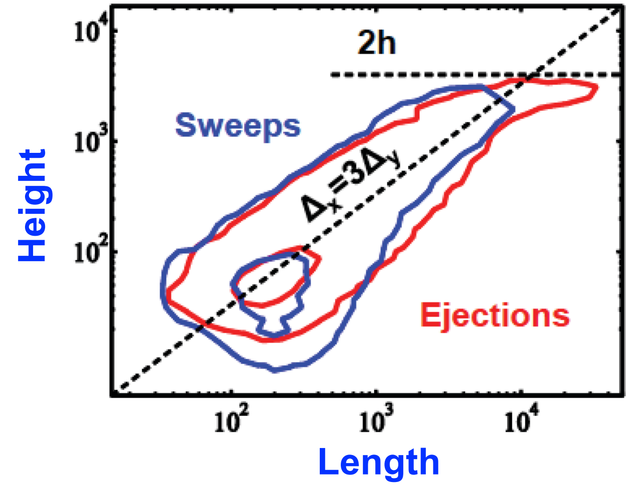

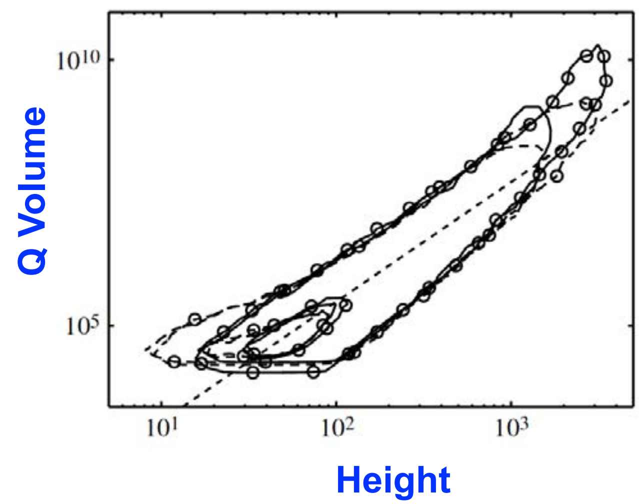

Evidence for self-similarity

- Hwang (2015), Hwang & Bengana (2016), Cossu & Hwang (2016)

Self-similar "minimal" coherent structures (attached eddies)

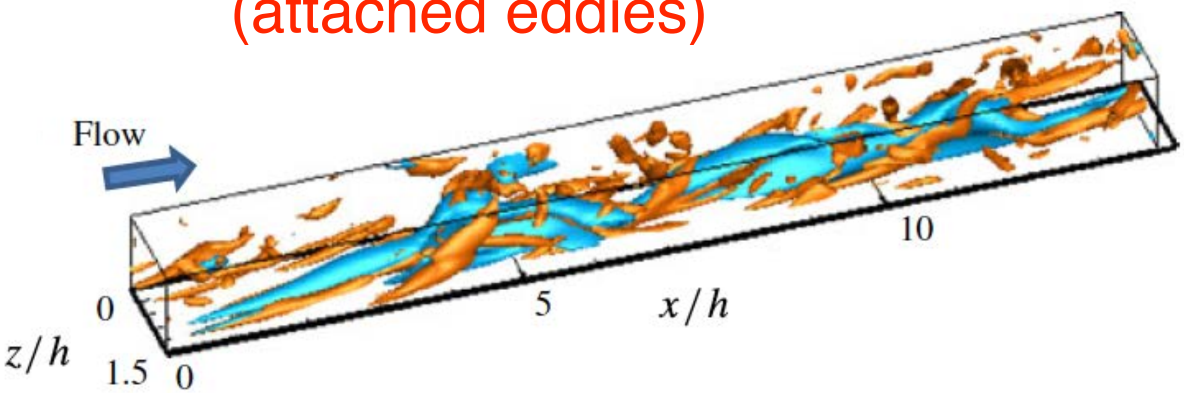

Self-sustaining and organised around invariant solutions of filtered-NSE (cf. Exact Coherent Structures)

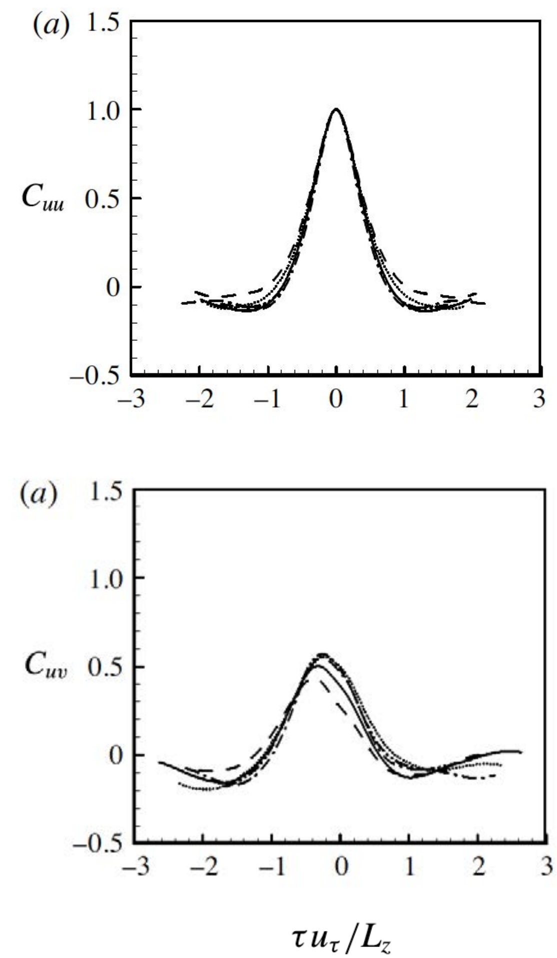

3. Spatial distribution and independence of attached eddies?

Clues looking at high-order moments

• Random and independent positioning in plane of the wall equates to a Poisson point process.

• Attached eddy hypothesis assumes a statistical independence among summands (representative eddies). Consequently, adopting the central limit theorem leads to Gaussian behaviour, for which

$$\left\langle (u^+)^{2p} \right\rangle \to (2p-1)!! \; \left\langle (u^+)^2 \right\rangle^p$$

where

$$n!! \equiv n(n-2)(n-4)\ldots.1$$

is the double factorial.

High-order moments

- Consequently, we expect

$$\langle (u^+)^{2p} \rangle^{\frac{1}{p}} = B_p - A_p \ln(z/\delta)$$

$$= D_p(Re_\tau) - A_p \ln z^+$$

where, for Gaussian behaviour

$$A_p = A_1[(2p-1)!!]^{1/p}$$

Meneveau & Marusic (2013) *J. Fluid Mech*, 719, R1

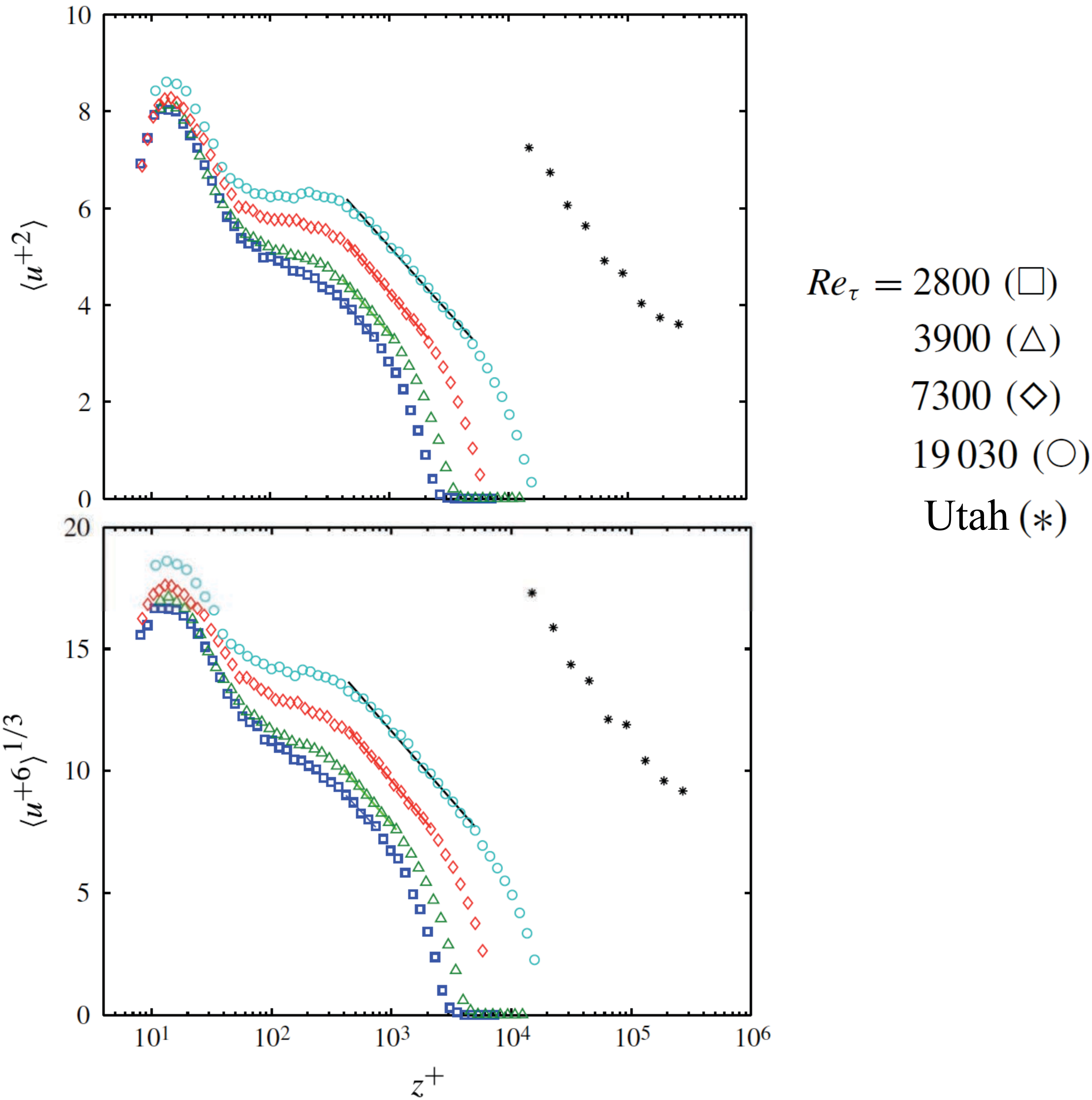

10
8
6
4
2
0
20
15
10
5
0
$\langle u^{+2} \rangle$
$\langle u^{+6} \rangle^{1/3}$
10^1
10^2
10^3
10^4
10^5
10^6
z^+
Re_τ = 2800 (□)
3900 (△)
7300 (◇)
19 030 (○)
Utah (∗)

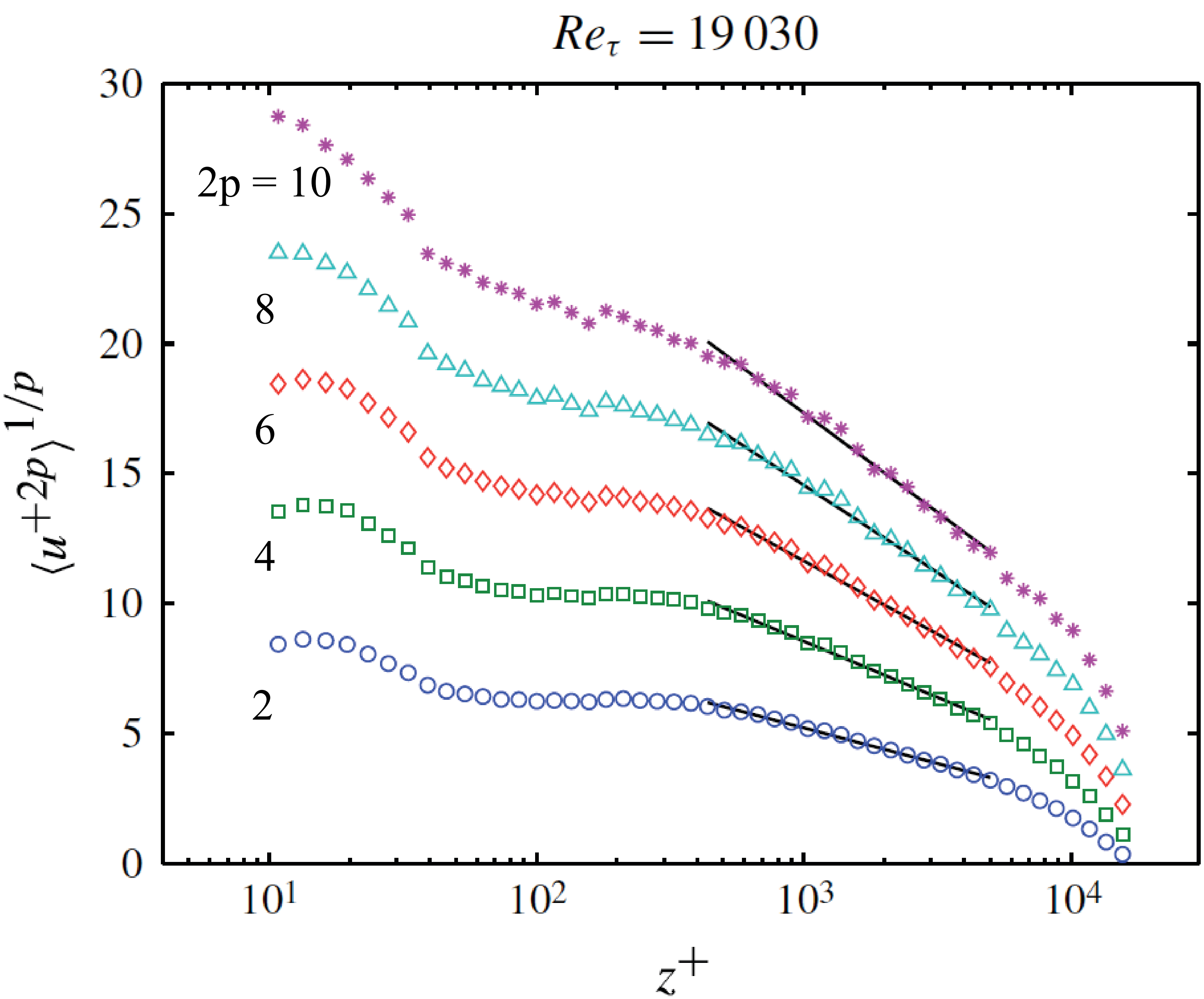

$Re_\tau = 19\,030$
30
25
20
15
10
5
0
2p = 10
8
6
4
2
$\langle u^{+2p} \rangle^{1/p}$
10^1
10^2
10^3
10^4
z^+

Streamwise velocity: $\langle (u^+)^{2p} \rangle^{1/p} = B_p - A_p \ln(z/\delta)$

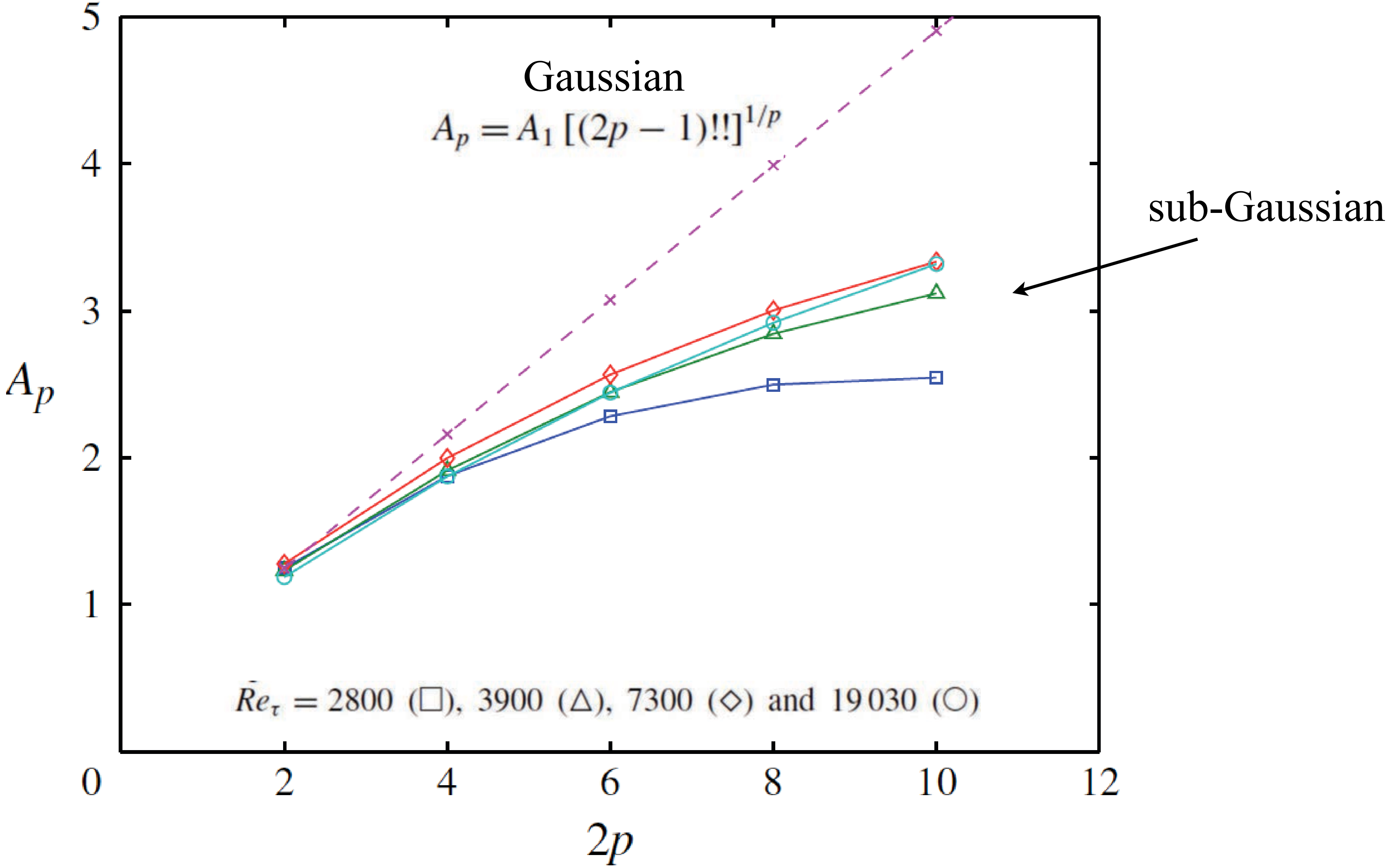

Spanwise velocity: $\langle (v^+)^{2p} \rangle^{1/p} = B_{p,v} - A_{p,v} \ln(z/\delta)$

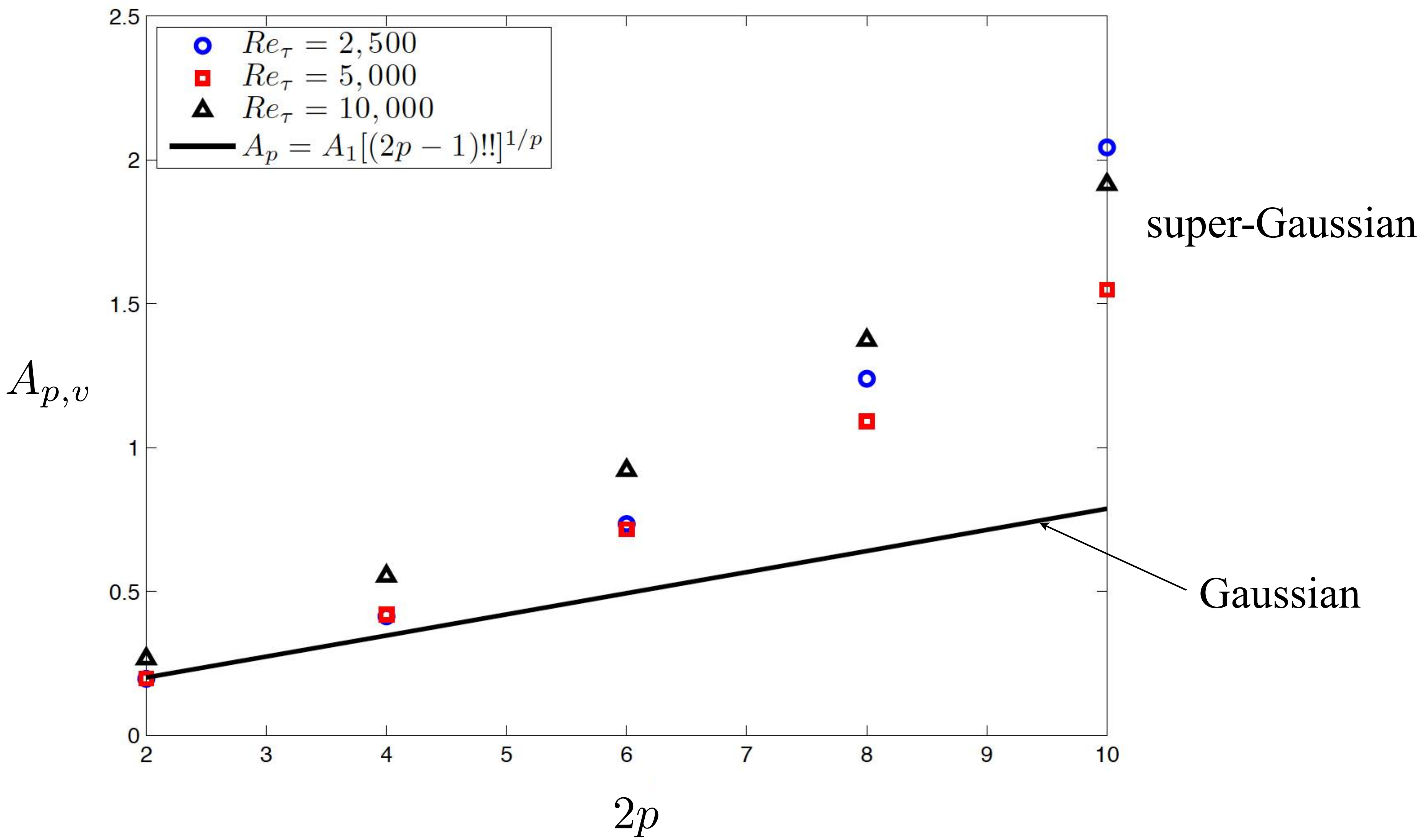

Revisit mathematical basis for attached eddy model

- beyond mean flow and 2nd order statistics

Woodcock & Marusic (2015) *Phys. Fluids*

Representative attached eddy

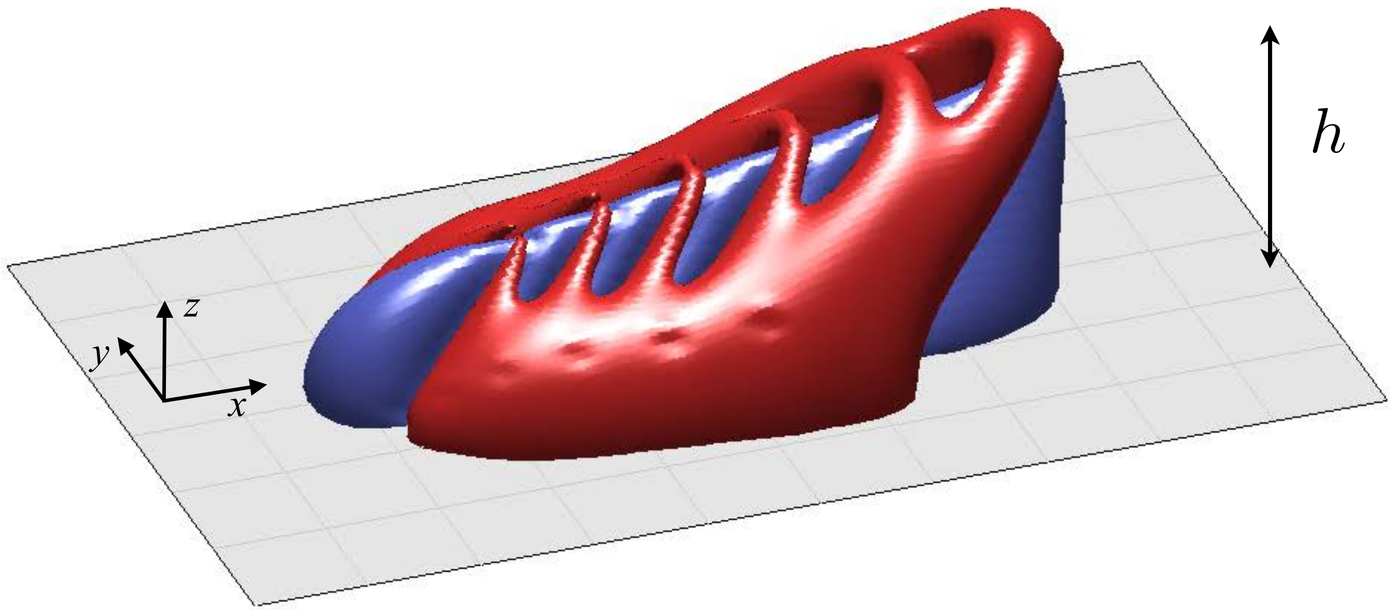

$$\mathbf{U}_{one\,eddy} = \mathbf{Q}\left(\frac{\mathbf{x} - \mathbf{x}_e}{h}\right)$$

$$\mathbf{U}(\mathbf{x}) = \sum_k \mathbf{Q}\left(\frac{\mathbf{x} - \mathbf{x}_{e_k}}{h_k}\right)$$

Campbell's theorem (1909)

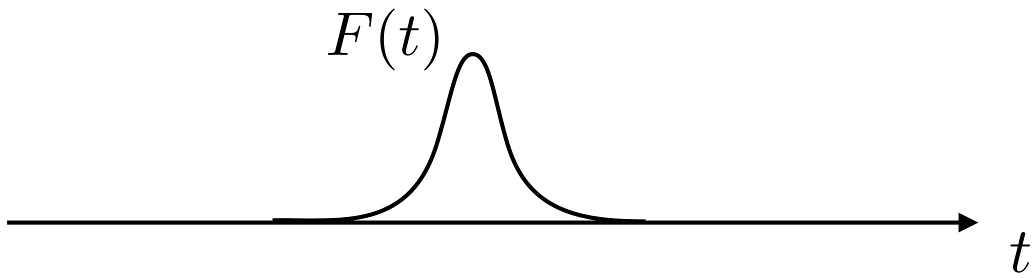

$$I(t) = \sum_k F(t - t_k)$$

Where t_k is random and β = average number of pulses per second

$$\text{mean: } \langle I \rangle = \beta \int F dt$$

$$\text{variance: } \langle \sigma_I^2 \rangle = \beta \int F^2 dt$$

Using Campbell's theorem for randomly positioned uncorrelated eddy velocity signatures and integrating over a range of scales weighted with inverse power-law p.d.f. gives for $z \ll h_{max}$:

$$\langle U \rangle = \frac{1}{\kappa} \log\left(z^+\right) + C, \qquad \langle u^2 \rangle = B_1 - A_1 \log\left(\frac{z}{h_{max}}\right)$$

$$\langle w^2 \rangle = A_3, \qquad \langle v^2 \rangle = B_2 - A_2 \log\left(\frac{z}{h_{max}}\right)$$

➡ Which returns the Townsend (1976) and Perry & Chong (1982) results

Implications for universality of von Karman's constant ?

Townsend (1976, see also Davidson 2000):

Proposed that increases in turbulence intensity in log region as per attached eddy hypothesis (cf. inactive motions) will lead to κ varying with Reynolds number

"the difference (in κ) is unlikely to be detectable in ordinary circumstances, although, in principal, it would become important at extremely large Reynolds numbers."

$$\frac{1}{\kappa} = \frac{1}{\kappa_\infty}\frac{\left(1-10^6 Re_\tau^{-3}\right)^2}{\left(1-10^4 Re_\tau^{-2}\right)^3}; \qquad \kappa_\infty = \frac{9k_x k_y}{8\iint_{-\infty}^{\infty} Q_x\left(\frac{x}{h},\frac{y}{h},0\right)\,\mathrm{d}\!\left(\frac{x}{h}\right)\mathrm{d}\!\left(\frac{y}{h}\right)}$$

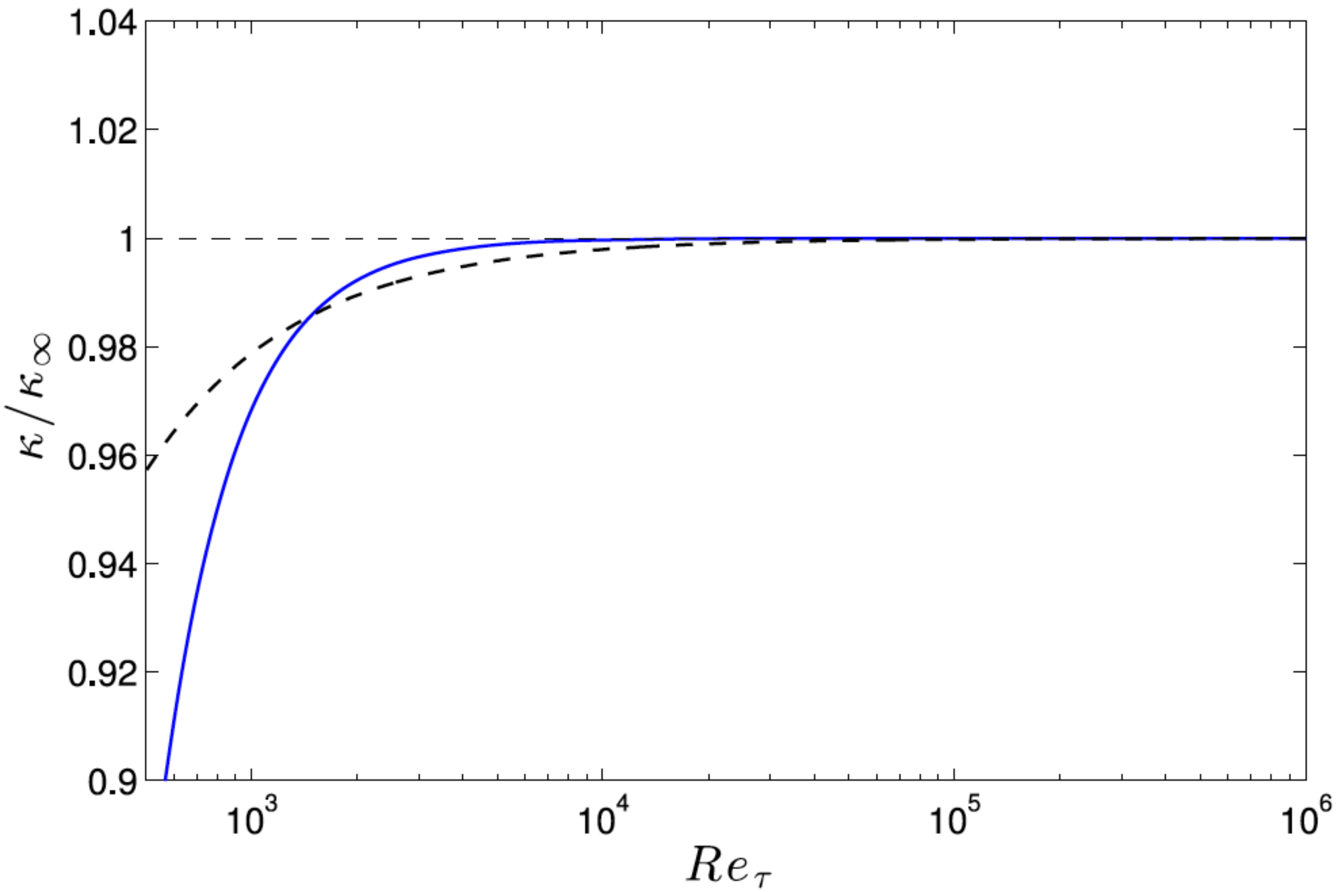

Extend to general order moments and cross-correlations

Define eddy contribution functions

$$I_{k,l,m}(Z) \stackrel{\text{def}}{=} \iint_{-\infty}^{\infty} Q_x^k(\mathbf{X})\, Q_y^l(\mathbf{X})\, Q_z^m(\mathbf{X})\, \mathrm{d}X\, \mathrm{d}Y$$

$$\mathbf{X} \equiv (X, Y, Z) \stackrel{\text{def}}{=} \frac{\mathbf{x}}{h}$$

and cumulants of the velocity

$$\lambda_{k,l,m}(z) \stackrel{\text{def}}{=} \beta \int_{h_{min}}^{h_{max}} I_{k,l,m}(Z) h^2 P(h)\, \mathrm{d}h$$

where

$\beta \equiv \dfrac{N}{L^2}$: average density (per area) of eddies at the wall

$P(h)$: probability that an eddy has size h

Define eddy contribution functions

$$I_{k,l,m}(Z) \stackrel{\text{def}}{=} \iint\limits_{-\infty}^{\infty} Q_x^k(\mathbf{X})\, Q_y^l(\mathbf{X})\, Q_z^m(\mathbf{X})\, \mathrm{d}X\, \mathrm{d}Y$$

$$\mathbf{X} \equiv (X, Y, Z) \stackrel{\text{def}}{=} \frac{\mathbf{x}}{h}$$

and cumulants of the velocity

$$\lambda_{k,l,m}(z) \stackrel{\text{def}}{=} \beta \int\limits_{h_{min}}^{h_{max}} I_{k,l,m}(Z) h^2 P(h)\, \mathrm{d}h$$

where

$$\beta \equiv \frac{N}{L^2} :$$ average density (per area) of eddies at the wall

$P(h)$: probability that an eddy has size h

$$P(h) \propto \frac{1}{h^3} = 2\left(h_{min}^{-2} - h_{max}^{-2}\right)^{-1} \frac{1}{h^3}$$

Using an extended form of Campbell's theorem for randomly positioned uncorrelated eddies (which can be formally proved) gives:

$$\lambda_{k,l,m} = i^{-(k+l+m)} \frac{\partial^k}{\partial \gamma_x^k} \frac{\partial^l}{\partial \gamma_y^l} \frac{\partial^m}{\partial \gamma_z^m} \log_e \left\langle e^{i\mathbf{U}\cdot\boldsymbol{\gamma}} \right\rangle \Big|_{\boldsymbol{\gamma}=\mathbf{0}}$$

$$\lambda_{k,l,m}(z) \stackrel{\text{def}}{=} \beta \int_{h_{min}}^{h_{max}} \left[\iint_{-\infty}^{\infty} Q_x^k(\mathbf{X})\, Q_y^l(\mathbf{X})\, Q_z^m(\mathbf{X})\, \mathrm{d}X\, \mathrm{d}Y \right] h^2 P(h)\, \mathrm{d}h$$

Using an extended form of Campbell's theorem for randomly positioned uncorrelated eddies (which can be formally proved) gives:

$$\langle U \rangle = \lambda_{1,0,0} \qquad \langle V \rangle = \lambda_{0,1,0} \qquad \langle W \rangle = \lambda_{0,0,1}$$

$$\langle u^2 \rangle = \lambda_{2,0,0} \qquad \langle v^2 \rangle = \lambda_{0,2,0} \qquad \langle w^2 \rangle = \lambda_{0,0,2}$$

$$\lambda_{k,l,m}(z) \stackrel{\text{def}}{=} \beta \int_{h_{min}}^{h_{max}} \left[\iint_{-\infty}^{\infty} Q_x^k\left(\mathbf{X}\right) Q_y^l\left(\mathbf{X}\right) Q_z^m\left(\mathbf{X}\right) \, \mathrm{d}X \, \mathrm{d}Y \right] h^2 P(h) \, \mathrm{d}h$$

Using an extended form of Campbell's theorem for randomly positioned uncorrelated eddies (which can be formally proved) gives:

$$\langle U \rangle = \lambda_{1,0,0} \qquad \langle V \rangle = \lambda_{0,1,0} \qquad \langle W \rangle = \lambda_{0,0,1}$$

$$\langle u^2 \rangle = \lambda_{2,0,0} \qquad \langle v^2 \rangle = \lambda_{0,2,0} \qquad \langle w^2 \rangle = \lambda_{0,0,2}$$

$$\lambda_{k,l,m}(z) \stackrel{\text{def}}{=} \beta \int_{h_{min}}^{h_{max}} \left[\iint_{-\infty}^{\infty} Q_x^k(\mathbf{X})\, Q_y^l(\mathbf{X})\, Q_z^m(\mathbf{X})\, \mathrm{d}X\, \mathrm{d}Y \right] h^2 P(h)\, \mathrm{d}h$$

$$\lambda_{k,l,m}(z) = A_{k,l,m} \log\left(\frac{z}{h_{max}}\right) + B_{k,l,m}, \qquad \text{for } z \ll h_{max}$$

$$A_{k,l,m} = \begin{cases} \text{constant}, & \text{if } m = 0 \\ 0, & \text{if } m \neq 0 \end{cases}$$

Using an extended form of Campbell's theorem for randomly positioned uncorrelated eddies (which can be formally proved) gives:

$$\langle U \rangle = \lambda_{1,0,0} \qquad \langle V \rangle = \lambda_{0,1,0} \qquad \langle W \rangle = \lambda_{0,0,1}$$

$$\langle u^2 \rangle = \lambda_{2,0,0} \qquad \langle v^2 \rangle = \lambda_{0,2,0} \qquad \langle w^2 \rangle = \lambda_{0,0,2}$$

$$\lambda_{k,l,m}(z) \stackrel{\text{def}}{=} \beta \int_{h_{min}}^{h_{max}} \left[\iint_{-\infty}^{\infty} Q_x^k(\mathbf{X})\, Q_y^l(\mathbf{X})\, Q_z^m(\mathbf{X})\, \mathrm{d}X\, \mathrm{d}Y \right] h^2 P(h)\, \mathrm{d}h$$

$$\lambda_{k,l,m}(z) = A_{k,l,m} \log\left(\frac{z}{h_{max}}\right) + B_{k,l,m}, \qquad \text{for } z \ll h_{max}$$

➡ Which returns the Townsend (1976) and Perry & Chong (1982) results

In addition to expressions for general cross-correlations:

$$\begin{aligned}
\langle uv \rangle &= \lambda_{1,1,0}, \\
\langle u^2 v \rangle &= \lambda_{2,1,0}, \\
\langle uvw \rangle &= \lambda_{1,1,1}, \\
\langle u^2 v^2 \rangle &= \lambda_{2,2,0} + \lambda_{2,0,0}\lambda_{0,2,0} + 2\lambda_{1,1,0}^2, \\
\langle u^3 v \rangle &= \lambda_{3,1,0} + 3\lambda_{1,1,0}\lambda_{2,0,0}, \\
\langle u^2 vw \rangle &= \lambda_{2,1,1} + \lambda_{0,1,1}\lambda_{2,0,0} + 2\lambda_{1,0,1}\lambda_{1,1,0}
\end{aligned}$$

and any order u-moments (using short-hand $\lambda_n \equiv \lambda_{n,0,0}$):

$$
\begin{aligned}
\langle U\rangle &= \lambda_1, \\
\langle u^2\rangle &= \lambda_2, \\
\langle u^3\rangle &= \lambda_3, \\
\langle u^4\rangle &= \lambda_4 + 3\lambda_2^2, \\
\langle u^5\rangle &= \lambda_5 + 10\lambda_2\lambda_3, \\
\langle u^6\rangle &= \lambda_6 + 15\lambda_2\lambda_4 + 10\lambda_3^2 + 15\lambda_2^3, \\
\langle u^7\rangle &= \lambda_7 + 21\lambda_2\lambda_5 + 35\lambda_3\lambda_4 + 105\lambda_2^2\lambda_3, \\
\langle u^8\rangle &= \lambda_8 + 28\lambda_2\lambda_6 + 56\lambda_3\lambda_5 + 35\lambda_4^2 + 210\lambda_2^2\lambda_4 + 280\lambda_2\lambda_3^2 + 105\lambda_2^4, \\
\langle u^9\rangle &= \lambda_9 + 36\lambda_2\lambda_7 + 84\lambda_3\lambda_6 + 126\lambda_4\lambda_5 + 378\lambda_2^2\lambda_5 + 1260\lambda_2\lambda_3\lambda_4 + 280\lambda_3^3 \\
&\quad + 1260\lambda_2^3\lambda_3, \\
\langle u^{10}\rangle &= \lambda_{10} + 45\lambda_2\lambda_8 + 120\lambda_3\lambda_7 + 210\lambda_4\lambda_6 + 630\lambda_2^2\lambda_6 + 126\lambda_5^2 + 2520\lambda_2\lambda_3\lambda_5 \\
&\quad + 1575\lambda_2\lambda_4^2 + 2100\lambda_3^2\lambda_4 + 3150\lambda_2^3\lambda_4 + 6300\lambda_2^2\lambda_3^2 + 945\lambda_2^5,
\end{aligned}
$$

and any order u-moments (using short-hand $\lambda_n \equiv \lambda_{n,0,0}$):

$$
\begin{aligned}
\langle U\rangle &= \lambda_1, \\
\langle u^2\rangle &= \lambda_2, \\
\langle u^3\rangle &= \lambda_3, \\
\langle u^4\rangle &= \lambda_4 + 3\lambda_2^2, \\
\langle u^5\rangle &= \lambda_5 + 10\lambda_2\lambda_3, \\
\langle u^6\rangle &= \lambda_6 + 15\lambda_2\lambda_4 + 10\lambda_3^2 + 15\lambda_2^3, \\
\langle u^7\rangle &= \lambda_7 + 21\lambda_2\lambda_5 + 35\lambda_3\lambda_4 + 105\lambda_2^2\lambda_3, \\
\langle u^8\rangle &= \lambda_8 + 28\lambda_2\lambda_6 + 56\lambda_3\lambda_5 + 35\lambda_4^2 + 210\lambda_2^2\lambda_4 + 280\lambda_2\lambda_3^2 + 105\lambda_2^4, \\
\langle u^9\rangle &= \lambda_9 + 36\lambda_2\lambda_7 + 84\lambda_3\lambda_6 + 126\lambda_4\lambda_5 + 378\lambda_2^2\lambda_5 + 1260\lambda_2\lambda_3\lambda_4 + 280\lambda_3^3 \\
&\quad + 1260\lambda_2^3\lambda_3, \\
\langle u^{10}\rangle &= \lambda_{10} + 45\lambda_2\lambda_8 + 120\lambda_3\lambda_7 + 210\lambda_4\lambda_6 + 630\lambda_2^2\lambda_6 + 126\lambda_5^2 + 2520\lambda_2\lambda_3\lambda_5 \\
&\quad + 1575\lambda_2\lambda_4^2 + 2100\lambda_3^2\lambda_4 + 3150\lambda_2^3\lambda_4 + 6300\lambda_2^2\lambda_3^2 + 945\lambda_2^5,
\end{aligned}
$$

$$\langle u^{2p}\rangle = \lambda_{2p} + ... + (2p-1)!!\lambda_2^p; \qquad p = 2, 3, 4...$$

Comparison to Gaussian behaviour

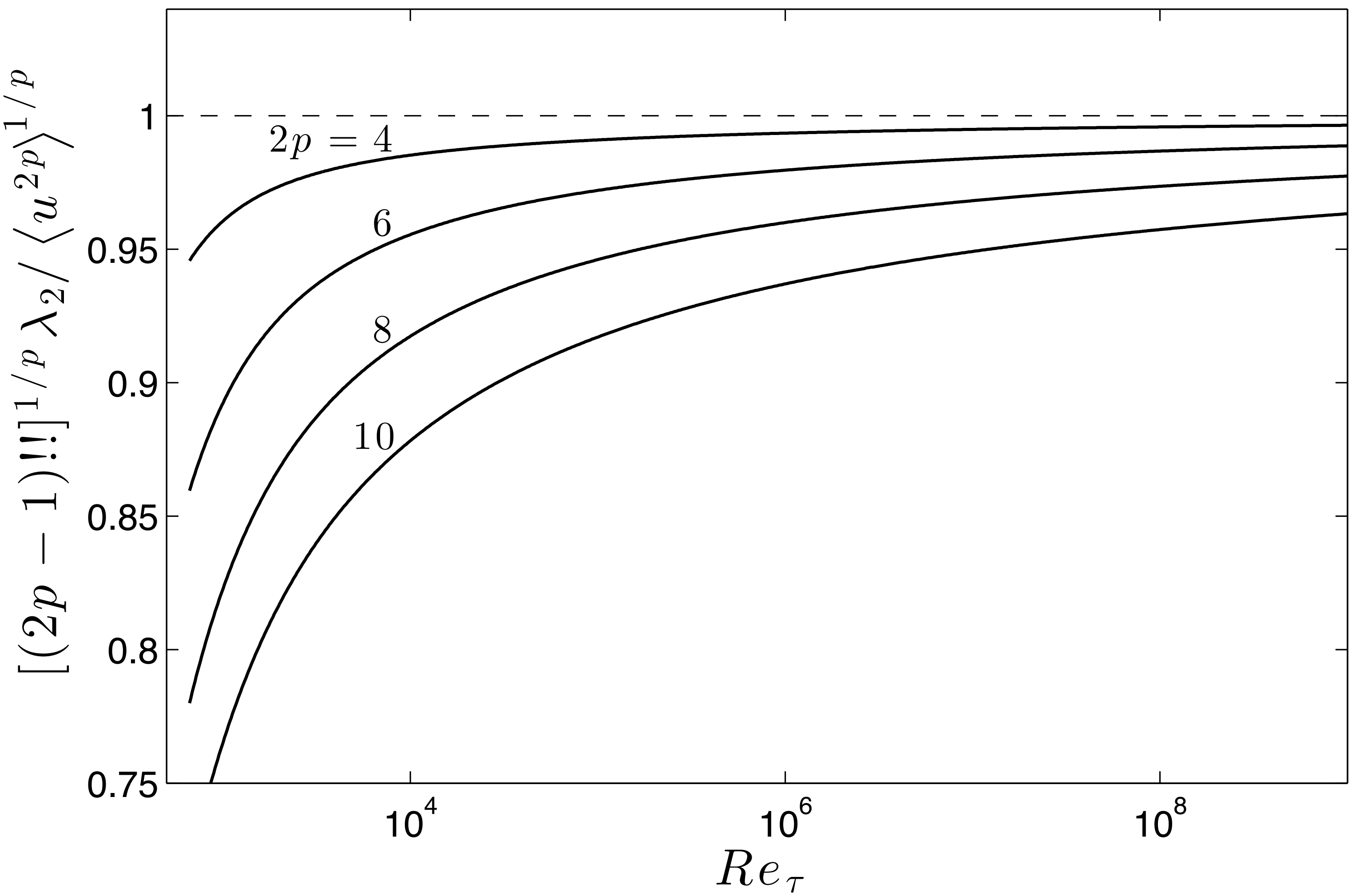

$$\langle u^{2p}\rangle = \lambda_{2p} + ... + (2p-1)!!\lambda_2^p$$

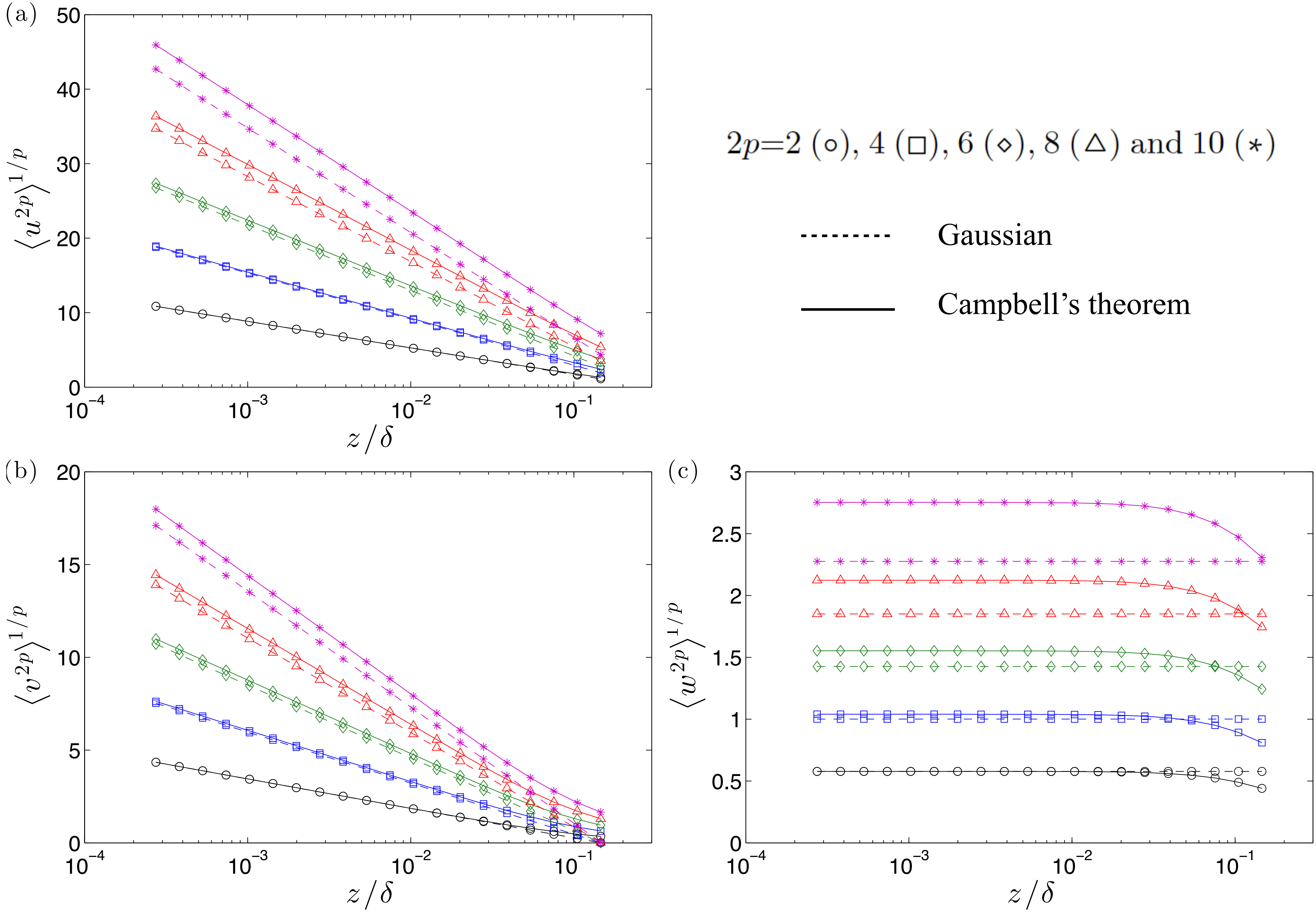

(a)
$\langle u^{2p} \rangle^{1/p}$
z/δ
$2p$=2 (∘), 4 (□), 6 (⋄), 8 (△) and 10 (∗)
Gaussian
Campbell's theorem
(b)
$\langle v^{2p} \rangle^{1/p}$
z/δ
(c)
$\langle w^{2p} \rangle^{1/p}$
z/δ

Skewness

$$S_u = \frac{\langle u^3 \rangle}{\langle u^2 \rangle^{3/2}}, \qquad S_v = \frac{\langle v^3 \rangle}{\langle v^2 \rangle^{3/2}}, \qquad S_w = \frac{\langle w^3 \rangle}{\langle w^2 \rangle^{3/2}}$$

$$S_u = \frac{\lambda_3}{\lambda_2^{3/2}} \to 0, \quad \text{for } Re_\tau \to \infty$$

$$S_w = \frac{\lambda_{0,0,3}}{\lambda_{0,0,2}^{3/2}} = \frac{B_{0,0,3}}{B_{0,0,2}^{3/2}} \to \text{constant}, \quad \text{for } Re_\tau \to \infty$$

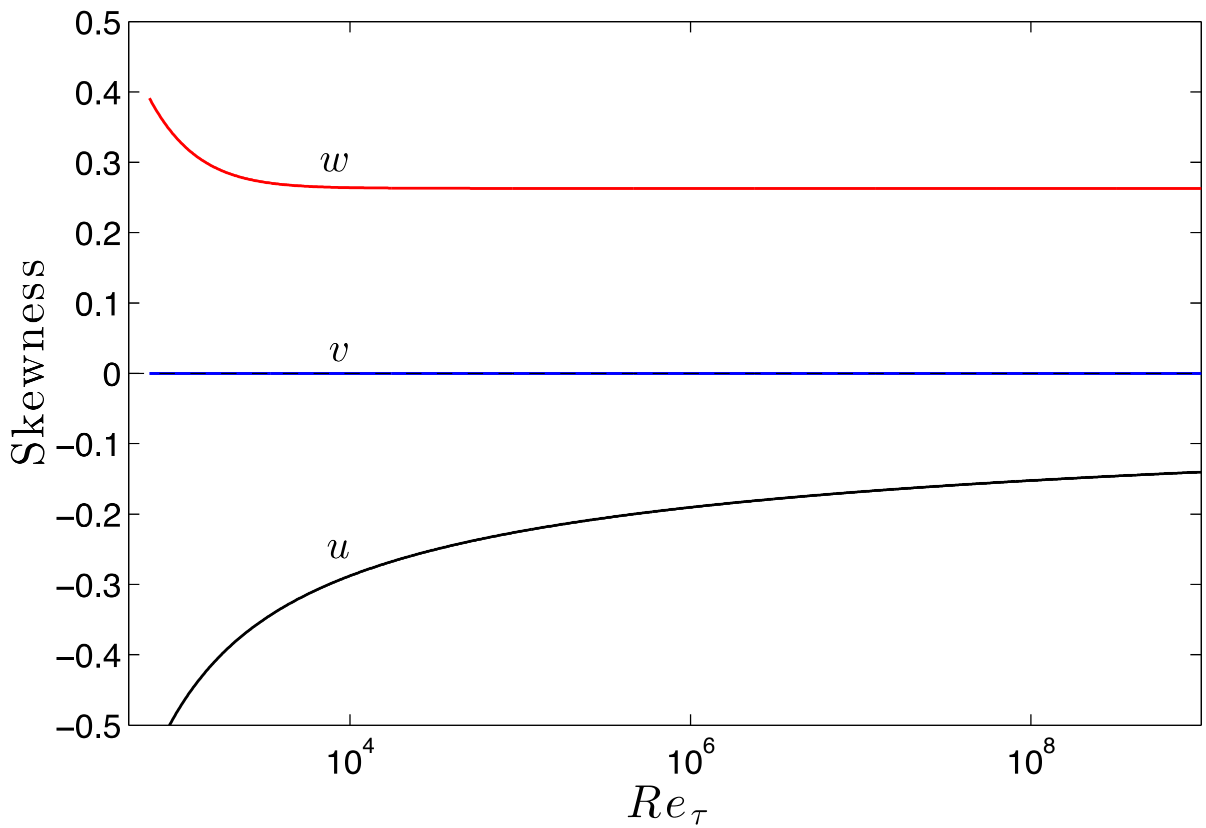

Flatness

$$F_u = \frac{\langle u^4 \rangle}{\langle u^2 \rangle^2}, \qquad F_v = \frac{\langle v^4 \rangle}{\langle v^2 \rangle^2}, \qquad F_w = \frac{\langle w^4 \rangle}{\langle w^2 \rangle^2}$$

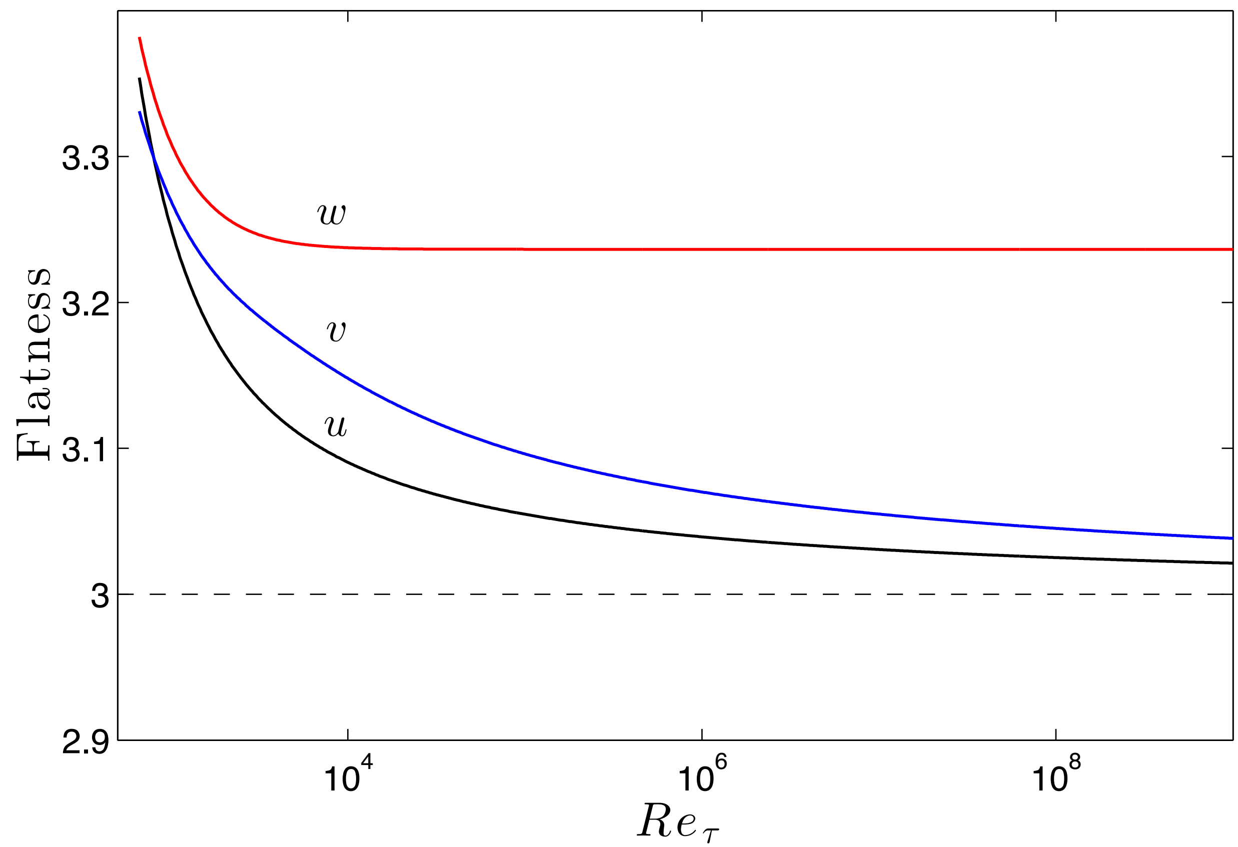

Flatness

$$F_u = \frac{\langle u^4 \rangle}{\langle u^2 \rangle^2}, \qquad F_v = \frac{\langle v^4 \rangle}{\langle v^2 \rangle^2}, \qquad F_w = \frac{\langle w^4 \rangle}{\langle w^2 \rangle^2}$$

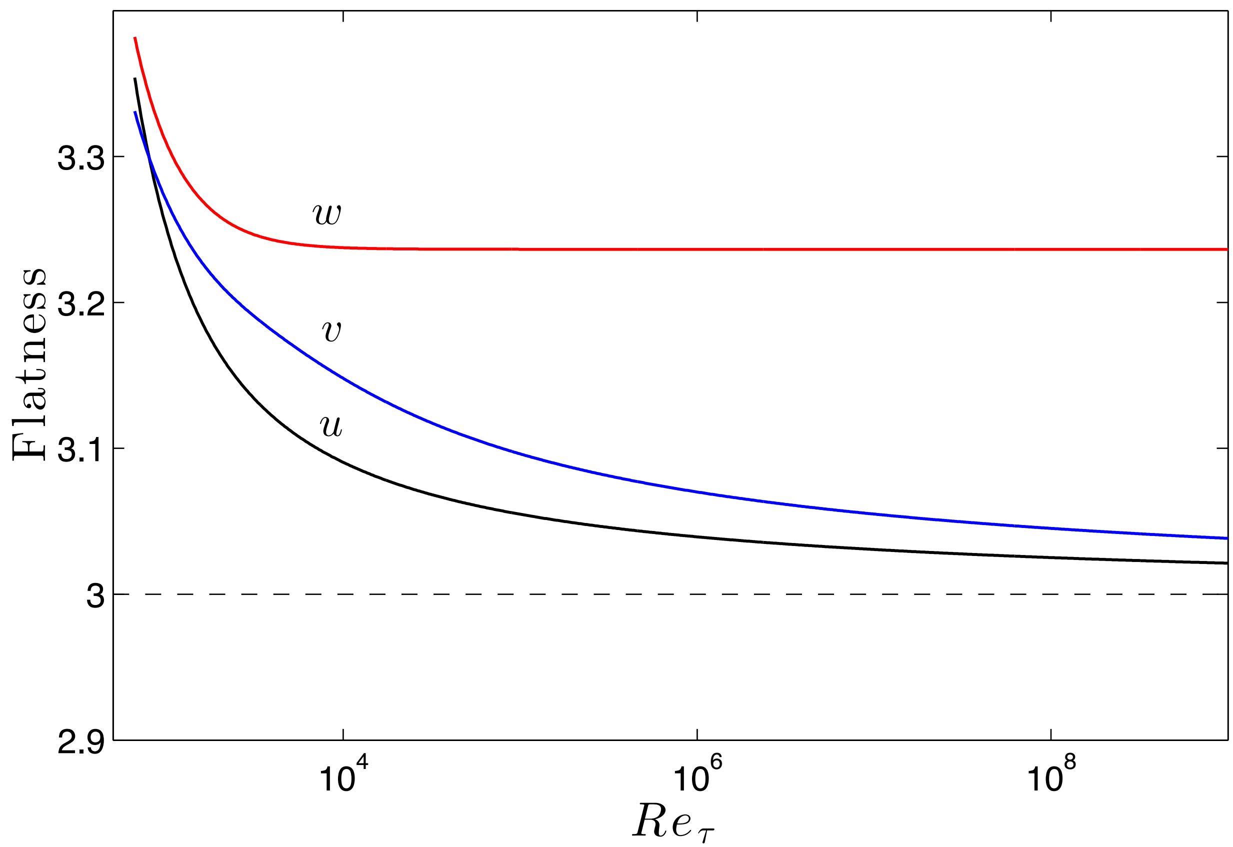

Experiments (Fernholz & Finley 1996): $F_u \approx 2.8,\ F_v \approx 3.4$ and $F_w \approx 3.4$

Spatial Exclusion

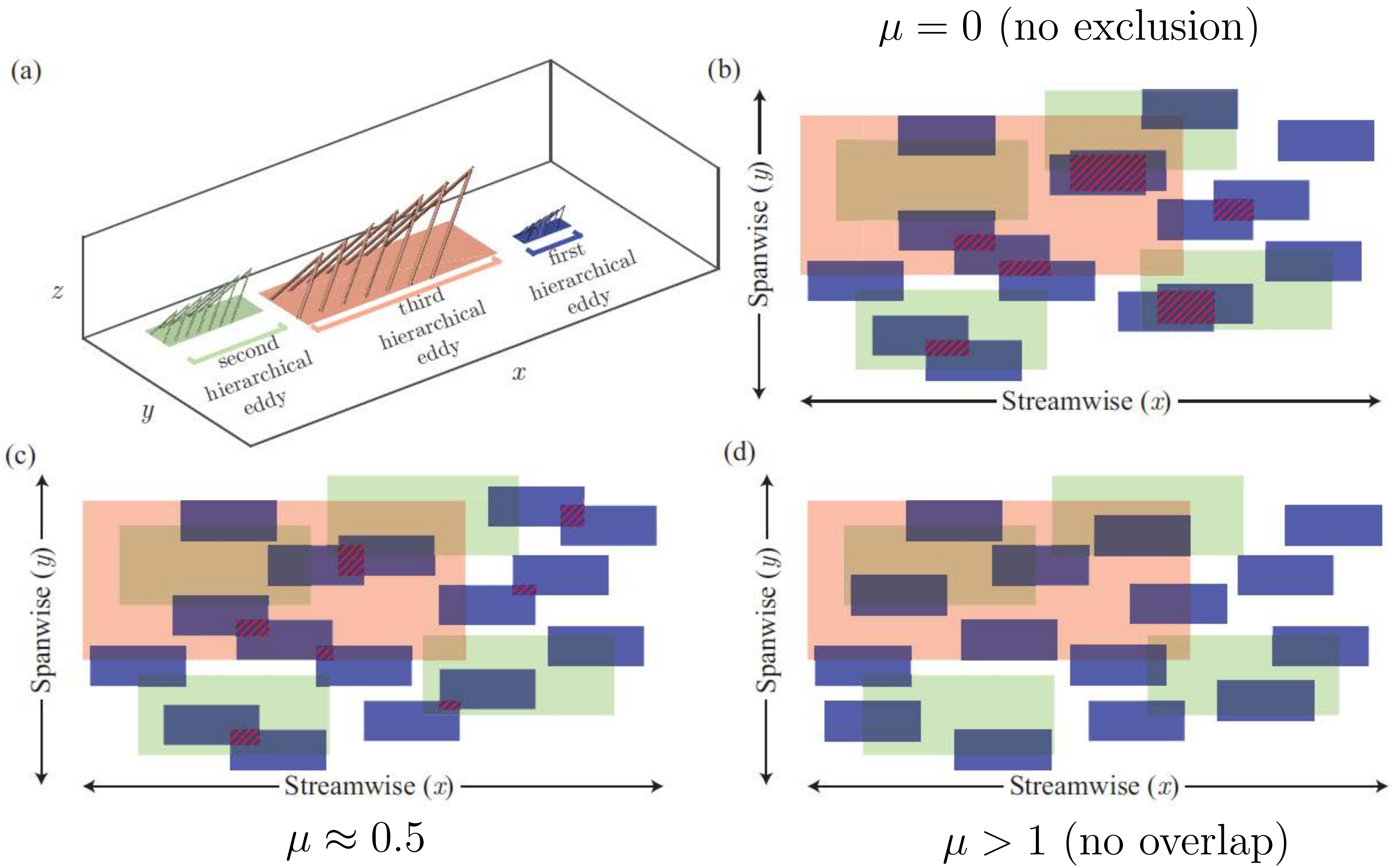

$\mu = 0$ to 1

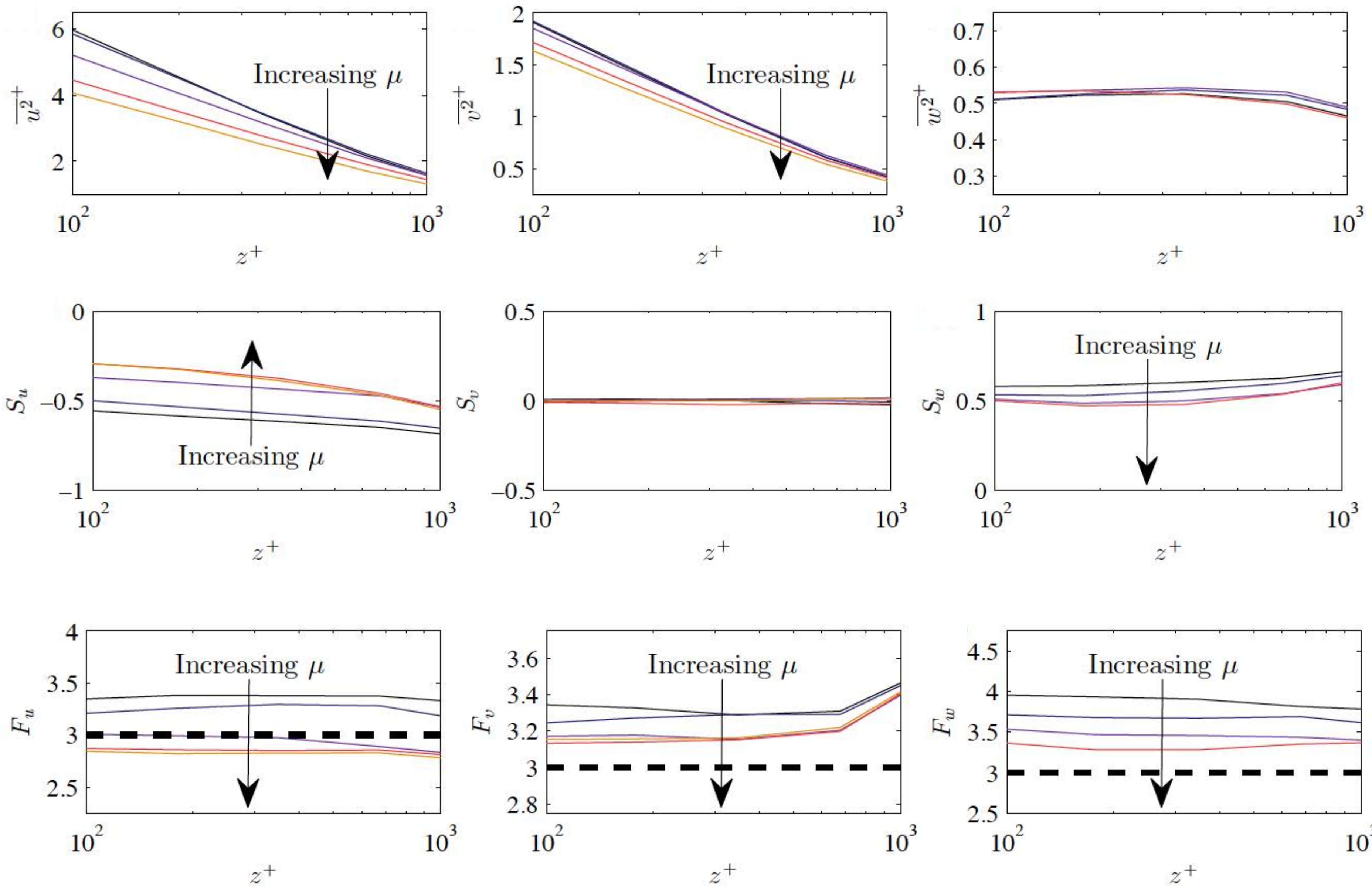

Increasing μ
$\overline{u^2}^+$
$\overline{v^2}^+$
$\overline{w^2}^+$
S_u
S_v
S_w
F_u
F_v
F_w
z^+

$Re_\tau = 6400$. (mid-log layer)

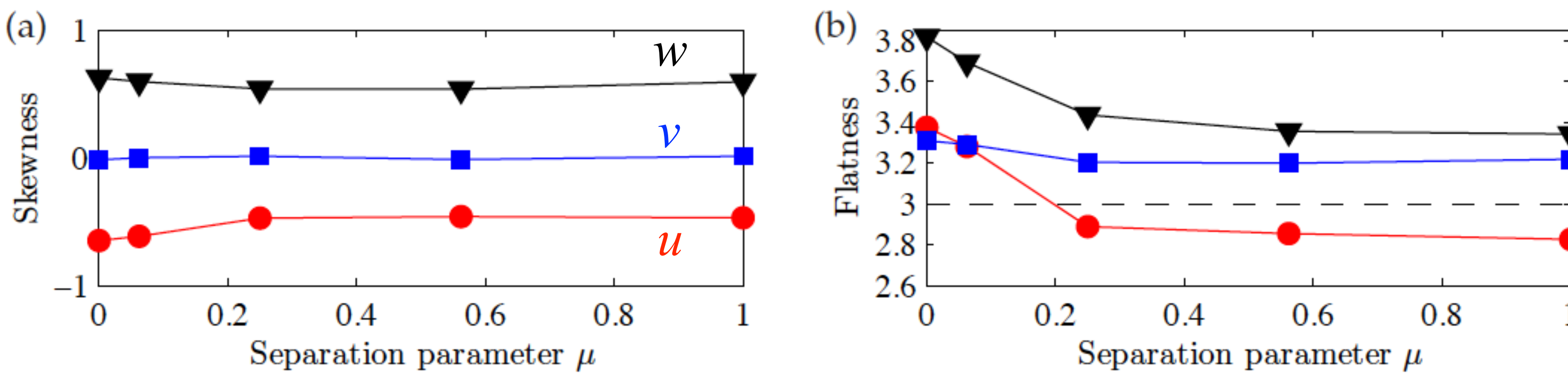

Similar analysis can be carried out for structure functions

$$\langle \Delta u^n(r) \rangle = \langle [u(\boldsymbol{x} + \boldsymbol{i}r) - u(\boldsymbol{x})]^n \rangle$$

$$\langle \Delta u_+^{2p} \rangle^{1/p} = E_p + D_p \ln \frac{r}{z}$$

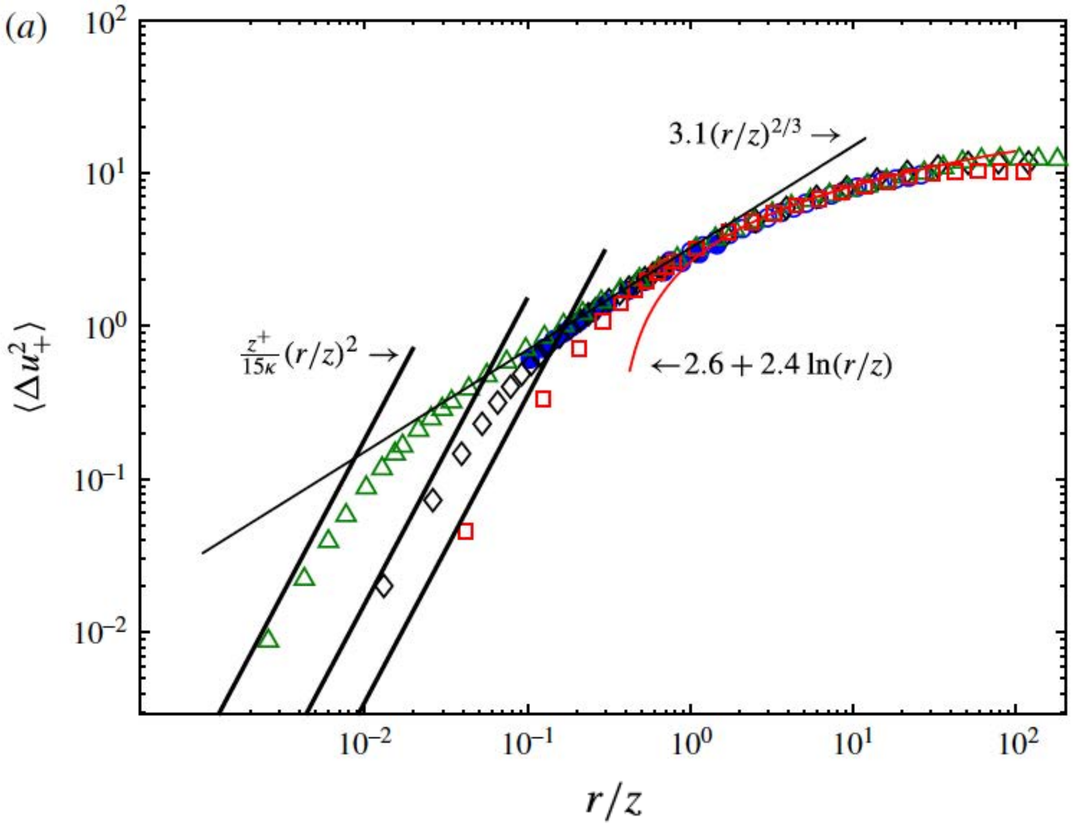

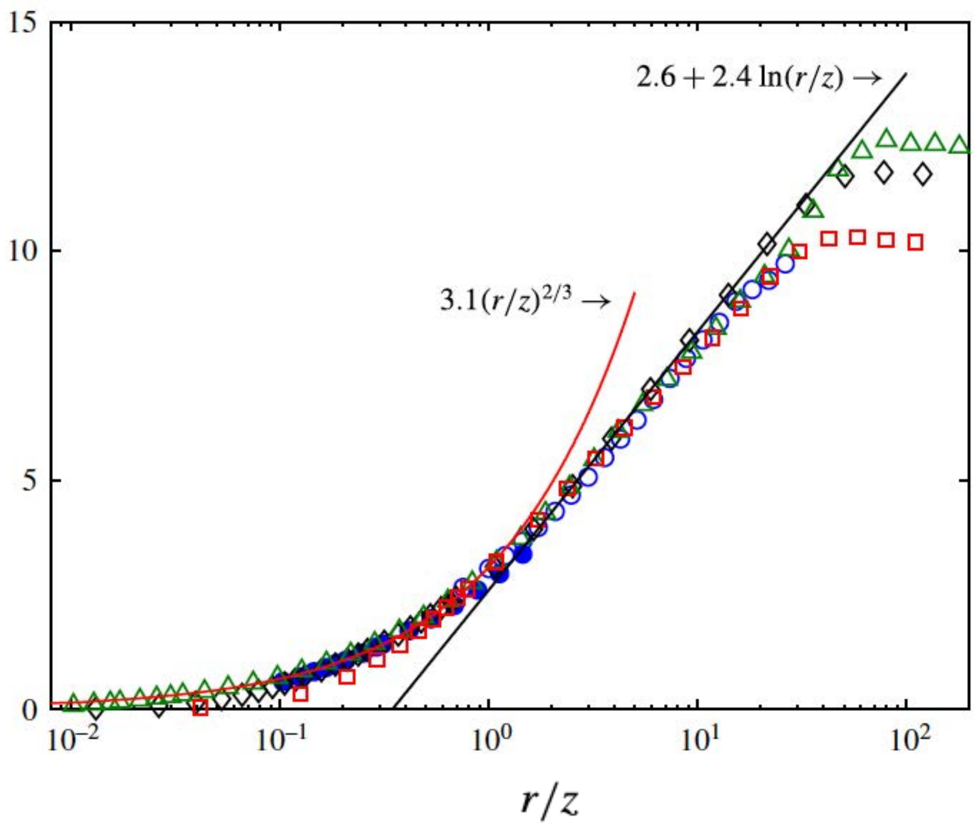

de Silva, Marusic,Woodcock & Meneveau (2015)

Similar analysis can be carried out for structure functions

$$\langle \Delta u^n(r) \rangle = \langle [u(\boldsymbol{x} + \boldsymbol{i}r) - u(\boldsymbol{x})]^n \rangle$$

$$\langle \Delta u_+^{2p} \rangle^{1/p} = E_p + D_p \ln \frac{r}{z}$$

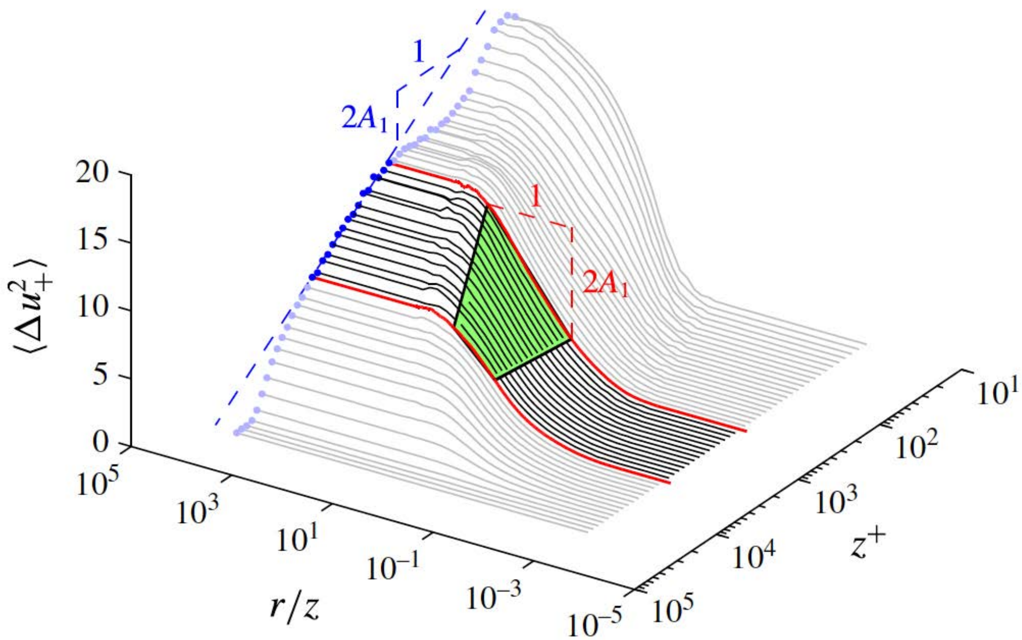

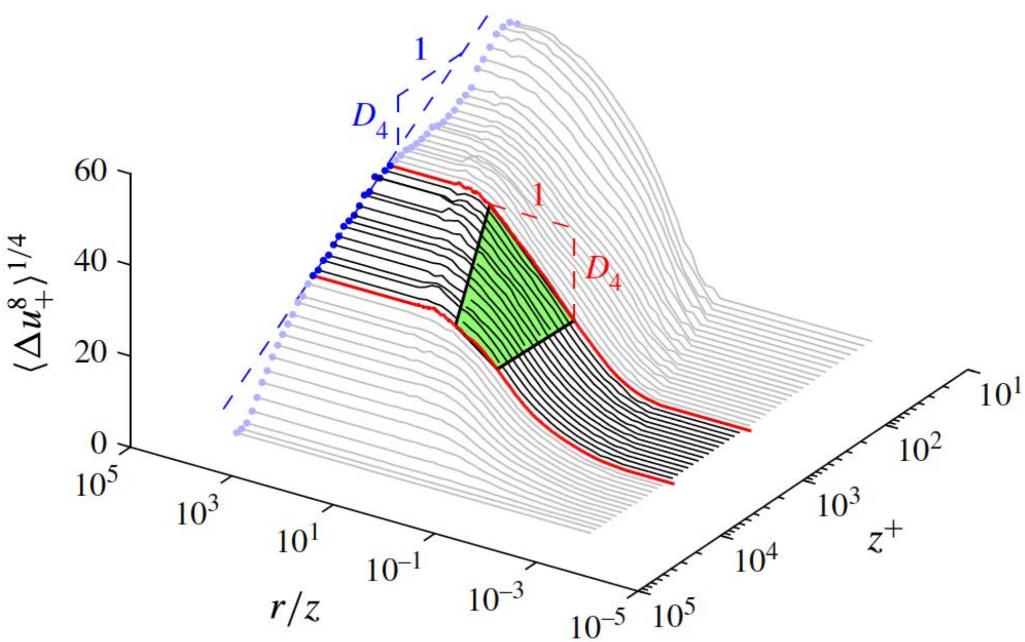

de Silva, Marusic,Woodcock & Meneveau (2015)

Conclusions

- The logarithmic region becomes the dominant region in wall turbulence at very high Reynolds numbers.

- In addition to the mean flow, the log region is found to also exhibit generalised logarithmic functions for

  - $\langle u^2 \rangle$, $\langle v^2 \rangle$: Townsend (1976); Perry & Chong (1982)
  - $\langle u^{2p} \rangle^{1/p}$, $\langle v^{2p} \rangle^{1/p}$; Meneveau & Marusic (2013)
  - Structure functions: $\langle \Delta u^{2p} \rangle^{1/p}$; de Silva *et al.* (2015)

- Attached eddy model with an extended form of Campbell's theorem formally shown to agree with these observations, including admitting an asymptotically universal von Karman constant, and capturing the finite skewness of w (which conflicts with central-limit theorem).

- Quantitative differences, such as experiments showing sub-Gaussian behavior of u, point to the need to modify assumption of spatial independence of attached eddies.

- Discrete, quantized version of attached eddies, is supported by current observations.